

Measurements and modelling of liquid-liquid equilibria

of ϵ -caprolactam + water + solvent + ammonium sulfate systems

Author : Gerard van Bochove

**Supervisors : Ir. M. Wijtkamp
Dr. Ir. Th. W. de Loos
Prof. Dr. Ir. J. de Swaan Arons**

July 1998

Delft University of Technology
Faculty of Applied Sciences
Subfaculty of Chemical Engineering and Materials Sciences
Laboratory of Applied Thermodynamics and Phase Equilibria

Preface

This report is the result of graduation work, performed at the Laboratory of Applied Thermodynamics and Phase Equilibria of the Delft University of Technology from September 1997 to July 1998. This graduation work is part of the last year of the education Chemical Engineering of the Delft University of Technology. The work was carried out within the Ph.D.-work of Mark Wijtkamp. Mark Wijtkamps Ph.D. project was concerned with the measuring and modelling of liquid-liquid equilibria of ϵ -caprolactam + water + solvent + ammonium sulfate systems and is funded by DSM Research.

The author would like to thank his supervisors, ir Mark Wijtkamp and dr ir Th. de Loos for their support. The author also wants to thank the other colleagues of the section Applied Thermodynamics and Phase Equilibria for their help, their kind approach and their contribution to the pleasant atmosphere.

Gerard van Bochove, July 1998

Abstract

ϵ -Caprolactam, the monomer of Nylon-6, is obtained from the production process as an aqueous solution of ammonium sulfate and ϵ -caprolactam. The crude ϵ -caprolactam is purified by extraction with an organic solvent. To be able to model this extraction process, thermodynamic modelling of liquid-liquid equilibria of ϵ -caprolactam + water + solvent + ammonium sulfate is required. Since the number of models in literature is scarce, a dedicated model for the description of liquid-liquid equilibria of mixed solvent electrolyte systems has to be developed.

In this work liquid-liquid equilibria were experimentally determined for the systems ϵ -caprolactam + water + 1-heptanol + ammonium sulfate at 20°, 40° and 60°C. In addition to this experimental work, a program was developed to correlate experimental liquid-liquid equilibrium data of mixed solvent electrolyte systems. The program is based on an activity coefficient model, that consists of a nonelectrostatic contribution and an electrostatic contribution. The Non Random Two Liquid (NRTL) theory is used to describe the nonelectrostatic contribution. The statistical mechanical Mean Spherical Approximation (MSA) theory is used to account for the electrostatic interactions. The MSA is a physically more correct model than the Debye-Hückel model, since it takes into account ion size effects. The new NRTL-MSA activity coefficient model is compared with the existing electrolyte NRTL models of Chen and Liu.

The experimental work showed that 1-heptanol may be a suitable solvent for the extraction of ϵ -caprolactam. The presence of ammonium sulfate in the system favours the dissolution of ϵ -caprolactam in the organic phase and salts out the aqueous phase. At increasing temperature, the solubility of ϵ -caprolactam in 1-heptanol increases to a greater extent than the solubility in water.

The NRTL-MSA model, built up from an electrolyte NRTL contribution and an electrostatic MSA contribution without explicit hard sphere contribution produces promising results for the representation of liquid-liquid equilibria of mixed solvent electrolyte systems. For the system water + 2-propanol + sodium chloride, an average deviation of 0.006 w/w could be reached. It might be concluded carefully that the NRTL-MSA performs better than the electrolyte NRTL. However, the model still needs more testing. It is also recommended to extend and apply the nonprimitive MSA to mixed solvent systems and compare it with the results of the NRTL-MSA model, presented here.

Table of contents

1. Introduction	1
2. Scope & Basic thermodynamics	2
2.1 Properties and production of ϵ -caprolactam	2
2.2 Extraction of caprolactam	2
2.3 Thermodynamic modelling of the extraction process	3
2.4 Liquid-liquid equilibria	3
3. Thermodynamics of electrolyte solutions	5
3.1 Introduction	5
3.2 Statistical mechanical background	6
3.2.1 Statistical mechanics of liquids	6
3.2.2 McMillan-Mayer approach	7
3.2.3 Conversion to Lewis-Randall systems	8
3.3 Debye-Hückel model	9
3.3.1 Approach	9
3.3.2 Extensions	10
3.4 Electrolyte NRTL model	11
3.4.1 The Non-Random-Two-Liquid (NRTL) theory	11
3.4.2 Electrolyte NRTL activity coefficient model	13
3.4.3 Modification by Liu	15
3.4.4 Ionic Equilibrium in the electrolyte NRTL model	15
3.5 Other electrolyte models	15
4. Mean Spherical Approximation theory	17
4.1 Principles	17
4.2 Solution of the primitive MSA	18
4.3 Hard sphere contribution	19
4.4 Activity coefficients: MSA vs. Debye-Hückel	20
4.5 EXP-modification	21
4.6 Nonprimitive MSA	22
4.7 Reported applications of the MSA theory	23
5. Experimental work	26
5.1 Introduction	26
5.2 Description of experiments	26
5.3 Results	27
5.3.1 Caprolactam + water + cyclohexane	27
5.3.2 Caprolactam + water + 1-heptanol	27
5.3.3 Caprolactam + water + 1-heptanol + ammonium sulfate	29
5.4 Error analysis	30
5.5 Conclusions	31

6. Modelling	32
6.1 Introduction	32
6.2 Activity coefficient subroutine	32
6.2.1 Solution properties	32
6.2.2 MSA contribution	33
6.2.3 NRTL contribution	34
6.2.4 Other contributions	34
6.3 Flash routine	35
6.4 Regression routine	36
6.5 Levenberg-Marquardt routine	38
6.6 Chemical equilibrium	38
7. Calculations	39
7.1 Examination of the MSA activity coefficient	39
7.2 Prediction of ionic activity coefficients	39
7.3 Modelling liquid-liquid equilibria of electrolyte solutions	41
7.3.1 Model 1: MSA + molecular NRTL	41
7.3.2 Model 2: MSA + electrolyte NRTL	43
7.3.3 Model 3: No hard sphere contribution	44
7.3.4 Model 4: Electrolyte NRTL of Liu	46
7.4 Modelling of experimental results	47
8. Conclusions & recommendations	48
References	50
List of symbols	53
Appendices	55
I : Analyses	55
II : Error analysis experiments	58
III : Experimental results	61
IV : Electrolyte NRTL model	64
V : Electrostatic contribution neutral species	65
VI : Example of an input file	68
VII : Source code CHEMEQ	71
VIII : Source code ACTCOEFF	73

1. Introduction

Nylon 6 belongs to the most heavily used nylons for fibre manufacture. Nylon 6 is a polyamide formed by polymerization of ϵ -caprolactam. ϵ -caprolactam may be produced via various routes from cyclohexane, benzene, toluene or phenol. The production process yields ammonium sulfate as a byproduct that has to be separated from the aqueous caprolactam solution by extraction with an organic solvent. In modelling the extraction process, thermodynamic modelling of liquid-liquid equilibria of ϵ -caprolactam + water + solvent + ammonium sulfate is required. Because the number of models known in literature is scarce, a dedicated model for the description of liquid-liquid equilibria of mixed solvent electrolyte systems has to be developed.

In this study experimental liquid-liquid equilibrium data are measured for the system water + caprolactam + solvent + ammonium sulfate at three different temperatures (20°, 40° and 60°C). The purpose is to use the experimental data to model liquid-liquid equilibria of these systems. The modelling will be performed using an activity coefficient model based on a Non Random Two Liquid model (NRTL; Renon [35]) and the Mean Spherical Approximation (MSA; Blum [6]). This model will be compared with the existing electrolyte NRTL (Chen et al. [12], later modified by Austgen et al. [4] and Liu [25]). It is expected that the combination of MSA with NRTL will perform better than the electrolyte NRTL, since the MSA accounts for ion size effects and is physically more correct.

The structure of this report is the following. First a short discussion is given of the scope of the project and the basic thermodynamics underlying the modelling of liquid-liquid equilibria of multicomponent systems. Consequently, in chapter 3 some theories on equilibria of electrolyte solutions are discussed. The next chapter then discusses the Mean Spherical Approximation theory. A description of the experiments on liquid-liquid equilibria of the systems water + ϵ -caprolactam + 1-heptanol, water + ϵ -caprolactam + cyclohexane and water + ϵ -caprolactam + 1-heptanol + ammonium sulfate is given in chapter 5. The results are also presented in this chapter. The next chapter describes the development of a FORTRAN program able to regress and to correlate liquid-liquid equilibria of electrolyte systems, using an activity coefficient model such as the NRTL-MSA. The calculations and the results are presented in chapter 7, followed by the conclusions and recommendations.

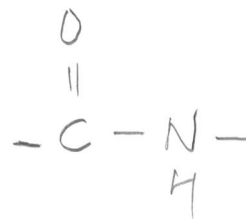


Figure 2.1: Caprolactam (left) is the monomer of nylon-6 (right)

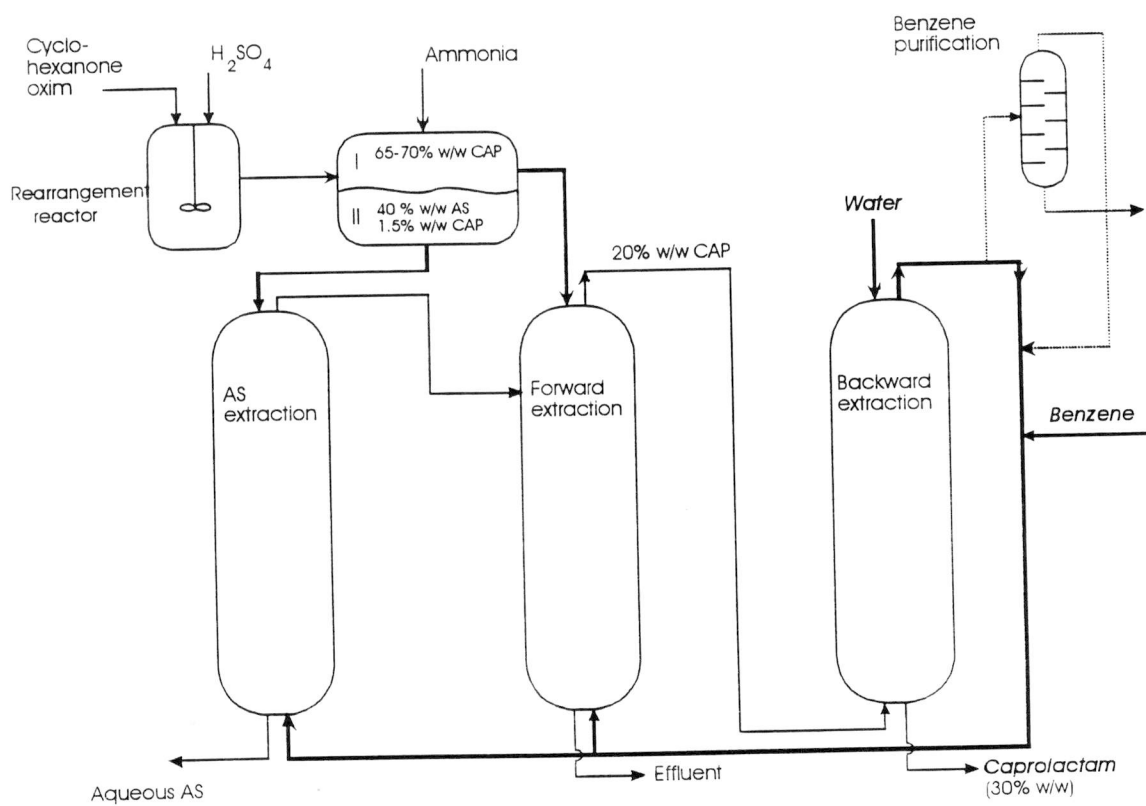


Figure 2.2 : Purification process of caprolactam with benzene as solvent [40]

2. Scope & Basic thermodynamics

2.1 Properties and production of ϵ -caprolactam

ϵ -Caprolactam (further called caprolactam) is one of the most widely used chemical intermediates. World caprolactam production is about four million tons per year. Most of the production is consumed for nylon-6 fibres and plastics (see figure 2.1). Caprolactam or 6-amino-hexanoic acid-lactam is a white, hygroscopic crystalline solid at ambient temperature, with a characteristic odour. It is very soluble in water and most organic solvents and is hardly soluble in high molecular weight aliphatic hydrocarbons. The compound melts at 69°C. It can be hydrolyzed, N-alkylated, O-alkylated, halogenated and is readily converted to high molecular weight linear nylon-6 polymers.

Several commercial processes exist for the manufacture of caprolactam. The synthesis of caprolactam consists of three steps. First, cyclohexanone is produced (in the process in use at DSM, phenol is converted to cyclohexanone by catalytic hydrogenation). Subsequently, the cyclohexanone reacts with a hydroxyl amine (e.g. $\text{NH}_2\text{OH}\cdot\text{H}_2\text{SO}_4$). Currently, two processes are used to produce the cyclohexanone oxime. First, the conventional Raschig process is used. This process produces large amounts of ammonium sulfate as byproduct. The second process is the Hydroxylamine Phosphate-Oxime (HPO) process; much less byproduct ammonium sulfate is produced. The cyclohexane oxime from both processes is converted to caprolactam by Beckmann rearrangement in the presence of oleum ($\text{H}_2\text{SO}_4/\text{SO}_2$). [19]

2.2 Extraction of caprolactam

To reduce the organic and inorganic impurities to a very low level, a series of purification steps is applied. These include extraction, chemical and physical treatment and final vacuum distillation. The mixture from the Beckmann rearrangement is first neutralized with ammonia. Water is added to prevent the formed ammonium sulfate from precipitation. Because of this neutralization two immiscible phases are formed that can be separated mechanically. The top layer consists of circa 65-70% w/w caprolactam and a small amount of ammonium sulfate. The bottom layer contains about 40% w/w ammonium sulfate and 1.5% w/w caprolactam. The ammonium sulfate rich layer is subjected to a separate extraction process with an organic solvent. The caprolactam in this layer dissolves in the organic solvent, the extract. This extract is transported to the forward extraction. The forward extraction uses the same organic solvent as the ammonium sulfate extraction. The crude caprolactam top layer is also lead to the forward extraction. All impurities that are more soluble in water than in the organic solvent are left behind in the aqueous raffinate. The organic extract, containing about 20% w/w caprolactam, still contains impurities that dissolve better in the organic solvent than in water. These impurities are removed by a re-extraction or backward extraction with water. The organic solvent is reused after partial distillation to avoid accumulating of impurities. The bottom product of the backward extraction is a 30% w/w aqueous solution of caprolactam and is treated further by means of ionic exchangers, hydrogenation, evaporation and vacuum distillation. The full extraction process of caprolactam is shown in figure 2.2. [40]

hinderijk
zonder namen &
jaartallen

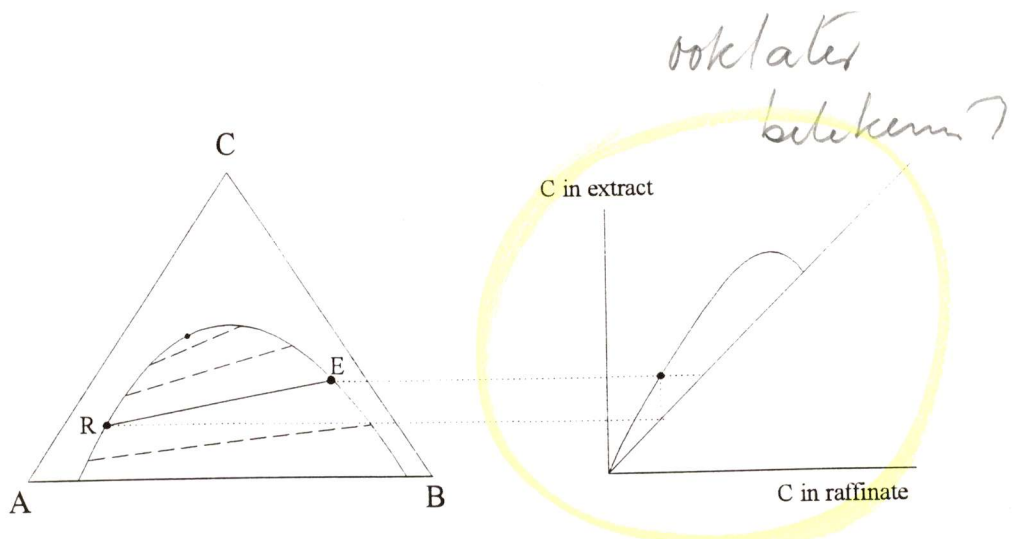


Figure 2.3: Liquid-liquid extraction is only possible when the feed solvent (A) and the extracting solvent (B) show a phase split. The streams leaving the extraction step (the raffinate R and the extract E) are in equilibrium with each other. In the figure, the liquid-liquid equilibrium is represented in a triangular diagram (left) and a distribution curve (right). [19]

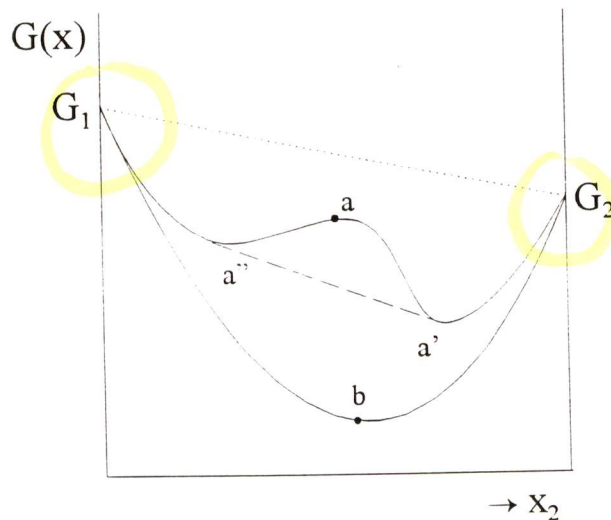


Figure 2.4: Gibbs energies of binary mixtures as functions of composition. The portion a'-a-a'' of the upper curve represents an unstable region. In this region the lowest Gibbs energy is reached by splitting into two phases with compositions a' and a''. The lower curve is that of a completely miscible mixture.[48]

2.3 Thermodynamic modelling of the extraction process

Liquid-liquid extraction or solvent extraction is the separation of a dissolved component from its solvent by transfer to a second solvent. The second solvent has to be immiscible with the first solvent and preferably has a higher affinity to the transferred component. Liquid-liquid extraction can purify a component with respect to dissolved components that are not soluble in the second solvent. Regarding the caprolactam recovering process: in the forward extraction caprolactam is transferred from the aqueous solution with ammonium sulfate to the organic solvent, leaving most water soluble impurities in the aqueous phase. In the backward extraction, caprolactam is transferred from the organic solvent to water, leaving the organic impurities in the organic solvent. In the extraction device the solution of solvent 1 with the solute is contacted with solvent 2. The solute distributes between both solvents until liquid-liquid equilibrium is reached. Since solvent 1 and 2 are immiscible, the two phases can be separated and the process may be repeated at different conditions. [19]

To be able to make reliable predictions of the solute fractions in both solutions leaving the extraction process in a simulation program like ASPEN Plus, an accurate thermodynamic model is required to calculate the liquid-liquid equilibria and the distribution of the solute between the liquid phases. These predictions are also needed for the choice of an appropriate solvent. In the project this work contributes to, DSM wants to have a reliable model for the extraction process and data for different types of solvent, in order to find a substitute for the currently being used benzene. The presence of ammonium sulfate as byproduct complicates this modelling (although it has a positive effect on the extraction it self). The model must be able to account for the effects of electrolytes (ammonium sulfate) and impurities. The problem arising here is the concentration of the ammonium sulfate. Few models can cope with electrolyte concentrations of up to 40% w/w and are applicable to mixed solvent systems.

Of course the availability of a good model for liquid-liquid equilibria of electrolyte systems would not only benefit the extraction process of caprolactam. Most chemical processes comprise processes that involve multicomponent electrolyte solutions. Even small amounts of salt may have considerable effects on the properties of these solutions. The development of engineering methods for the prediction of phase equilibria of complex systems containing both electrolytes and nonelectrolytes therefore is an important challenge for engineers. Damage prevention of industrial equipment requires accurate knowledge of the concentration of electrolytes through a process. Recent environmental concerns require precise control of electrolytes in final products and waste streams. Unfortunately and in spite of several decades of research, thermodynamic models for the prediction of thermodynamic properties of mixed solvent electrolyte solutions are scarce, often lead to different predictions and require many empirical adjustable parameters. However, accurate prediction of phase equilibria using thermodynamic models for mixed solvent electrolyte systems is essential to the success of computer-aided design and simulation of separation processes. [25]

2.4 Liquid-liquid equilibria

Liquid-liquid extraction is only possible when the feed solvent and the extracting solvent show a phase split. Whether a mixture with a certain composition will demix or not and how the solute will distribute between the liquid phases can be described using thermodynamics. In general, the equilibrium conditions for phase equilibria can be derived using the Gibbs energy. A closed system not at equilibrium will always go to a minimum in the total Gibbs energy with respect to all possible changes at given pressure and temperature, according to the second law of thermodynamics. In other words, at the equilibrium

state differential variations can occur in the system at constant pressure and temperature without producing any change in the total Gibbs energy: $dG_{T,P} = 0$.

For a given liquid mixture at fixed temperature and pressure the necessary equilibrium condition is that the Gibbs energy for the system is minimum. If the mixture achieves the lowest Gibbs energy by splitting into two or maybe three liquid phases, this is what actually happens (see figure 2.4). Thus, mixtures of two solvents will only mix when the mixed state has the lowest Gibbs energy. This directly leads to the usual equilibrium conditions

$$\mu_i^I = \mu_i^{II} \quad (2.1)$$

$$\begin{aligned} &\Downarrow \\ [\mu_i^0 + RT \ln(x_i \gamma_i)]^I &= [\mu_i^0 + RT \ln(x_i \gamma_i)]^{II} \quad (2.2) \end{aligned}$$

$$\begin{aligned} &\Downarrow \\ (x_i \gamma_i)^I &= (x_i \gamma_i)^{II} \quad (2.3) \end{aligned}$$

where R = Universal gasconstant
 T = Temperature
 x_i = Mole fraction component i
 μ_i = Chemical potential component i in phase I or II
 γ_i = Activity coefficient component i

The Gibbs energy of mixing is defined as:

$$\Delta G_m = G - \sum_i x_i G_i \quad (2.4)$$

where G_i = Gibbs energy component i

The molar Gibbs energy is built up from two contributions: an ideal contribution and a contribution that takes into account the non-ideality: the excess Gibbs energy. The excess Gibbs energy is interrelated with the activity coefficient γ by the following relationships:

$$G^E = RT \sum_i x_i \ln \gamma_i \quad (2.5)$$

$$RT \ln \gamma_i = \left(\frac{\partial n_T G^E}{\partial n_i} \right)_{T,P,n_j} \quad (2.6)$$

where n_i = Number of moles i

Liquid-liquid equilibria can be modelled using the equilibrium condition in equation (2.3). In order to calculate the activity coefficients, one needs a model describing the excess Gibbs energy as a function of composition and temperature or an equation of state. [41]

3. Thermodynamics of electrolyte solutions

3.1 Introduction

For many years, standard texts on solution theories only dealt with nonelectrolytes. This represents the difficulties in treating electrically charged species. In 1923 Debye and Hückel published a model for electrolyte solutions where the ions are treated as point electric charges. This model has been of historical significance in electrolyte theories. In this chapter the Debye-Hückel model will shortly be discussed in order to be able to compare it with the Mean Spherical approximation theory in the next chapter. Also, some statistical mechanical background in dealing with electrolyte solutions will be discussed as a basis for the discussion of the Mean Spherical Approximation theory: both the Debye-Hückel model and the MSA model make use of the primitive model of electrolyte solutions, also called the McMillan-Mayer theory of solutions. The Debye-Hückel model, although only accurate at low concentrations, has been used in combination with models for nonelectrolyte solutions, such as NRTL and UNIQUAC. The resulting models have been of great importance in chemical engineering and will also be presented here.

The strong nonideal behaviour of electrolyte solutions is caused by the long range forces between the ions. The thermodynamic properties of a mixture depend on the forces that exist between the components in the mixture. In electrolyte systems both molecular and ionic species are present, resulting in molecule-molecule interactions, molecule-ion interactions and ion-ion interactions. The ion-ion interactions are dominated by the electrostatic Coulomb interactions, except for high electrolyte concentrations. Electrostatic interactions are inversely proportional to the distance of separation, while other intermolecular interactions are inversely proportional to a higher power of the distance of separation. [28]

An important phenomenon caused by the presence of ionic species in a solution is the salting-out behaviour in mixed solvents. The addition of salt to a solution leads to a change in the solubility of other solutes in the mixture. This effect is of industrial importance in separation processes such as extractive distillation and azeotrope distillation. Addition of salt to a mixed solvent system, changes the structure of the liquid phase with the highest dielectric constant, usually water. The water molecules that surround the ions become unavailable for the solvation of the nonelectrolyte and the nonelectrolyte becomes salted out from the aqueous phase. This effect may also be described by a lowering of the dielectric constant in the direct neighbourhood of an ion. This leads to an increase in the activity coefficient and the formation of dielectric holes around the ions. The dielectric holes or cavities have a much lower polarizability and other ions are repelled from these cavities. The cavities thus act as a shield around the ions. As will become clear in chapter 4 these short range electrostatic effects are largely dependent on ion size differences. [28]

Some conventions exist in literature on dealing with electrolyte solutions. It is customary to define a mean ionic activity coefficient γ_{\pm} for the electrolyte by:

$$\gamma_{\pm} = \left(\gamma_+^{v_+} \gamma_-^{v_-} \right)^{\frac{1}{v_+ + v_-}} \quad (3.1)$$

where v_i Stoichiometric coefficient
 γ_i Single-ion activity coefficient

For the electrolyte, the condition for liquid-liquid equilibria is equated as:

$$\mu_{\pm}^I = \mu_{\pm}^{II} \quad (3.2)$$

$$(x_{\pm}\gamma_{\pm})^I = (x_{\pm}\gamma_{\pm})^{II} \quad (3.3)$$

where x_{\pm} is the mean ionic mole fraction and is calculated in the same way as the mean ionic activity coefficient.

3.2 Statistical mechanical background

3.2.1 Statistical mechanics of liquids

In statistical mechanics the structure of a liquid is expressed in terms of probabilities: Molecular distribution functions give the time-averaged spatial arrangement of the molecules. They describe how the molecules in a liquid are distributed with respect to one another. Knowing the molecular distribution functions, all thermodynamic properties of a fluid can be calculated. Molecular distribution functions can be obtained experimentally by X-ray or neutron diffraction, by computer simulations and from integral equations (which will be discussed later). [28]

The most important distribution functions are the pair correlation functions or radial distribution functions g_{ij} . The pair correlation function is related to the total correlation function h_{ij} by:

$$h_{ij}(r_{ij}) = g_{ij}(r_{ij}) - 1 \quad (3.4)$$

where r_{ij} = r = Distance between centres molecule i and j

The total correlation between molecule i and j is split up into a contribution for the direct correlation, the direct correlation function C_{ij} , and an indirect correlation contribution. Ornstein and Zernike defined it by:

$$h_{ij} = C_{ij} + \rho \int h_{ik} C_{ik} dr_k \quad (3.5)$$

where ρ = Density, molecules per volume

It has been shown that the asymptotic behaviour for the total correlation function is:

$$C_{ij} \rightarrow -\beta u_{ij}(r_{ij}) \quad \text{for } r \rightarrow \infty \quad (3.6)$$

where u_{ij} = Interaction energy
 β = Boltzmann thermal factor = $(kT)^{-1}$
 k = Boltzmann constant
 T = Temperature

The solution for the pair correlation function can only be derived if there is an additional relation between C_{ij} and g_{ij} . These relations are the closure relations or integral equations, like the Hypernetted

Chain approximation and the Percus-Yevick approximation. Another integral equation, especially designed for electrolyte solutions, is the Mean Spherical Approximation. This theory will be discussed more extensively in the next chapter. [21]

Once the system is solved and g_{ij} is known, the internal energy U per unit volume is obtained from [46]:

$$U(\rho, \beta) = \sum_{i,j=1}^2 \rho_i \rho_j \int_{d_{ij}}^{\infty} u_{ij}(r) g_{ij}(r) 4\pi r^2 dr \quad (3.7)$$

where: ρ_i = numerical density of i

Integrating the internal energy with respect to β yields the Helmholtz free energy A :

$$\frac{A}{VkT} = \int_0^{\beta} U^*(\rho, \beta') d\beta' \quad (3.8)$$

3.2.2 McMillan-Mayer approach

In statistical thermodynamics, macroscopic properties of a system are calculated from the microscopic nature of the system. One way to do this is the ensemble method introduced by Gibbs. An ensemble is defined as a great number of independent systems identical in nature, but differing in state. By making a statistical count of all the possible states, average properties can be calculated corresponding to the macroscopical state of the system.

Several ensembles are distinguished in statistical thermodynamics:

- If the number of particles N , the total volume V and the internal energy are kept constant, the system is called a microcanonical ensemble.
- In a canonical ensemble every system has the same number of particles, volume and temperature. The work function of this ensemble is the Helmholtz free energy.
- If all systems have the same (constant) volume, temperature T and chemical potential μ , a grand canonical ensemble is produced. In a grand canonical ensemble the internal energy and the number of particles may vary. Macroscopically it corresponds to an open system, with heat and mass transfer across the boundaries.
- An ensemble with a constant number of particles, constant pressure P and constant temperature T is called an N,P,T -ensemble, also referred to as a Lewis-Randall ensemble or isothermal-isobaric ensemble. This ensemble is related to the Gibbs-energy.

A special ensemble is the McMillan-Mayer (MM) ensemble for solutions [21,29], also called the primitive model of electrolytes. The McMillan-Mayer ensemble is based on the grand canonical ensemble and is used for the description of electrolyte solutions. The solvent molecules, unlike in the grand canonical ensemble, do not appear explicitly. The assumption is made that the solvent molecules form a dielectric continuum, a uniform background. The ions are considered as charged spheres or points in a continuous medium. This reduces the level of difficulty considerably. "Averaged" quantities are used where the solvent molecules have been 'smoothed out' and replaced by a dielectric continuum. For

example the MM partition function in the grand canonical ensemble is defined as the quotient of the partition function for a solution (II) and the one of the reference state (I), namely the pure solvent(s) at the same T. (The relative quantity is denoted with *.)

$$\Xi^{*II} \equiv \frac{\Xi^{II}}{\Xi^I} = \frac{\exp(\beta^{II} \cdot P^{II} \cdot V^{II})}{\exp(\beta^I \cdot P^I \cdot V^I)} = \exp(\beta \cdot \Pi \cdot V) \quad (3.9)$$

where V^I = Volume of pure solvent
 V^{II} = Volume of pure solvent + solutes
 Π = Osmotic pressure = $P^{II} - P^I$
 Ξ = Partition function of the grand canonical ensemble

Characteristic of the McMillan-Mayer ensemble is that an excess Helmholtz free energy is derived, whereas a Lewis-Randall ensemble yields an expression in terms of an excess Gibbs free energy. It is recalled that the Helmholtz free energy of the system can be found from the partition function of the grand canonical ensemble by:

$$\Xi(V, T, \mu) = \exp\left(\frac{pV}{kT}\right) = \sum_N Q(N, V, T) \cdot \exp\left(\frac{N\mu}{kT}\right) \quad (3.10)$$

$$Q(N, V, T) = \sum_j \exp\left(-\frac{U_j}{kT}\right) \quad (3.11)$$

$$A(N, V, T) = -kT \ln Q(N, V, T) \quad (3.12)$$

where: Q = partition function
 U_j = energy of the j-th quantum state

The Debye-Hückel theory and the MSA theory are obtained in the McMillan-Mayer theory, not from equation (3.12) but from the Ornstein-Zernike equation. In most electrolyte theories the assumption of ions in a dielectric continuum is made and the properties are expressed as relative to that of a pure solvent. Illustrative may be that a model derived with the McMillan-Mayer ensemble does not give the pressure, but the osmotic pressure. (Theories that do not use the McMillan-Mayer framework are called nonprimitive models, see for instance the description of the nonprimitive MSA in section 4.6)

3.2.3 Conversion to Lewis-Randall systems

Many theories have been derived in the primitive model to describe the single-solvent and multisolvent systems. Until 1982 they merely focussed on properties of the salt rather than of the solvents and were not applicable to correlate the effects of salts on phase equilibria in multisolvent systems. However, in 1982 the electrolyte NRTL and in 1986 the extended UNIQUAC model were published and these models were able to predict phase equilibria for electrolyte systems. These models combine a long range electrostatic term with another model such as NRTL and UNIQUAC for the short range interactions. UNIQUAC and NRTL are Lewis-Randall models, where the models for long range electrostatic interaction are McMillan-Mayer models. Correct use of a combination of both models requires a conversion. Formulae have been derived for this conversion, but they are very complex and will not be given here.

One consequence of ignoring the conversion is that the solvent activity coefficient does not include a contribution from the electrostatic interactions. Cardoso and O'Connell [9] and Lloyd Lee [22] derived by means of different methods an expression for the solvent activity coefficient which gives the correct dependence on the electrostatic forces (see appendix V):

$$\ln \gamma_i = \ln \gamma_i^{LR} - \frac{\langle \bar{v}_i \rangle \Pi}{RT} \quad (3.13)$$

where $\langle \bar{v}_i \rangle$ = Partial molar volume
 γ_i^{LR} = Activity coefficient from Lewis-Randall model (short range interactions)
 γ_i = Solvent activity coefficient

For the ionic activity coefficients the following equation is then used:

$$\ln \gamma_i = \ln \gamma_i^{LR} + \ln \gamma_i^{MM} \quad (3.14)$$

where γ_i^{MM} is the electrostatic contribution.

3.3 Debye-Hückel model

3.3.1 Approach

The Debye-Hückel model can be derived either from electrostatics (Poisson's equation) or from classical mechanics. Both derivations are described extensively in literature (for instance Lee [21]). Major assumptions are: the solvent is replaced by a dielectric background, the ions have no diameter or volume and the salt concentration is low. A short description will now be given of the classical derivation from electrostatics.

In the Debye-Hückel theory the ions are point charges and the solvent is replaced by a dielectric continuum, according to the McMillan-Mayer theory. For charged hard spheres the interaction potential between ion 1 and ion 2 is given by the Coulomb interaction subject to hard core repulsion:

$$u_{ij} = \frac{z_i z_j e^2}{\epsilon r_{ij}} \quad \text{for } r > \sigma \quad (3.15)$$

where e = Charge of an electron
 z = Valence
 ϵ = Dielectric constant = $4\pi \cdot 8.8542 \times 10^{-12} \cdot \epsilon_r$
 σ = Mean ionic diameter

The ions are assumed to be point charges and thus have no hard core (the diameter of the ions σ is taken to be zero) or volume: it is assumed that the different behaviour of electrolyte solutions can be described by the Coulomb interaction only. Starting point of the derivation of the Debye-Hückel model is the insertion of Boltzmann's distribution law into Poisson's equation, which is a relation between the distribution of charges and the electrostatic potential ψ . The resulting equation is called the Poisson-

Boltzmann equation and describes the distribution of charge around an ion: by assuming a Boltzmann distribution:

$$\nabla^2\psi(r) = -\frac{1}{\epsilon} \sum_i z_i e \rho_i \exp\left(\frac{z_i e \psi(r)}{kT}\right) \quad (3.16)$$

The Debye-Hückel theory further assumes that $kT \gg z_i e \psi$ so that the exponential term can be linearized:

$$\nabla\psi(r) = \kappa^2\psi(r) \quad (3.17)$$

$$\kappa^2 = \frac{e^2}{\epsilon kT} \sum_i \rho_i z_i^2 \quad (3.18)$$

where κ is the Debye-Hückel shielding parameter. The reciprocal of this parameter is called the Debye-length and is an indication of the range of electrostatic interaction between the ions. The electrostatic potential of the ions is shielded by the ionic atmosphere and decreases by a factor $1/\exp(1)$ over the Debye length.

The expression for the activity coefficient is written as:

$$\ln\gamma_i = -\frac{z_i^2 e^2 \kappa}{8\pi\epsilon kT} \quad (3.19)$$

3.3.2 Extensions

Several modifications have been proposed to extend the range of applicability to higher concentrations:

- Extended Debye-Hückel: In contrary to the former Debye-Hückel model, in the extended model the charge density within a radius a from the centre of the ion is assumed to be zero, resulting in:

$$\ln\gamma_i = -\frac{z_i^2 e^2}{8\pi\epsilon kT} \frac{\kappa}{1+\kappa a} \quad (3.20)$$

Often the radius a is referred to as the closest approach parameter and is treated as an empirical constant.

- Pitzer-Debye-Hückel: Pitzer suggested an extension of the Debye-Hückel model. It actually is the long range contribution for ion-ion interaction from the so called Pitzer ion interaction model. It contains one adjustable parameter, the closest approach parameter ρ . Dependence on the composition is given by the true mole fraction based ionic strength I_x . The equation, which was derived using the principles of the McMillan-Mayer theory, gives some recognition to the repulsive forces between ions. [12]

$$\ln\gamma_i^{PDH} = -\left(\frac{2\pi N_A d}{M_B}\right)^{\frac{1}{2}} \left(\frac{e^2}{\epsilon_w kT}\right)^{\frac{3}{2}} \left(\frac{2z_i^2}{\rho} \ln(1 + \rho\sqrt{I_x}) + \frac{z_i^2 \sqrt{I_x} - 2I_x \sqrt{I_x}}{1 + \rho\sqrt{I_x}}\right) \quad (3.21)$$

$$I_x = \frac{1}{2} \sum_i x_i z_i^2 \quad (3.22)$$

where d = Solution density
 M_B = Solvent molar mass
 N_A = Avogadro's number

- Many other attempts have been made to improve the Debye-Hückel model. The basic form of these equations is usually (just like the extended Debye-Hückel):

$$\ln\gamma_i = \frac{A|z^+z^-|\sqrt{I}}{1 + Ba\sqrt{I}} + C \cdot I \quad (3.23)$$

$$I = \frac{1}{2} \sum_i \rho_i z_i^2 \quad (3.24)$$

where I = Ionic strength
 A, B, C = Parameters dependent on the physical properties

3.4 Electrolyte NRTL model

3.4.1 The Non-Random-Two-Liquid (NRTL) theory

The Non Random Two Liquid equation is based on the concept of local compositions. Local compositions, different from overall compositions, are presumed to account for the short range order and nonrandom molecular orientations that result from differences in molecular size and intermolecular forces. Local mole fractions are given as X_{ij} , which is the local mole fraction of molecule i in the immediate neighbourhood of molecule j . In the NRTL model, the local mole fraction of molecules i in the neighbourhood of molecule j , X_{ij} , is related to the local mole fraction of molecules i in the neighbourhood of a molecule i , by:

$$\frac{X_{ij}}{X_{ii}} = \frac{x_j \exp(-\alpha_{ij} g_{ij}/RT)}{x_i \exp(-\alpha_{ij} g_{ii}/RT)} \quad (3.25)$$

where g_{ij} = energy of interaction between molecules of type i and j
 x_i = overall mole fraction of molecule i
 α = nonrandomness factor

The original NRTL model was proposed by Renon and Prausnitz [35]. They introduced the nonrandomness factor α into the relation between the local mole fractions. This factor is an empirical constant that takes into account the nonrandomness of mixing: the different molecules are not fully statistically distributed through the liquid. Renon and Prausnitz combined equation (3.25) with the Two

Liquid theory, which assumes two kinds of cells in a binary mixture: one with molecule 1 in the centres, the other with molecule 2 in the centres. The residual Gibbs energy (that is the Gibbs energy compared to the ideal gas at the same conditions) for the centre molecule is then given by the sum of the interaction energies between the centre molecule and the surrounding molecules:

$$g^{(1)} = X_{11}g_{11} + X_{21}g_{21} \quad (3.26)$$

The molar excess Gibbs energy is the sum of the changes in the residual Gibbs energy of transferring molecules i from a pure liquid to the centre of a cell and may be written as:

$$G^E = x_1X_{21}(g_{21} - g_{11}) + x_2X_{12}(g_{12} - g_{22}) \quad (3.27)$$

Combining equation (3.25), (3.27) and the fact that the local mole fractions must sum to unity gives the Non Random, Two-Liquid (NRTL) equation. Differentiation of equation (3.27) gives the activity coefficient for a binary solution. The NRTL equation can easily be generalized to multicomponent mixtures:

$$\frac{G^E}{RT} = \sum_{i=1}^n x_i \frac{\sum_{j=1}^n \tau_{ji} G_{ji} x_j}{\sum_{k=1}^n G_{ki} x_k} \quad (3.28)$$

where:

$$\tau_{ji} = (g_{ji} - g_{ii})/RT \quad (3.29)$$

$$G_{ji} = \exp(-\alpha_{ij}\tau_{ji}) \quad (3.30)$$

The NRTL model contains two adjustable parameters, which can be found by data regression: the binary interaction parameter τ_{ji} which is the difference of the dimensionless interaction energies and the nonrandomness factor $\alpha_{ij} = \alpha_{ji}$. Although the nonrandomness factor α_{ij} was vaguely related by Renon and Prausnitz to the reciprocal of the coordination number (the number of molecules i just touching the central molecule j), the range of numerical values found in literature shows that it may be regarded as an empirical constant. Values from 0.01 to 100 can be found from correlations of experimental data [48]. Walas [48] examined the parameters published for a large number of VLE systems and found a large variation with an average of 0.3 for nonaqueous mixtures and 0.4 for aqueous-organic systems. For liquid-liquid equilibria of molecular components the nonrandomness factor is often fixed at 0.2. The binary NRTL parameters are temperature dependent.

The advantages of the Non Random Two Liquid theory are its algebraic simplicity, the applicability of the model to mixtures that give liquid phase splitting, the applicability to multicomponent systems using only binary parameters and the fact that no specific volume or surface area data are required like in the UNIQUAC model. Main disadvantage is the large number of parameters that have to be fitted for multicomponent mixtures (although they can often be obtained from binary systems.) Also, the NRTL overpredicts the area under the binodal curve compared with experiments.

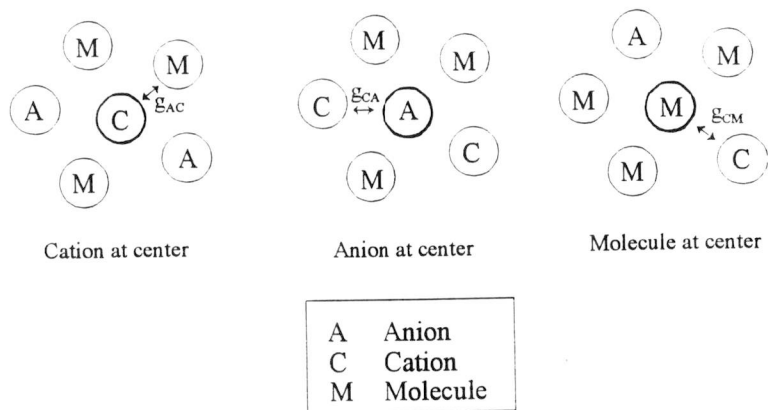


Figure 3.1: Three types of cells in the electrolyte NRTL, according to the like-ion repulsion and local electroneutrality assumptions. [13]

3.4.2 Electrolyte NRTL activity coefficient model

Chen et al. [12,13] extended the NRTL local composition model for use with electrolyte systems. They also added a long-range and a short range interaction contribution to the excess Gibbs energy of this extended NRTL model. In the Chen model as modified by Austgen et al. [4] and used in the simulation program ASPEN Plus [1], the excess Gibbs energy is built up from three contributions: one contribution to account for the short-range interactions among all species, one contribution to model the long range electrostatic interactions and a contribution, required to make pure water the reference state in a mixture of pure solvents. The long range electrostatic contribution is calculated with the Pitzer-Debye-Hückel equation (see section 3.3.2).

$$G^E = G^{E,PDH} + G^{E,Born} + G^{E,NRTL} \quad (3.31)$$

The short-range contribution is modelled using the NRTL theory, which has been adapted for modelling of electrolytes: In addition to the cells with a solvent molecule in the centre of the NRTL model of Renon and Prausnitz, in the electrolyte NRTL also cells with a cation c or an anion a in the centre are considered (see figure 3.1). Therefore, the original NRTL model was modified to take into account two fundamental assumptions on the structure of electrolyte solutions. First, the local composition of cations in a cell with a cation in the centre, as well as the local composition of anions around an anion is assumed to be zero. This assumption is called the like-ion repulsion assumption and is equivalent to the assumption of g_{cc} and g_{aa} being much greater than other interaction energies. The second assumption states that the distribution of cations and anions around a centre solvent molecule is such that the net local ionic charge is zero; this is the local electroneutrality assumption:

$$\begin{aligned} X_{cc} &= X_{aa} = 0 \\ X_{am} \cdot Z_a &= X_{cm} \cdot Z_c \end{aligned}$$

where Z is an absolute charge number. The assumptions lead to a slightly different treatment for the molecular NRTL model. For instance, the excess Gibbs energy is now calculated by:

$$\begin{aligned} G^{E,lc} &= x_m(g^{(m)} - g_{ref}^{(m)}) + x_c(g^{(c)} - g_{ref}^{(c)}) + x_a(g^{(a)} - g_{ref}^{(a)}) \\ g^{(a)} - g_{ref}^{(a)} &= Z_a(X_{ma}g_{ma} + x_{ca}g_{ca}) - Z_a g_{ca} \\ g^{(c)} - g_{ref}^{(c)} &= Z_c(X_{mc}g_{mc} + x_{ac}g_{ac}) - Z_c g_{ac} \\ g^{(m)} - g_{ref}^{(m)} &= (X_{am}g_{am} + X_{cm}g_{cm} + X_{mm}g_{mm}) - g_{mm} \end{aligned} \quad (3.32)$$

Pure completely dissociated electrolyte is taken as the reference state. (If partial dissociation is accounted for, the molecular salt is dealt with as an additional molecular species.) The electrolyte NRTL local composition contribution results in the following equation for a multicomponent system with one salt:

$$\frac{G^{E,lc}}{RT} = \sum_m X_m \frac{\sum_j X_j G_{jm} \tau_{jm}}{\sum_k X_k G_{km}} + X_c \frac{\sum_j X_j G_{jc} \tau_{jc}}{\sum_k X_k G_{jc}} + X_a \frac{\sum_j X_j G_{ja} \tau_{ja}}{\sum_k X_k G_{ja}} - x_c \ln \gamma_c^\infty - x_a \ln \gamma_a^\infty \quad (3.33)$$

where:

$$X_j = C_j x_j \quad (C_j = Z_j \text{ for ions, } C_j = 1 \text{ for molecules})$$

$$\alpha_{jc} = \alpha_{ja} = \alpha_{cj} = \alpha_{aj} = \alpha_{j,ca}$$

$$\tau_{jc} = \tau_{ja} = \tau_{j,ca}$$

$$\tau_{cj} = \tau_{aj} = \tau_{ca,j}$$

The last contributions in equation (3.33) are added in order to make the symmetric normalized $G^{E,lc}$ compatible with the unsymmetric reference condition (normalized to mole fractions of unity for solvent and zero for electrolytes) of the Pitzer-Debye-Hückel formula. Therefore, an infinite dilution reference condition is needed.

The electrolyte NRTL activity coefficients, that can be derived from equation (3.33), can be found in appendix IV. The binary parameters $\tau_{ca,m}$, $\tau_{m,ca}$ and $\alpha_{j,ca}$ are the only adjustable parameters. If $\alpha_{j,ca}$ is fixed at 0.2, two adjustable parameters remain for a pair of an anion and a cation. These parameters are referred to as the salt-molecule parameter and the molecule-salt parameter, respectively. The salt-molecule parameter is the difference of the dimensionless interaction energies between the ion-molecule pair and the molecule-molecule pair. The molecule-salt parameter is the difference of the dimensionless interaction energies between the molecule-ion pair and the cation-anion pair. Since the interaction between cation and anion is stronger than the interaction between the solvents and the ionic species, which is stronger than the interaction between solvent molecules, all $\tau_{ca,m}$'s are expected to be negative and all $\tau_{m,ca}$'s are expected to be positive.

The third contribution to the excess Gibbs energy is a Born contribution. In order to be able to calculate liquid-liquid equilibria, the activity coefficients of a component must have the same reference state in both phases. For solvents the pure component liquid state is used as the reference state. This is not possible for the ions and neither is a reference state of infinite dilution, since the reference state would be solvent composition dependent. That is the reason Austgen et al. [4] added a Born expression to account for the Gibbs energy of the transfer of the ions from a dielectric medium (Debye-Hückel theory) of mixed solvents to a dielectric medium of a pure solvent, usually water. After the addition of this Born term the reference state is the infinite dilute state in water. [25]

The Born theory of ion hydration [34] is a method to estimate the solvation energy of ions. Like in the Debye-Hückel theory, ions are viewed as charged spheres in a dielectric continuum. The Born model can be used to calculate the difference in solvation energies between ions in different solvents and this is how it is applied in the electrolyte NRTL. The Born contribution to the excess Gibbs energy and the Born contribution to the ionic activity coefficient are respectively given by:

$$\frac{G^{E,Born}}{RT} = \frac{e^2}{2kT} \left(\frac{1}{\epsilon} - \frac{1}{\epsilon_w} \right) \sum \frac{x_i z_i^2}{r_i^{Born}} \quad (3.34)$$

$$\ln \gamma_i^{Born} = \frac{e^2 z_i^2}{2kT} \left(\frac{1}{\epsilon} - \frac{1}{\epsilon_w} \right) \frac{1}{r_i^{Born}} \quad (3.35)$$

where r_i^{Bom} is the ionic cavity radius or Born radius, the radius of the dielectric cavity formed by the ion. In literature equation (3.34) and (3.35) are often multiplied by 10^{-2} , presumably due to the use of different unities.

3.4.3 Modification by Liu

The three contribution NRTL model can successfully be used for the calculation of vapour-liquid equilibria of mixed solvent systems. However, for liquid-liquid equilibria of mixed solvent systems the model still needs improvement. In 1996 Liu and Watanasari [25] proposed the addition of a fourth contribution to the excess Gibbs energy: an empirical Brønsted-Guggenheim term, given by:

$$\frac{G^{E,BG}}{RT} = \sum x_m M_{s,m} \sum_c \sum_a \frac{100\beta_{ca}}{T} x_c x_a \quad (3.36)$$

This equation should compensate for inadequacies of the Debye-Hückel and Born equation when used for mixed solvent electrolyte systems. Since the extension of the Pitzer-Debye-Hückel equation to mixed solvents still needs more study and the Born expression gives poor results compared with experiments, the three contribution electrolyte NRTL model does not always give satisfactory results. According to modelling work done in Delft, a first impression says that this model is still not able to describe liquid-liquid equilibria with electrolytes well.

3.4.4 Ionic Equilibrium in the electrolyte NRTL model

When salts such as NaCl dissolve in water, the ions dissociate and separate from each other. However, the attractive Coulombic force should recombine the ions. The reason that Na^+ and Cl^- do not form a molecule in water is the large dielectric constant of water. The high permittivity reduces the forces of attraction that much that thermal motions can overcome these forces. In a solvent with a much lower dielectric constant the ionic dissociation is reduced and accounting for the ionic equilibrium in the model may be worthwhile. This can be achieved by introducing the undissociated salt as an additional molecular component and calculating the ionic equilibrium. The parameters for the undissociated salt have to be fitted, can be assumed to be the same as for the ion pair or are set to zero [13,26].

3.5 Other electrolyte models

Some other models exist that are capable of modelling liquid-liquid equilibria of mixed solvent electrolyte systems. Best known among them is the extended UNIQUAC equation. UNIQUAC stands for Universal Quasi-Chemical. UNIQUAC is often used since it is the basis of a group contribution method for obtaining activity coefficients, the UNIFAC method. In the original (not extended to electrolytes) UNIQUAC model the Gibbs energy is made up of two parts. The first part is the so called configurational or combinatorial part. This is a contribution due to differences in sizes and shapes of the molecules. The second part is the residual part and accounts for the interactions between these molecules. The extended UNIQUAC model adds a third contribution, a Debye-Hückel term and introduces a salt concentration dependence of the interaction energy parameters. Like the NRTL model the UNIQUAC model is applicable to multicomponent mixtures using only binary parameters. The UNIQUAC equation is algebraically more complex than the NRTL equation. It utilizes knowledge of molecular surfaces and volumes of the pure components, which makes it applicable to mixtures of widely different molecular sizes [48]. For liquid-liquid equilibria of molecular systems, Sørensen et al. [41] found a slightly better correlation by the UNIQUAC equation.

Another model to describe equilibria of electrolyte solutions is the Extended Bromley-Flory-Huggins excess Gibbs energy model [11]. This model uses the Flory-Huggins theory of polymer solutions, combined with the Bromley model, which is an extension of the Debye-Hückel model. The Extended Bromley-Flory-Huggins model describes liquid-liquid equilibria of water-alcohol-salt systems rather accurately. The model requires three parameters for ternary systems and five parameters for quaternary systems. Looking at the structure, the Bromley-Flory-Huggins model looks a lot like the electrolyte NRTL by Austgen [4].

Recently, Zerres and Prausnitz [50] published a model for multisolvent electrolyte systems. Their model consists of three contributions: (1) chemical solvation effects, (2) physical, non-ionic short range effects (Van Laar) and (3) long range electrostatic effects. For a ternary system the model contains seven adjustable parameters. Liu [25] compared the model of Zerres and Prausnitz with his modification of the electrolyte NRTL and found a better representation by the NRTL for the three systems he studied.

4. Mean Spherical Approximation theory

4.1 Principles

The Mean Spherical Model was originally proposed as a model for Ising ferromagnets. In 1966 it was generalized for continuum systems by Lebowitz and Percus [20]. They extended the mean spherical model to lattice gases. (In the lattice model molecules of a mixture of gases are arranged on a regular lattice and the properties of the mixture are calculated from the possible combinations of the molecules.) Lebowitz and Percus went over from a lattice gas to a continuum fluid by approximating a continuum fluid by a lattice gas with infinitely small lattice spacing. In the Mean Spherical Approximation theory (MSA), the total correlation function and the direct correlation function of Ornstein and Zernike satisfy the following conditions:

$$h_{ij}(r) = -1 \quad \text{for } r \leq \sigma_{ij} \quad (4.1)$$

$$C_{ij}(r) = -\beta u_{ij}(r) \quad \text{for } r > \sigma_{ij} \quad (4.2)$$

$$\sigma_{ij} = \frac{1}{2}(\sigma_i + \sigma_j) \quad (4.3)$$

where: σ_i = Hard core diameter of molecule i
 σ_{ij} = Closest distance of approach
 u_{ij} = Pair potential

Equation (4.1) is an exact relation. Penetrating within the hard core of another molecule is impossible for a molecule. The relation for C_{ij} is only valid for $r \rightarrow \infty$, but in the MSA theory it is used as an approximation for all $r > \sigma_{ij}$. For hard spheres, MSA corresponds with the Percus-Yevick theory for hard sphere fluids. Together, equation (4.1) and (4.2) provide the information to solve the Ornstein-Zernike equation.

The MSA theory was proposed for a continuum fluid, but is mainly used as a model to account for the effects of the charge of electrolytes. Following the primitive model of electrolytes (MM-ensemble), the solvent molecules are replaced by a dielectric background. In equation (4.3) σ_i and σ_j now refer to the hard sphere diameter of the hydrated ions of type i and j , respectively. The pair potential u_{ij} , relative to that of the pure solvent, is given by the electrostatic interaction potential:

$$u_{ij}(r)^* = \frac{q_i q_j}{\epsilon r} = \frac{z_i z_j e^2}{\epsilon r} \quad (4.4)$$

here: q_i = Charge on i -th type ion
 z_i = Valency of ion of type i
 e = Charge of a proton
 ϵ = Dielectric constant of the solvent = $4\pi\epsilon_0\epsilon_r$

This system has been solved for a system of ions with equal diameters, the restricted primitive model, and for a system with ions of different size. These solutions will be dealt with in paragraph 4.2.

4.2 Solution of the primitive MSA

Waisman and Lebowitz [45,46,47] solved this for the restricted (primitive) model. In the restricted primitive model the cations and anions are charged hard spheres of equal size and charge. Waisman and Lebowitz found explicit analytical expressions for the thermodynamic properties, such as the internal energy and the Helmholtz free energy A :

$$\frac{U^{MSA}}{VkT} = \frac{x^2 + x - x(1+x)^{1/2}}{4\pi\sigma^3} \quad (4.5)$$

$$\frac{A^{MSA}}{VkT} = \frac{3x^2 + 6x - 2(1+2x)^{3/2} + 2}{12\pi\sigma^3} \quad (4.6)$$

$$x^2 = \kappa^2\sigma^2 = \frac{4\pi\sigma^2}{\epsilon kT} \sum_{j=+,-} \rho_j q_j^2 \quad (4.7)$$

where: κ = Debye-Hückel parameter
 σ = $\sigma_i = \sigma_j$

This solution has been shown to provide satisfactory results. However, assuming equal diameters is quite unrealistic. In the not restricted primitive model the cations and anions are treated as charged hard spheres of unequal diameters. This model has been solved by Blum and Hoye [6,7]. The only restriction they used, is the electroneutrality condition: $\sum \rho_j z_j = 0$. Their solution is an one parameter model, where the only parameter is Γ , the shielding parameter. Like κ in the Debye-Hückel-theory, this parameter is a characteristic length. The shielding parameter is given by the following set of equations:

$$\Gamma^2 \equiv \frac{\pi e^2}{\epsilon kT} \left[\sum_{j=1}^n \rho_j \left(\frac{z_j - \frac{\pi}{2\Delta} \sigma_j^2 P_n}{1 + \Gamma \sigma_j} \right)^2 \right] \quad (4.8)$$

$$P_n \equiv \frac{1}{\Omega} \sum_k \frac{\rho_k \sigma_k z_k}{1 + \Gamma \sigma_k} \quad (4.9)$$

$$\Omega \equiv 1 + \frac{\pi}{2\Delta} \sum_k \frac{\rho_k \sigma_k^3}{1 + \Gamma \sigma_k} \quad (4.10)$$

$$\Delta \equiv 1 - \frac{\pi \sum_k \rho_k \sigma_k^3}{6} \quad (4.11)$$

where P_n = Coupling parameter (electrostatic effects to geometric effects)
 Δ = Volume fraction of the solvent
 Ω = Unnamed parameter

The summations are over the number of ions. The shielding parameter or inverse shielding length Γ has to be determined by iteration. A good starting value would be $\kappa/2$. For $\sigma_+ = \sigma_-$ the solution of Blum is

consistent with the Waisman-Lebowitz solution. The internal energy and the Helmholtz free energy are given by:

$$\frac{U^{MSA}}{VkT} = \frac{e^2}{\epsilon kT} \left(\Gamma \sum_{i=1}^n \frac{\rho_i z_i^2}{1+\Gamma\sigma_i} + \frac{\pi}{2\Delta} \Omega P_n^2 \right) \quad (4.12)$$

$$\frac{A^{MSA}}{VkT} = \frac{U^{MSA}}{VkT} + \frac{\Gamma^3}{3\pi} \quad (4.13)$$

The MSA single-ion activity coefficient γ_i and the osmotic coefficient ϕ are obtained from the Helmholtz free energy by:

$$\phi^{MSA} = \rho \frac{\partial}{\partial \rho} \left(\frac{\beta A^{MSA}}{\rho} \right) \quad (4.14)$$

$$\ln \gamma_i^{MSA} = \beta \frac{\partial A^{MSA}}{\partial \rho_i} \quad (4.15)$$

resulting in:

$$\phi^{MSA} = -\frac{\Gamma^3}{3\pi\rho} - \frac{\pi e^2}{2\epsilon\rho kT} \frac{P_n^2}{\Delta^2} \quad (4.16)$$

$$\ln \gamma_i^{MSA} = -\frac{e^2}{\epsilon kT} \frac{\Gamma z_i^2}{1+\Gamma\sigma_i} - \frac{\pi e^2}{\epsilon kT} \frac{P_n}{2\Delta} \left(\frac{2z_i\sigma_i}{1+\Gamma\sigma_i} - \frac{\pi P_n \sigma_i^3}{2\Delta(1+\Gamma\sigma_i)} + \frac{\pi P_n \sigma_i^3}{6\Delta} \right) \quad (4.17)$$

The ion activity coefficient is built up from two contributions. The first contribution is a Debye-Hückel like term and accounts for the long range electrostatic interactions. The second term describes the short range electrostatic interactions and reflects the shielding ability according to their size.

If concentration dependent dielectric constants or ionic diameters are used, additional terms are required since a correct derivation would introduce the derivatives to the concentration in the relation for the activity coefficient [38]:

$$\ln \gamma_i^{MSA} = (4.17) + \sum_j \frac{\rho_j e^2}{\epsilon kT} \left(\frac{\Gamma^2 z_j^2}{(1+\Gamma\sigma_j)^2} + \frac{\pi^2 P_n^2 \sigma_j^2 (2-\Gamma^2 \sigma_j^2)}{4\Delta^2 (1+\Gamma\sigma_j)^2} - \frac{\pi z_j P_n}{\Delta(1+\Gamma\sigma_j)^2} \right) \frac{\partial \sigma_j}{\partial \rho_i} + \frac{U^{MSA}}{\epsilon kT} \frac{\partial \epsilon}{\partial \rho_i} \quad (4.18)$$

4.3 Hard sphere contribution

From the former equations, relations can be obtained for the osmotic coefficient and the (mean) ionic activity coefficient. MSA was first applied to aqueous electrolyte solutions without including nonelectrostatic terms in the calculation of the activity coefficients. This led to large errors in concentrated solutions. MSA could be applied to calculate mean and single-ion activity coefficients, but the agreement with experimental results was only satisfactory for dilute aqueous electrolyte solutions, even when concentration dependent ionic diameters were used. [14]

Using only the MSA contribution for the calculation of ionic activity coefficients corresponds to assuming that the contribution of the salt is restricted to the contribution arising from the charges of the ions. Therefore, including also the contribution from the uncharged reference system is necessary: the hard sphere contributions. Humffray [17] introduced the addition of a hard sphere contribution and found that it greatly improved the results on aqueous solutions of sodium chloride and calcium chloride.

$$\ln\gamma_i = \ln\gamma_i^{MSA} + \ln\gamma_i^{HS} \quad (4.19)$$

Usually, the hard sphere contribution is calculated with the Carnahan-Starling equation for mixtures of unequal sized hard spheres, as derived by Mansoori et al. [27]:

$$Z = \frac{(1+\xi+\xi^2)-3\xi(y_1+y_2\xi)-\xi^3}{(1-\xi)^3} \quad (4.20)$$

where Z is the compressibility factor and ξ , y_1 and y_2 are functions of the size and composition of the spheres. The Helmholtz free energy can be obtained from this equation. Subsequently, the activity coefficient can be derived from the Helmholtz energy. The equations are rather complex, but fortunately the expression for the activity coefficient has been derived and been simplified by Simonin et al. [38]:

$$\begin{aligned} \ln\gamma_i^{HS} &= -\ln(1-X_3) + \sigma_i \frac{3X_2}{1-X_3} + \sigma_i^2 F_2 + \sigma_i^3 F_3 \\ F_2 &= \frac{3X_1}{1-X_3} + \frac{3X_2^2}{X_3(1-X_3)^2} + \frac{3X_2^2}{X_3^2} \ln(1-X_3) \\ F_3 &= \frac{1}{1-X_3} \left(X_0 - \frac{X_2^3}{X_3^2} \right) + \frac{3X_1X_2 - X_2^3/X_3^2}{(1-X_3)^2} + \frac{2X_2^3}{X_3(1-X_3)^3} - \frac{2X_2^3}{X_3^3} \ln(1-X_3) \\ X_n &= \frac{\pi}{6} \sum_i \rho_i \sigma_i^n \end{aligned} \quad (4.21)$$

The equation gets even more complicated when concentration dependent ionic diameters are used:

$$\ln\gamma_i^{HS} = -\ln(1-X_3) + \sigma_i \frac{3X_2}{1-X_3} + \sigma_i^2 F_2 + \sigma_i^3 F_3 + \sum_j \rho_j \left(\frac{3X_2}{1-X_3} + 2\sigma_j F_2 + 3\sigma_j^2 \right) \frac{\partial \sigma_j}{\partial \rho_i} \quad (4.22)$$

4.4 Activity coefficients: MSA vs. Debye-Hückel

The MSA mean ionic activity coefficient can be obtained from equation (3.1) and (4.17). When this mean ionic activity coefficient is compared with the mean ionic activity coefficient from the Debye-Hückel theory (DH) and the Extended Debye-Hückel theory (EDH), a striking resemblance is found:

$$DH : \quad \ln\gamma_{\pm} = - \frac{|z_c z_a| e^2 \kappa}{2\epsilon kT} \quad (4.23)$$

$$EDH: \quad \ln\gamma_{\pm} = - \frac{|z_c z_a| e^2}{2\epsilon kT} \frac{\kappa}{1 + \kappa a} \quad (4.24)$$

$$MSA: \quad \ln\gamma_{\pm} = \ln\gamma_{\pm}^{HS} - \frac{e^2 \Gamma}{\epsilon kT} \sum_i \frac{(\rho_i/\rho) z_i^2}{1 + \Gamma \sigma_i} - \frac{(\alpha P_n \Omega)^2}{8\rho} \left[\frac{1}{\Omega \Delta} + \frac{1}{(\Omega \Delta)^2} \right] \quad (4.25)$$

Since the Debye-Hückel theory considers ions as point charges, the hard sphere term immediately drops out. For low concentrations the third term, the short term electrostatic interaction term may be ignored. Thus, for low concentrations only the long range electrostatic contribution is important. From the equations the MSA may clearly be seen as an extension of the Debye-Hückel theory: for low numerical concentrations and zero diameter the MSA shielding parameter approaches $\frac{1}{2}\kappa$. In this case the MSA activity coefficient is equal to the Debye-Hückel activity coefficient. The difference between the Debye-Hückel model and the MSA model also becomes clear from the assumptions made for their derivation from statistical mechanics:

$$MSA : \quad h_{ij}(r) = -1 \quad \text{for } r < \frac{1}{2}(\sigma_i + \sigma_j) \quad (4.1)$$

$$C_{ij}(r) = \frac{u_{ij}(r)}{kT} \quad \text{for } r > \frac{1}{2}(\sigma_i + \sigma_j) \quad (4.2)$$

$$DH : \quad C_{ij}(r) = \frac{u_{ij}(r)}{kT} \quad \text{for all } r \quad (4.26)$$

The Debye-Hückel model neglects the excluded volume effects: ions can approach each other to a zero distance. It may be concluded from this comparison that the MSA theory is a more physically correct extension of the Debye-Hückel theory, which in contrary to this Debye-Hückel theory takes into account ion size effects. This is particularly important in mixed solvents since "salting out" is closely associated with ion sizes.

4.5 EXP-modification

Some inadequacies have been found to occur with the MSA-theory. The ion-ion correlation function can become negative at high concentrations and the short range electrostatic contributions give the wrong sign, compared with other electrolyte theories. Therefore a modification of the MSA has been developed to overcome these problems, the EXP-modification (abbreviated by EXP-MSA) of Anderson and Chandler [10]. They proposed that the pair correlation function can be approximated by:

$$g_{ij}^{EXP}(r) = g_{ij}^{HS}(r) \exp(\zeta_{ij}(r)) \quad (4.27)$$

Here, ζ is the chain sum, which for Coulomb forces (ions) is given as the screened Coulomb potential:

$$\zeta_{ij}(r) = - \frac{z_i z_j e^2}{\epsilon kT} \frac{\exp(-\kappa r)}{r} \quad (4.28)$$

The EXP-MSA theory has been worked out by Gering et al. [15]. They used the theory to predict osmotic coefficients. In the MSA theory, the osmotic coefficient can be calculated from equation (4.14). This is the approach using the energy route. Another way to derive the osmotic coefficient is using the virial equation, where the molar osmotic coefficient can be calculated from:

$$\Phi_c - 1 = \frac{2\pi e^2}{3\rho\epsilon kT} \sum_i \sum_j \rho_i \rho_j z_i z_j \int_{\sigma_{ij}}^{\infty} r g_{ij}(r) dr + \frac{2\pi}{3\rho} \sum_i \sum_j \rho_i \rho_j d_{ij}^3 g_{ij}(\sigma_{ij}) \quad (4.29)$$

where the first term accounts for the long range forces and the second term for the short range contributions. The long range forces are electrostatic forces. The short range contribution has two sources: the neutral hard sphere repulsion and the short range electrostatic interactions. In the MSA-EXP theory the pair correlation function in the last term is approximated by equation (4.27). In the work of Gering et al. the first term is replaced by a correlation, which gives absolute deviations of less than one percent compared with the exact solution. This correlation is given by:

$$\Phi_{LR-EXP} = -\frac{1}{3\pi\rho} \left(\Gamma_{MSA} - 4\rho \ln\rho - 25\rho + 300\rho^2 \right)^3 \quad (4.30)$$

The activity coefficient of the solvent can be computed from the molal osmotic coefficient (this requires numerical integration). The molal activity coefficient is obtained by converting the molar osmotic coefficient to the molal osmotic coefficient.

The EXP-MSA theory as used by Gering et al. was successfully used to predict osmotic coefficients and activity coefficients for various (multisolute) 1:1 electrolyte systems. Sun et al. [42] compared the EXP-MSA with a simplified MSA (which gave comparable results to the original MSA) for 120 electrolyte systems. They found the EXP-MSA to give better fits for 60 electrolytes, but worse for 30 electrolytes, which typically contained complex anions as SO_4^{2-} or multichlorides. Sun et al. concluded it to be likely that the short range term is not always positive in sign.

4.6 Nonprimitive MSA

The primitive model of the Mean Spherical Approximation has been extended to a nonprimitive model by Planche and Renon [5,33] and by Blum and Wei [8] resulting in two different models. They solved the MSA for a model where the solvent molecules are considered as hard spheres of different sizes and are not replaced by a dielectric background. In the nonprimitive model of Planche and Renon [5] molecule-molecule and ion-molecule attractive forces, ion-ion Coulombic interaction and hard sphere repulsion among all particles are assumed. The solution is based on the following expression for the interaction between two species i and j (where i and j may refer to both ionic and nonionic species):

$$\frac{u_{ij}(r)}{kT} = \frac{4\pi e^2 z_i z_j}{\epsilon kT r} + \frac{W_{ij}}{2\pi r N_A} \delta'(r - \sigma_{ij}) \quad (4.31)$$

$$u_{ij}(r) = \infty \text{ for } r < \sigma_{ij} \quad (4.32)$$

where δ' stands for the derivative of the Dirac function and W_{ij} is a temperature dependent parameter. Using this pair interaction potential and the Mean Spherical Approximation (equation (4.1) and (4.2)),

the Ornstein-Zernike equation is solved. The solution requires an exact definition of the dielectric constant and W_{ij} . For W_{ij} an empirical relation is used, introducing two new adjustable parameters per ion. The dielectric constant is considered both temperature and concentration dependent and is calculated with one adjustable parameter per ion. The parameters cannot be assigned any definite physical meaning. The nonprimitive MSA of Planche and Renon [33] has been used successfully for the representation of vapour liquid equilibria and liquid phase compositions of the system $\text{H}_2\text{O} + \text{HNO}_3 + \text{N}_2\text{O}_5$ by Passarello [31]. If the interaction parameter is zero, the model reduces to the primitive MSA of Blum [6]

In the nonprimitive Mean Spherical Approximation model of Blum and Wei [8] the electrolyte solution is modelled as an ion-dipole mixture. The system consists of a mixture of $(n-1)$ charged hard spheres and a solvent of hard spheres with a dipole moment. The pair potentials for $r > \sigma_{ij}$ are expressed as:

$$u_{ij} = \frac{z_i z_j e^2}{r} \quad (4.33)$$

$$u_{in} = \frac{z_i e \mu \Phi^{011}}{r^2} \quad (4.34)$$

$$u_{nn} = -\frac{\mu^2 \Phi^{112}}{r^3} \quad (4.35)$$

where n refers to the solvent and the angular function Φ^{mnl} accounts for the orientation of the dipole moment μ . The solution of this system produces three characteristic parameters, among which Γ that was also found in the primitive MSA. The nonprimitive MSA of Blum and Wei [8] reduces to the primitive MSA of Blum [6] for small solvent diameters and infinite dilution. Adjustable parameters are the hard sphere diameters of all components, the solvent density and the dipole moment μ of the solvent. The model does not contain the dielectric constant. Extension and application of the nonprimitive MSA of Blum and Wei [8] to mixed solvent is not known to have been published yet. It has been used to calculate the mean ionic activity coefficients of several water-salt systems and saturated vapour pressures of water with fair accuracy by Li et al. [23]

Since the nonprimitive model deals with the solvent explicitly, the model may be considered more physically correct. However, the nonprimitive MSA will not be applied in this work, because of the complexity of the solution of this models and because the model is not yet applicable to mixed solvent systems (model of Blum and Wei [8]) or because it uses many adjustable parameters (model of Planche and Renon [33]). Besides this, some parameters can only be found from vapour-liquid equilibrium data of the pure components.

4.7 Reported applications of the MSA theory

Many published uses of the Mean Spherical Approximation are concerned with predicting of osmotic coefficients. In this paragraph a short summary is given of some published applications of the MSA theory. (In the publications discussed the hard sphere contribution is included in the MSA.)

- Triolo et al. [43] used the solution of the MSA by Blum to fit experimental osmotic coefficients of a collection of monovalent salts at concentrations of 0 to 2 M. They used the Newton-Raphson method to solve the shielding parameter. No correction was used for the conversion of Lewis-Randall

to McMillan-Mayer ensemble. Triolo et al. fitted the predictions to experimental data by adjusting the hard core diameter of one ion. The Percus-Yevick approximation was used for the reference osmotic coefficient. It was found that the MSA theory gives “surprisingly” good agreement with experiments.

- Later, this work was improved by using a hard core diameter as a function of density (but not of temperature) and by making the dielectric constant density (concentration) dependent. Triolo et al. did not attempt to use both diameters and dielectric constant density dependent, since they expected convergence problems, both parameters not being totally independent. The differences between theory and experiments appeared to be within the uncertainties of the experimental values [44].
- Corti [14] showed that the unrestricted primitive MSA gives activity coefficients in mixed electrolytes (NaCl-CaCl₂) that are in close agreement with experimental data. Corti used best fits for the ionic diameters, without concentration dependency.
- Simonin et al. [38,39] used the MSA for several pure ionic solutions of nonassociating salts (alkalihalides and acids). Here, the variation of the dielectric constant and the cation diameter with concentration is taken into account explicitly for the calculation of the activity coefficient, using simple expressions:

$$\sigma = \sigma^{(0)} + \alpha^{(1)}C \quad (4.36)$$

$$\varepsilon = \frac{\varepsilon_0}{1 + \alpha C} \quad (4.37)$$

where

C	= Concentration
α	= Adjustable parameter
ε_0	= Pure solvent dielectric constant
$\sigma^{(i)}$	= Adjustable parameter

Good fittings for activity coefficients and osmotic coefficients were obtained in the concentration range 0 up to 15 mol/kg for strong electrolytes. In addition to this, the model was applied to mixtures of two and three salts, resulting in rather good agreement with experimental results.

- Lloyd Lee [22] combined the MSA theory with a UNIFAC model to form a so-called ElecGC model (Group Contribution method with ELEctrostatic contribution). This model was applied successfully to a multisalt multisolvent mixture (>20 components) for the calculation of vapour-liquid equilibria. Lee uses the MSA activity coefficient plus a Born contribution for the ionic activity coefficients. The ionic activity coefficients have no molecular UNIFAC contribution. The neutral components were modelled using a molecular UNIFAC model, combined with an MSA contribution to account for the electrostatic influence on the molecular components. This electrostatic contribution is related to the osmotic coefficient and was obtained from integration of the Gibbs-Duhem equation from a hypothetical neutral solution to the real situation (see appendix V). The resulting equation for the molecular species j is:

$$\ln \gamma_j = \ln \gamma_j^{UNIFAC} + \frac{1}{\sum_j \rho_j} \left[\frac{\Gamma^3}{3\pi} + \frac{\pi e^2}{2\varepsilon kT} \left(\frac{P_n}{\Delta} \right)^2 - \frac{\Pi^{HS}}{RT} \right] \quad (4.38)$$

- Wu and Lee [49] used a comparable method in 1992 for the calculation of vapour-liquid equilibria of mixed solvent electrolyte systems. Here they used the MSA mean ionic activity coefficient for LiCl in a mixture of methanol and water. They used the Gibbs-Duhem relation for the calculation of the activity coefficients of the molecular species by numerical integration from a low salt concentration to the desired concentration. Therefore, a hypothetical chain of osmotic cells was constructed with increasing salt concentrations. The activity coefficients of the salt free solution were calculated from a UNIQUAC model. The pseudo solvent approach of Gering and Lee [15] was used. (The physical properties of the solvents are averaged to those of one pseudo-solvent.) The ionic diameters in this pseudo solvent were averaged from diameters fitted to data of LiCl in the individual solvents. The conversion from the McMillan-Mayer to the Lewis-Randall ensemble was ignored.
- So far there are no publications on applying the MSA to liquid-liquid equilibria.

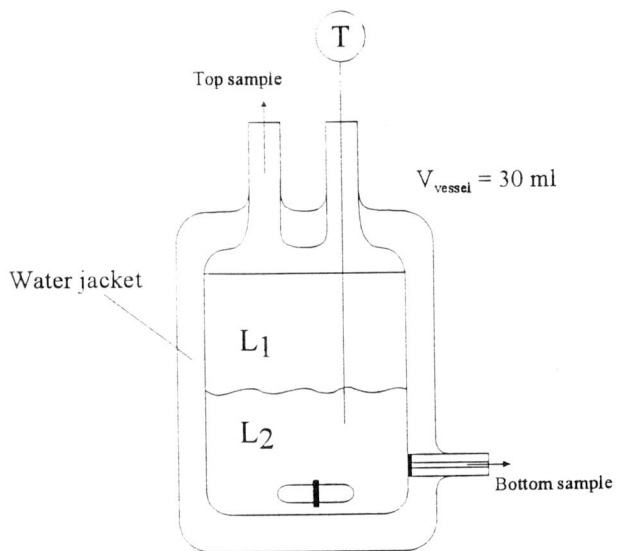


Figure 5.1: Equilibrium vessel for the measurement of liquid-liquid equilibria.

benzene?

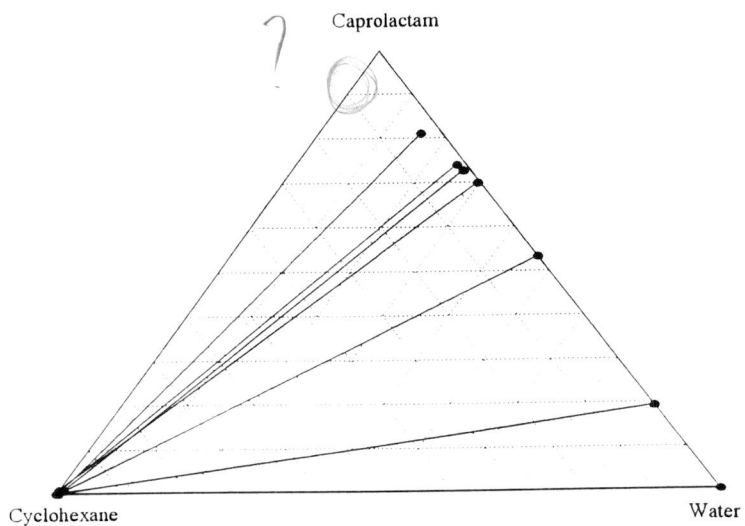


Figure 5.2: Liquid-liquid equilibrium of the system caprolactam + water + cyclohexane at 20°C. Solid lines represent experimental tie-lines. Data are plotted as mass fractions.

5. Experimental work

5.1 Introduction

Modelling of liquid-liquid equilibria requires experimental data. A considerable amount of liquid-liquid equilibrium data was already obtained by former work in the laboratory of Applied Thermodynamics and Phase Equilibria by Kristina Haase [16]. However, more data were needed. Therefore, a part of this work consisted of measuring experimental liquid-liquid equilibria of caprolactam + water + solvent + ammonium sulfate. The following ternary and quaternary systems were measured:

- | | |
|---|--------------------|
| - caprolactam + water + cyclohexane | at 20°C |
| - caprolactam + water + 1-heptanol | at 20, 40 and 60°C |
| - water + caprolactam + 1-heptanol + ammonium sulfate | at 40 and 60°C |

benzene

The solvents were chosen based on the need for group interaction parameters for UNIFAC. (The UNIFAC method will be used in the future to predict the solution behaviour.) For instance, 1-heptanol was chosen in order to obtain group interaction parameters for a primary alcohol with caprolactam. The fact that the extraction process of caprolactam is carried out within the temperature range of 20° to 60°C, has been the reason for measuring the systems at 20°, 40° and 60°C.

5.2 Description of experiments

The equilibria were measured using the following procedure:

1. A solution is made in such a way that two phases of almost the same volume were expected after settling.
2. The solution is stirred for about six hours in a small vessel (see figure 5.1), while the temperature is kept at a fixed temperature using a thermostatted water jacket. The temperature of the jacket could be controlled within 0.05°C.
3. Subsequently the solution is allowed to settle for about 14 hours, while the temperature is still kept constant at a certain temperature (20°, 40° or 60°C)
4. Samples are taken from both phases through the sample points using a syringe.
5. The samples are analyzed on caprolactam and organic solvents content by gas chromatography, on water content by Karl-Fischer titration and on ammonium sulfate content by titration with barium perchlorate. A short description of the analyses is given in appendix I.

Considering the quaternary systems, it was tried to work with almost equal concentrations of ammonium sulfate in the aqueous phase of 5, 15 and 30% w/w. This was done by making a solution of ammonium sulfate in water of the desired concentration, marking the liquid level, adding the caprolactam and 1-heptanol and after settling, adding water until the top of the bottom phase reaches the marked level. The experiments were carried out in a random order.

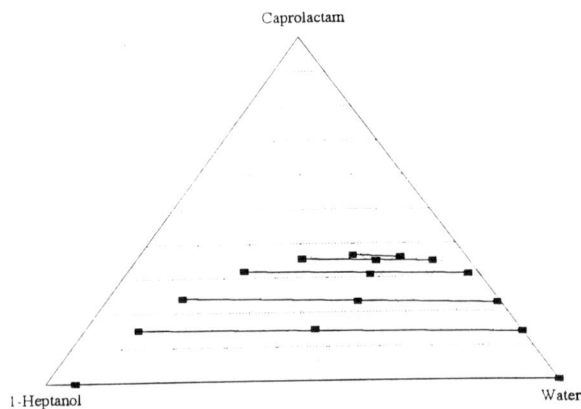


Figure 5.3: Liquid-liquid equilibrium of the system caprolactam + water + 1-heptanol at 20°C. Markers represent phase compositions and overall compositions. Solid lines represent experimental tie-lines

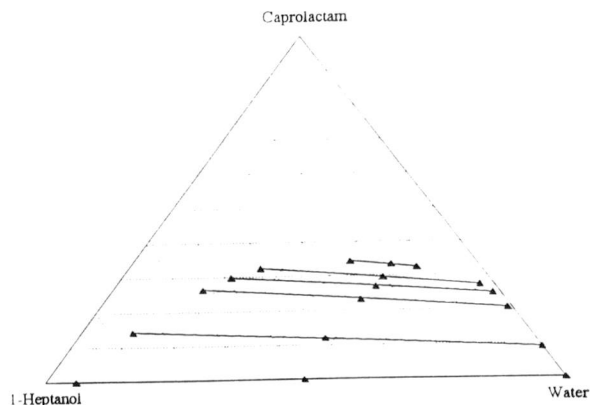


Figure 5.4: Liquid-liquid equilibrium of the system caprolactam + water + 1-heptanol at 40°C. Markers represent phase compositions and overall compositions. Solid lines represent experimental tie-lines

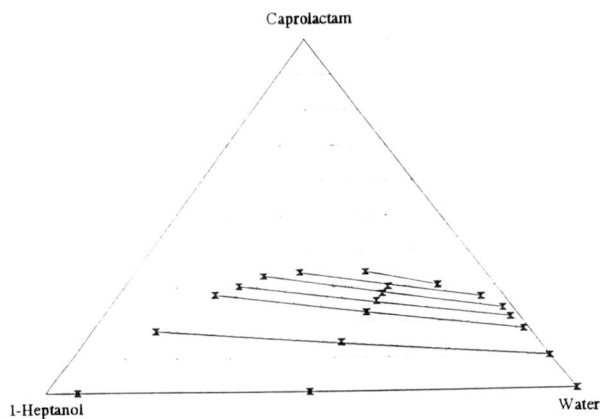


Figure 5.5: Liquid-liquid equilibrium of the system caprolactam + water + 1-heptanol at 60°C. Markers represent phase compositions and overall compositions. Solid lines represent experimental tie-lines

Table 5.1: Chemicals used in the experiments

Component	Source	Stated purity
Caprolactam	DSM	99.5 %
Cyclohexane	J.T.Baker	99.0 %
1-Heptanol	Merck	99.0 %
Ammonium sulfate	Merck	99.5 %

5.3 Results

5.3.1 Caprolactam + water + cyclohexane

Although it was intended to measure this system at several temperatures and salt concentrations, this was cancelled after the results of the ternary system at 20°C. As can be learnt from figure 5.2, hardly any caprolactam dissolves in the cyclohexane phases, which makes cyclohexane unsuitable to be used as a solvent in the extraction process of caprolactam. Besides this, it was found that a higher overall composition in the upper area of the Gibbs triangle resulted in the formation of solid caprolactam: the immiscibility area is crossing the solubility line and there is no critical point.

The results of the experiments are tabulated in table 5.2. The water content has not been measured for these equilibria. It was determined from the other fractions as $x_{\text{water}} = 1 - x_{\text{caprolactam}} - x_{\text{cyclohexane}}$.

Table 5.2: Liquid-liquid equilibria of the system cyclohexane + water + caprolactam at 20°C

Organic phase (w/w)		Aqueous phase (w/w)	
Caprolactam	Cyclohexane	Caprolactam	Cyclohexane
0.000	1.000	0.000	0.000
0.000	1.000	0.192	0.000
0.000	0.996	0.532	0.000
0.008	0.985	0.727	0.012
0.008	0.992	0.740	0.015
0.008	0.987	0.811	0.033

5.3.2 Caprolactam + water + 1-heptanol

This ternary system is needed for adequate modelling of the quaternary system caprolactam + water + 1-heptanol + ammonium sulfate. (The system caprolactam + water + ammonium sulfate had already been measured by Haase [16].) The system was measured at a temperature of 20°, 40° and 60°C. At higher caprolactam concentrations it was noticed that the organic phase became rather viscous, which may have some influence on the demixing behaviour. The results, normalized according to equation (5.1) are given in table 5.3 to 5.5. Full data including the uncorrected values and their sums are given in appendix III. The sum of all measured fractions varies from 0.982 to 1.019 w/w. The ternary diagrams of the systems are shown in figure 5.3 to 5.5. Figure 5.6 shows the influence of temperature on the distribution of caprolactam between the two phases.

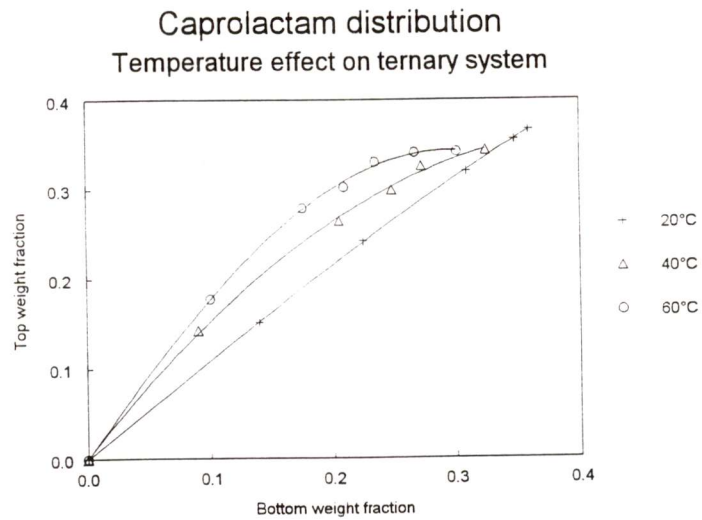


Figure 5.6: Distribution of caprolactam between aqueous (bottom) phase and organic (top) phase of the system caprolactam + water + 1-heptanol at 20, 40 and 60°C.

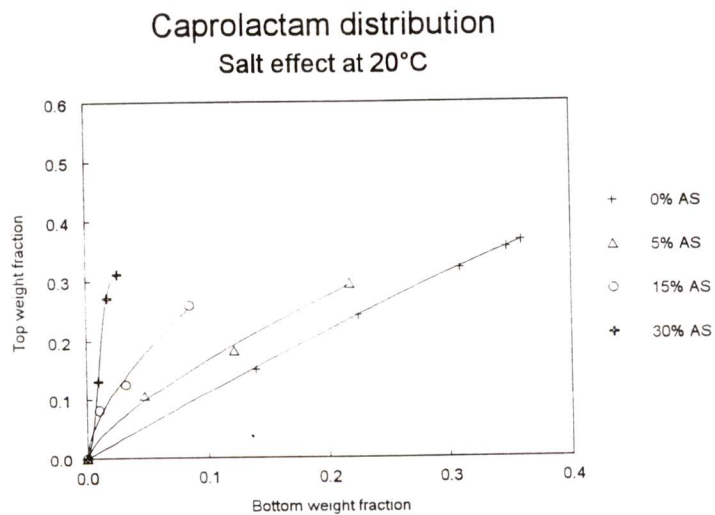


Figure 5.7: Distribution of caprolactam between aqueous (bottom) phase and organic (top) phase of the system caprolactam + water + 1-heptanol + ammonium sulfate at 20°C. Data measured by Kristina Haase. The salt concentrations in the aqueous phase were kept constant at approximately 0% w/w (+), 5% w/w (Δ), 15% w/w (○) and 30% w/w (⊕).

$$x_i^{normalized} = \frac{x_i}{\sum_{i=1}^3 x_i} \quad (5.1)$$

Table 5.3: Liquid-liquid equilibria of the system caprolactam + water + 1-heptanol at 20°C. Data are mass fractions, normalized according to equation (5.1)

Organic phase (w/w)			Aqueous phase (w/w)		
Caprolactam	Water	1-Heptanol	Caprolactam	Water	1-Heptanol
0.000	0.058	0.942	0.000	1.000	0.000
0.152	0.106	0.743	0.140	0.860	0.000
0.242	0.147	0.611	0.225	0.768	0.007
0.320	0.228	0.452	0.309	0.670	0.021
0.355	0.324	0.321	0.348	0.582	0.071
0.366	0.417	0.217	0.360	0.512	0.128

Table 5.4: Liquid-liquid equilibria of the system caprolactam + water + 1-heptanol at 40°C. Data are normalized mass fractions.

Organic phase (w/w)			Aqueous phase (w/w)		
Caprolactam	Water	1-Heptanol	Caprolactam	Water	1-Heptanol
0.000	0.061	0.939	0.000	1.000	0.000
0.143	0.100	0.757	0.090	0.910	0.000
0.265	0.175	0.561	0.205	0.786	0.008
0.299	0.212	0.488	0.249	0.736	0.015
0.326	0.256	0.418	0.273	0.699	0.028
0.344	0.417	0.239	0.325	0.554	0.121

Table 5.5: Liquid-liquid equilibria of the system caprolactam + water + 1-heptanol at 60°C. Data are normalized mass fractions.

Organic phase (w/w)			Aqueous phase (w/w)		
Caprolactam	Water	1-Heptanol	Caprolactam	Water	1-Heptanol
0.000	0.061	0.939	0.000	1.000	0.000
0.178	0.121	0.702	0.100	0.900	0.000
0.279	0.184	0.538	0.176	0.815	0.010
0.302	0.217	0.480	0.209	0.774	0.017
0.331	0.250	0.419	0.235	0.747	0.018
0.341	0.313	0.346	0.268	0.690	0.043
0.342	0.437	0.221	0.302	0.593	0.106

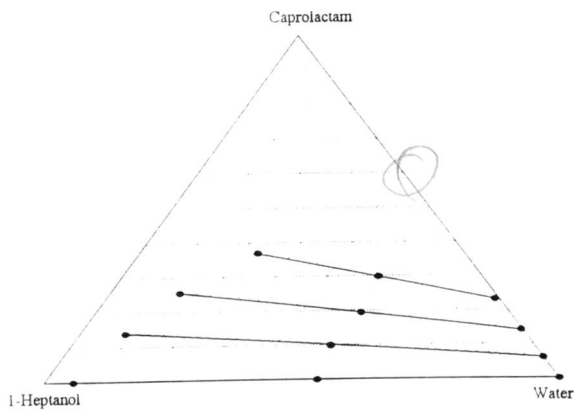


Figure 5.8: Liquid-liquid equilibrium of the system water + caprolactam + 1-heptanol + ammonium sulfate at 40°C. Data are plotted as mass fractions on a salt free basis. Solid lines represent experimental tielines, markers represent phase compositions and overall compositions. The ammonium sulfate content in the aqueous phase was approximately 5% w/w.

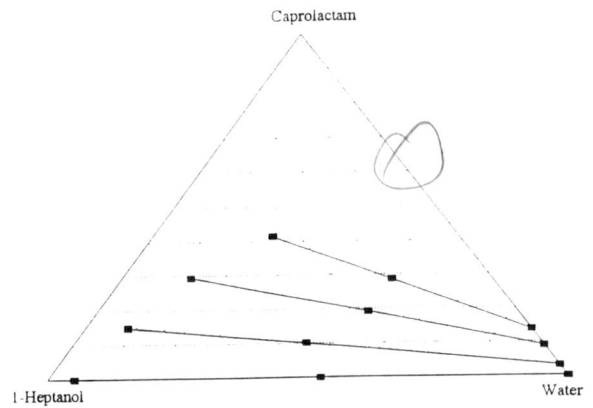


Figure 5.9: Liquid-liquid equilibrium of the system water + caprolactam + 1-heptanol + ammonium sulfate at 40°C. Data are plotted as mass fractions on a salt free basis. Solid lines represent experimental tielines, markers represent phase compositions and overall compositions. The ammonium sulfate content in the aqueous phase was approximately 15% w/w.

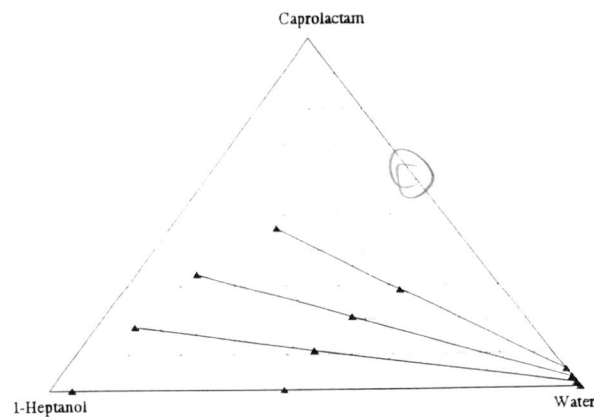


Figure 5.10: Liquid-liquid equilibrium of the system water + caprolactam + 1-heptanol + ammonium sulfate at 40°C. Data are plotted as mass fractions on a salt free basis. Solid lines represent experimental tielines, markers represent phase compositions and overall compositions. The ammonium sulfate content in the aqueous phase was approximately 30% w/w.

*Londer
heptanol?*

5.3.3 Caprolactam + water + 1-heptanol + ammonium sulfate

Experiments of the system caprolactam + water + 1-heptanol + ammonium sulfate at 20°C were carried out by Kristina Haase (see figure 5.7 and appendix III). So what remained was measuring liquid-liquid equilibria of these systems at 40° and 60°C. As indicated, it was tried to measure the systems at three different but fixed salt concentrations of the aqueous phase, namely 5, 15 and 30 wt % ammonium sulfate. The results are shown in the figures 5.8 up to 5.15 and table 5.6 and 5.7.

Table 5.6: Liquid-liquid equilibria of the system caprolactam + water + 1-heptanol + ammonium sulfate (AS) at 40°C. Data are normalized mass fractions.

Organic phase (w/w)				
	Caprolactam	Water	1-Heptanol	AS
1	0.000	0.056	0.944	0.000
2	0.139	0.088	0.772	0.000
3	0.256	0.135	0.609	0.000
4	0.369	0.231	0.399	0.002
5	0.000	0.052	0.948	0.000
6	0.149	0.083	0.767	0.000
7	0.294	0.134	0.572	0.000
8	0.413	0.233	0.352	0.003
9	0.000	0.044	0.956	0.000
10	0.181	0.073	0.746	0.000
11	0.335	0.115	0.550	0.000
12	0.463	0.201	0.334	0.002

Aqueous phase (w/w)				
	Caprolactam	Water	1-Heptanol	AS
1	0.000	0.950	0.000	0.050
2	0.058	0.895	0.000	0.047
3	0.134	0.814	0.003	0.049
4	0.220	0.722	0.009	0.050
5	0.000	0.857	0.000	0.143
6	0.026	0.813	0.000	0.161
7	0.077	0.785	0.000	0.139
8	0.117	0.740	0.000	0.143
9	0.000	0.689	0.000	0.311
10	0.009	0.687	0.000	0.304
11	0.020	0.703	0.000	0.277
12	0.038	0.708	0.000	0.255

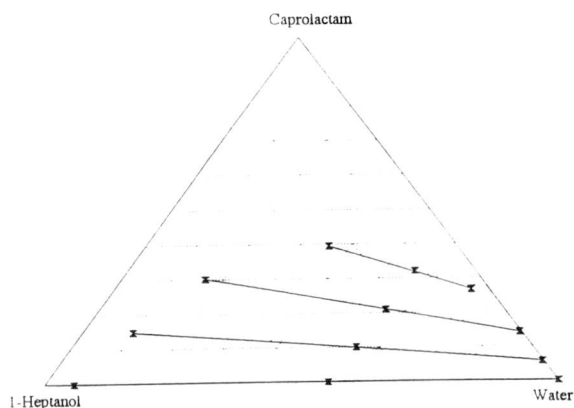


Figure 5.11: Liquid-liquid equilibrium of the system water + caprolactam + 1-heptanol + ammonium sulfate at 60°C. Data are plotted as mass fractions on a salt free basis. Solid lines represent experimental tielines, markers represent phase compositions and overall compositions. The ammonium sulfate content in the aqueous phase was approximately 5% w/w.

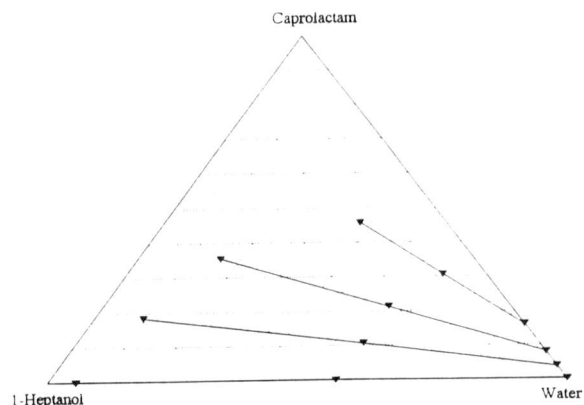


Figure 5.12: Liquid-liquid equilibrium of the system water + caprolactam + 1-heptanol + ammonium sulfate at 60°C. Data are plotted as mass fractions on a salt free basis. Solid lines represent experimental tielines, markers represent phase compositions and overall compositions. The ammonium sulfate content in the aqueous phase was approximately 15% w/w.

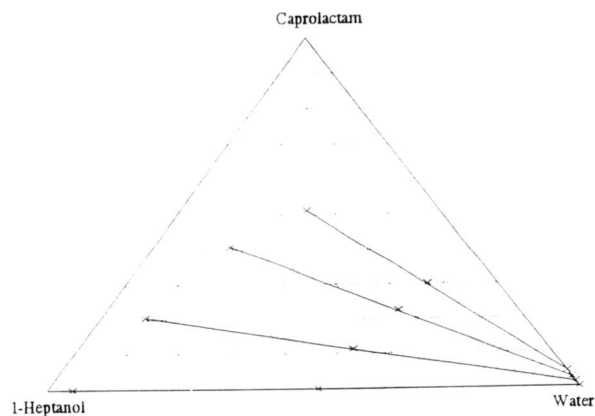


Figure 5.13: Liquid-liquid equilibrium of the system water + caprolactam + 1-heptanol + ammonium sulfate at 60°C. Data are plotted as mass fractions on a salt free basis. Solid lines represent experimental tielines, markers represent phase compositions and overall compositions. The ammonium sulfate content in the aqueous phase was approximately 30% w/w.

Table 5.7: Liquid-liquid equilibria of the system caprolactam + water + 1-heptanol + ammonium sulfate (AS) at 60°C. Data are normalized mass fractions.

Organic phase (w/w)				
	Caprolactam	Water	1-Heptanol	AS
1	0.000	0.057	0.943	0.000
2	0.149	0.098	0.753	0.000
3	0.302	0.164	0.534	0.000
4	0.392	0.354	0.247	0.008
5	0.000	0.056	0.945	0.000
6	0.185	0.095	0.720	0.000
7	0.354	0.161	0.484	0.001
8	0.450	0.373	0.164	0.013
9	0.000	0.047	0.953	0.000
10	0.206	0.084	0.709	0.000
11	0.410	0.146	0.444	0.001
12	0.512	0.240	0.245	0.004

Aqueous phase (w/w)				
	Caprolactam	Water	1-Heptanol	AS
1	0.000	0.954	0.000	0.046
2	0.054	0.899	0.002	0.045
3	0.134	0.808	0.004	0.055
4	0.254	0.664	0.034	0.048
5	0.000	0.854	0.000	0.146
6	0.031	0.820	0.000	0.148
7	0.066	0.772	0.000	0.162
8	0.137	0.713	0.000	0.150
9	0.000	0.709	0.000	0.291
10	0.010	0.695	0.000	0.296
11	0.019	0.679	0.000	0.303
12	0.032	0.684	0.000	0.284

5.4 Error analysis

A small error analysis has been carried out to estimate the errors of the analytical procedures. A more detailed description can be found in appendix II. The results of this analysis are: for the GC analyses an average absolute statistical error of 0.004 w/w for both caprolactam and 1-heptanol. For the water determinations a relative statistical error of 2.3% and 1.1% and absolute statistical errors of 0.004 and 0.009 w/w for the lower and the higher concentration ranges, respectively, was found. The ammonium sulfate determination introduces the largest errors: absolute statistical errors from 0.002 up to 0.014 w/w were calculated with an average value of 0.008 w/w and an average relative error of 4.5% w/w. (All statistical errors are based on a probability of 95%.) Normalization of the component mass fractions reduces the errors with about 25%

Caprolactam distribution Salt effect at 40°C

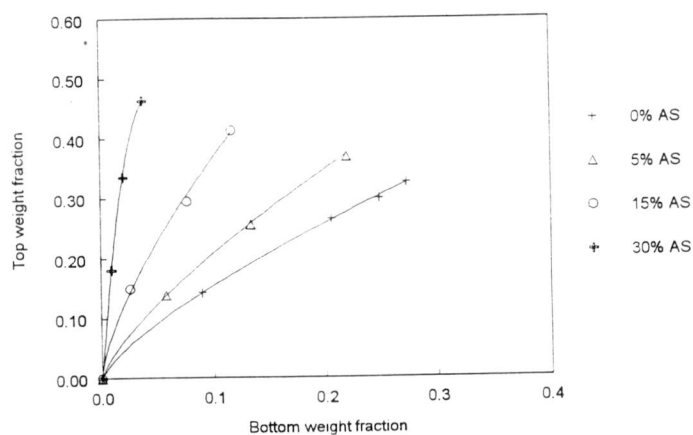


Figure 5.14: Distribution of caprolactam between aqueous (bottom) phase and organic (top) phase of the system caprolactam + water + 1-heptanol + ammonium sulfate at 20°C. The salt concentrations in the aqueous phase were kept constant at approximately 0% w/w (+), 5% w/w (Δ), 15% w/w (○) and 30% w/w (⊕)

Caprolactam distribution Salt effect at 60°C

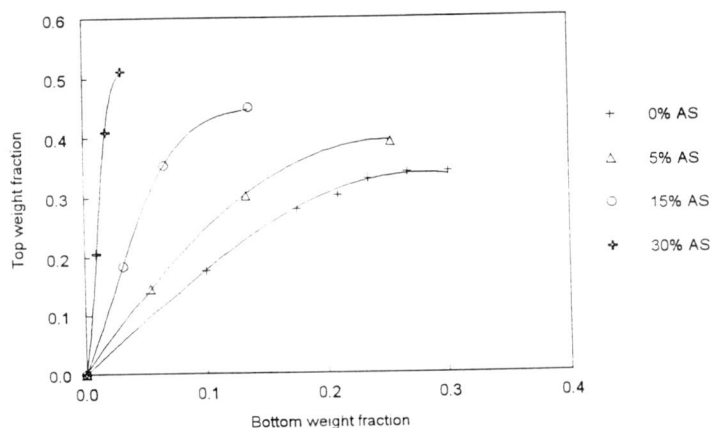


Figure 5.15: Distribution of caprolactam between aqueous (bottom) phase and organic (top) phase of the system caprolactam + water + 1-heptanol + ammonium sulfate at 60°C. The salt concentrations in the aqueous phase were kept constant at approximately 0% w/w (+), 5% w/w (Δ), 15% w/w (○) and 30% w/w (⊕)

Additional information on the errors can be found from the summation of the experimental results. It can be seen from the tables in appendix III that the deviation of the sum of the measured mole fraction from 100% only occasionally exceeds 1%. Based on the errors given above, a more frequent deviation might be expected. Perhaps the error analysis gives a pessimistic picture of the experimental errors, although it must be realized that errors may cancel out each other. However, the data in appendix III suggest the experiments are rather accurate within the feasible analysis methods. Also, the insertion of the overall compositions in the diagrams shows all the tie lines go through their overall compositions.

5.5 Conclusions

It was found in the experiments that cyclohexane is not a good solvent for the extraction of caprolactam. Hardly any caprolactam dissolves in the organic phase. In addition to this, at higher caprolactam concentrations there is a rather large chance of getting a third (solid) phase in the equilibrium vessel. It may be expected that presence of salt in the system will lead to the formation of a solid phase or phases over a wide range of concentrations.

A much better solvent seems 1-heptanol. Caprolactam dissolves very well in this solvent, above 20°C even better than in water. The solubility of caprolactam in the organic phases increases to a greater extent than the solubility of caprolactam in the aqueous phase. The presence of ammonium sulfate in the system has a positive influence on the (forward) extraction of caprolactam: almost all caprolactam dissolves in the organic phase. The caprolactam in the aqueous phase is salted out: nearly all caprolactam is transferred to the organic phase. This is especially made clear in the distribution curves in figure 5.6 and figure 5.7, 5.14 and 5.15. This illustrates the large effect the long range electrostatic forces have on the demixing behaviour.

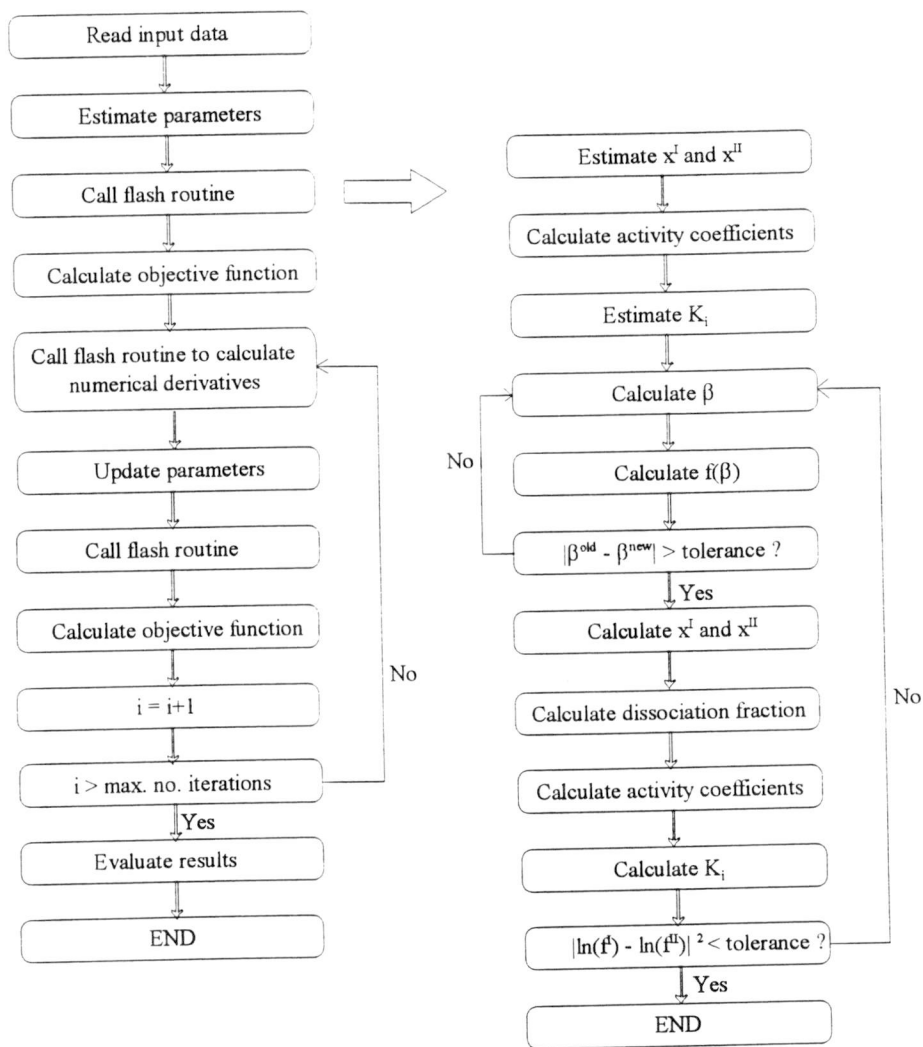


Figure 6.1: Structure of the program used to correlate experimental liquid-liquid equilibrium data of (electrolyte) solutions. Left side of the figure shows the structure of the flash routine.

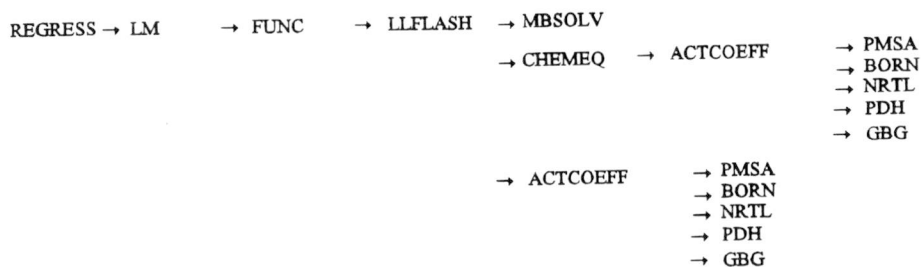


Figure 6.2: Structure of the regression part of the program used to correlate experimental liquid-liquid equilibrium data of (electrolyte) solutions. The figure contains the names of the subroutines in the FORTRAN source code. The subroutines are called from left to right and from top to bottom.

6. Modelling

6.1 Introduction

This chapter deals with the structure and the assumptions made in the modelling work. A model was programmed in Fortran that can perform liquid-liquid flash calculations using a combination of the Mean Spherical Approximation theory by Blum [6] and the NRTL activity coefficient model of Chen et al. [13]. The required parameters had to be obtained by fitting to experimental data, either from literature or from own experiments. The programming was started with a study after the performance of the MSA for the prediction of ionic activity coefficients. Consequently, the program was extended to the calculation of liquid-liquid equilibria and the regression of parameters. The electrolyte NRTL source code was obtained from Mark Wijtkamp. The regression routine is based on a Levenberg-Marquardt routine obtained from DSM Research.

Results of calculations will be given in the next chapter. In this chapter subsequently a description will be given of the activity coefficient subroutine, the flash routine, the regression routine and the chemical equilibrium routine. The structure of the whole program is shown in figure 6.1 and 6.2

6.2 Activity coefficient subroutine

The programmed activity coefficient subroutine can calculate activity coefficients of electrolyte systems using several models:

- Molecular NRTL [33]
- Electrolyte NRTL of Chen [12,13,4]
- Modified electrolyte NRTL of Liu [25]
- Models that are a combination of the NRTL model and the MSA theory (developed during this master's thesis). They will be specified more in the next chapter.

The subroutine for the activity coefficient itself consists of several subroutines, that account for different contributions. These contributions will be discussed in the following subsections:

6.2.1 Solution properties

All the electrolyte models require (physical) solution properties:

- *Solution density*: The density of the solvents is calculated from the correlations found in Perry's Chemical Engineer's Handbook [32, Table 2.30]. In the program, it was made possible to model the influence of the salt on the solution density by making the water density dependent on the salt concentration like Gering et al. [15] do. This can be achieved by the addition of a salt contribution, consisting of a salt parameter multiplied by the salt concentration. This salt parameter can be obtained from a linear fit of experimental densities [24] relative to the salt free solution versus the salt mass fraction (see figure 6.3). The mixing rule applied to get the solution density is based on the specific volume of the solvents. In equation (6.1) the density of water is the density of aqueous salt solution.

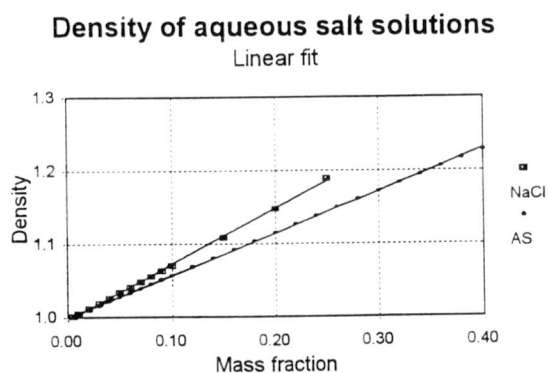


Figure 6.3: The salt effect on the density of an aqueous solution shows a linear relation with the mass fraction.

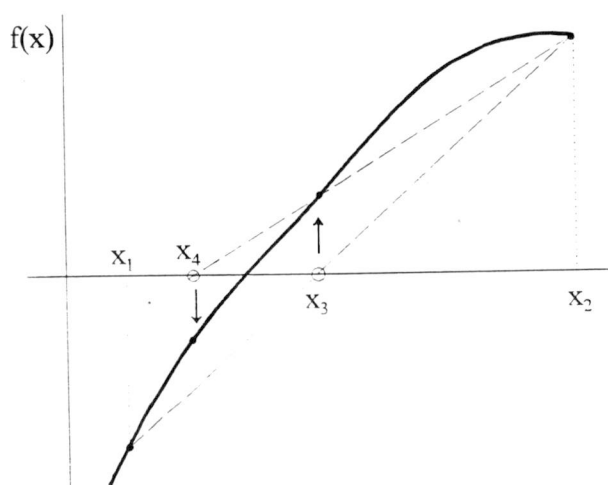


Figure 6.4: Secant method: New estimations are found by extrapolation or interpolation lines from the two most recently evaluated points. The points are numbered in the order they are used.

$$d_{mix} = \frac{\sum_i^{ns} w_i}{\sum_i^{ns} \frac{w_i}{d_i}} \quad (6.1)$$

where ns = Number of solvents
 w = Mass fraction

An important remark should be made here. The application of a mixing rule for a solution property that uses solvent mole fractions makes the ionic activity coefficient dependent on these solvent mole fractions. Although this has never been applied in literature until now, a correct derivation of the activity coefficient would then result in an electrostatic contribution to the solvent activities, which contains the derivatives with respect to the solvent mole fraction of the property to which the mixing rule is applied to. In the case of the electrolyte NRTL and the NRTL-MSA this means that a Born contribution and an electrostatic contribution (respectively Pitzer-Debye-Hückel or MSA) must be added to the expression for the solvent activity coefficient. This expression must account for the solvent concentration dependence of the dielectric constant, the density and for the MSA the numerical density. Unfortunately, this was recognized too late and has not been used in the program. The derivation would be very time consuming and complicated.

- *Dielectric constant*: The pure solvent dielectric constant is calculated from correlations in the Handbook of Chemistry and Physics [24]. The solvent dielectric constant is the mole averaged dielectric constant of the solvents. A mole averaged rather than a mass averaged dielectric constant was taken, because the dielectric constant is an indication of the polarizability of the solvent and it was assumed that this depends on the mole number of solvent molecules. Although the dielectric constant actually is salt concentration dependent, this was not taken into account in the model, because the salt effect on the dielectric constant is much less pronounced than the salt effect on the density. [49]
- *Ionic diameters*: For the ionic diameters as used in the MSA model, three options were built in:
 1. Use of one concentration independent ionic diameter
 2. Use of a mole averaged solvent dependent ionic diameter [15]
 3. Use of a salt concentration dependent diameter

6.2.2 MSA contribution

This subroutine calculates the activity coefficients from the unrestricted primitive MSA. It is usual to express the properties in the MSA model as a function of numerical densities instead of mole fractions. The numerical density in molecules or ions per volume is calculated with equation (6.2).

$$\rho_i = 10^3 N_A c_i = 10^3 N_A \frac{x_i d_{mix}}{\sum_i x_i M_i} \quad (6.2)$$

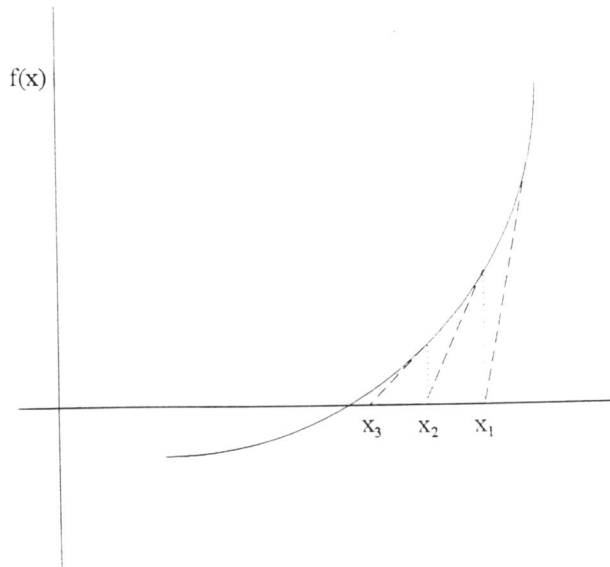


Figure 6.5: Newton-Raphson iteration: Extrapolation of the local derivatives gives the new estimation of the root. Points are numbered in the order they are used.

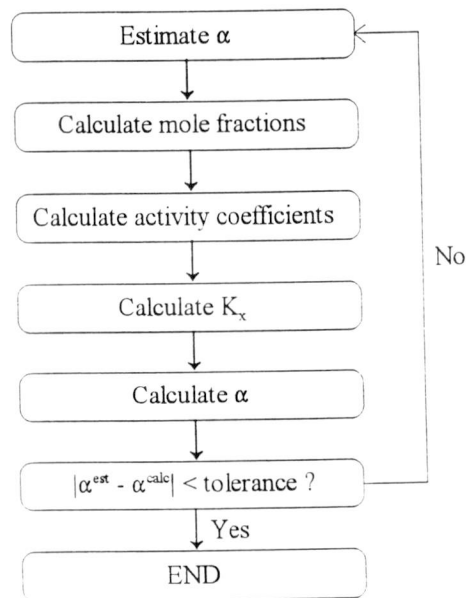


Figure 6.6: Structure of the routine to calculate the dissociation fraction.

where c = Concentration
 M = Molar weight

The shielding parameter Γ cannot be calculated explicitly and an iteration procedure is required to solve it. The secant method iteration is used for this purpose. (The secant method is briefly explained in figure 6.4.) As a first estimation the relation given by Simonin et al. [38] is used, which is:

$$\Gamma = \frac{\sqrt{1+2\kappa\sigma}-1}{2\sigma} \quad \text{with } \sigma = \frac{1}{2}(\sigma_c + \sigma_a) \quad (6.3)$$

Equation (3.1) and (4.17) are used to calculate the ionic activity coefficients. For the MSA contribution to the neutral species the equation derived by Lee [22] from Gibbs-Duhem integration (see section 4.7) is used. The (optional) hard sphere contribution in the MSA contribution is calculated with the Mansoori-Leland-Carnahan-Starling equation for hard sphere mixtures [27].

6.2.3 NRTL contribution

The NRTL routine was programmed by Mark Wijtkamp. The subroutine was modified to have the possibility to test the NRTL with MSA, where the NRTL is either a molecular NRTL and does not contribute to the ionic activity coefficients or is an electrolyte NRTL (like in the model of Chen) and does contribute to the ionic activity coefficients.

6.2.4 Other contributions

Born contribution

The Born contribution is calculated from equation (3.35). For the models including an MSA contribution the ionic diameters used in the MSA are also used in the Born term [22]. For the electrolyte NRTL models of Chen [1] and Liu [25] a fixed Born radius of 0.3 nm is used, in consequence with the literature on these models. The Born expression for mixed solvents with a solvent dependent diameter is [34]:

$$\ln \gamma_i^{Born} = \frac{e^2 z_i^2}{2kT} \left[\left(\frac{1}{\sigma_{i,mix} \epsilon_{mix}} - \frac{1}{\sigma_{i,w} \epsilon_w} \right) + \left(\frac{1}{\sigma_{i,mix}} - \frac{1}{\sigma_{i,w}} \right) \right] \quad (6.4)$$

When no solvent dependent diameter is used, the equation reduces to the common one, equation (3.35)

Pitzer-Debye-Hückel contribution

The electrolyte NRTL models use the Pitzer-Debye-Hückel contribution. A closest approach parameter of 14.9 was used. The Debye-Hückel parameter A_ϕ was not fixed, like in the article by Liu [25].

(Extended) Debye-Hückel contribution

In order to look at the performance of several Debye-Hückel models for the predictions of mean ionic activity coefficients, the Debye-Hückel and the Extended Debye-Hückel mean ionic activity coefficients were programmed, according to equation (3.19) and (3.20).

Bronsted-Guggenheim contribution

The modified electrolyte NRTL of Liu [25] uses a Bronsted-Guggenheim contribution.

6.3 Flash routine

The flash routine was obtained from Naveen Koak and had been modified for the prediction of liquid-liquid equilibria of electrolyte solutions by Mark Wijtkamp. An extensive description of the flash routine can be found in the thesis of Naveen Koak [18]. The solution method used is partially obtained from Walas [48].

Basic conditions for equilibrium are given by:

$$(\mu_i^{\text{II}} - \mu_i^{\text{I}}) = 0 \quad (6.5)$$

$$\ln(x_i \gamma_i)^{\text{II}} - \ln(x_i \gamma_i)^{\text{I}} = 0 \quad (6.6)$$

In the equations above and the following, the ion pair is seen as one component with a mean activity coefficient and a mean ionic mole fraction like in equation (3.1).

The distribution of component i between phase I and II is given by a distribution coefficient K_i :

$$x_i^{\text{II}} = K_i x_i^{\text{I}} \quad (6.7)$$

where:

$$K_i = \frac{\gamma_i^{\text{I}}}{\gamma_i^{\text{II}}} \quad (6.8)$$

The mole balance on component i gives:

$$z_i = (1 - \beta)x_i^{\text{I}} + \beta x_i^{\text{II}} \quad (6.9)$$

where z_i = Overall mole composition
 β = Fraction of phase I

Since the summation of the mole fractions of the components in both phases must be equal to unity, the following relation is valid:

$$\sum_i (x_i^{\text{II}} - x_i^{\text{I}}) = 0 \quad (6.10)$$

Combination of equation (6.7), (6.9) and (6.10) gives the equation that has to be solved to satisfy the mole balance:

$$f(\beta) = \sum_i \frac{z_i(K_i - 1)}{1 + \beta(K_i - 1)} = 0 \quad (6.11)$$

For a physically possible solution of the mole balance, β must satisfy $0 < \beta < 1$, leading to the following conditions:

$$\sum_i K_i z_i > 1 \quad (6.12)$$

$$\sum_i z_i / K_i > 1 \quad (6.13)$$

The mole balance is solved using Newton-Raphson iteration (see figure 6.5), equated as:

$$\beta^{new} = \beta^{old} + \frac{f(\beta)}{f'(\beta)} \quad (6.14)$$

$$f'(\beta) = -\sum_i \frac{z_i (K_i - 1)^2}{(\beta + (K_i - 1)\beta)^2} \quad (6.15)$$

After mole balance has been solved, new values are calculated for the phase compositions and the activity coefficients. These are then evaluated to check whether they satisfy equation (6.16) within the tolerance limits:

$$\sum_i \left[(\ln(x_i \gamma_i)^{II} - \ln(x_i \gamma_i)^I) \right]^2 \leq 10^{-12} \quad (6.16)$$

If the system is not converged, a new set of distribution functions is obtained from:

$$\ln K_i^{new} = \ln K_i^{old} - m \cdot \ln \left[\frac{(x_i \gamma_i)^{II}}{(x_i \gamma_i)^I} \right]^{old} \quad (6.17)$$

where m = Damping or acceleration factor

The full procedure for the flash calculation is:

1. If not specified, the overall composition is set to the average of the experimental values in both phases, this is equal to $\beta=0.5$. The experimental data are used as a first estimation of the phase compositions.
2. Based on the estimations for the compositions, the activity coefficients and the distribution coefficients are calculated
3. The mole balance is solved with the estimation for the distribution coefficient K_i
4. The activity coefficients are calculated for the new compositions
5. If an equilibrium constant has been specified, the equilibrium routine (section 6.6) is called and the new ionic equilibrium is calculated. [48]
6. The estimations for the distribution coefficients are updated.
7. The equilibrium condition is evaluated. If the specified tolerance is not reached, the calculations are repeated from step 3

6.4 Regression routine

This subroutine is in fact the driving force of the program. The subroutine reads the physical property data, the estimations for the parameters, the experimental data and the regression parameters (tolerance,

number of iterations) needed for the regression from file. The structure of the input files is given in appendix VI. The subroutine converts the experimental data (with salt concentrations) to the apparent mole fractions (where the salt mole fraction is split up into the ion mole fractions). If no dissociation constant has been specified, full dissociation is assumed. The physical property data are passed to the activity coefficient subroutine, the parameters for the regression are passed to the Levenberg-Marquardt routine.

The Levenberg-Marquardt routine minimizes the objective function supplied by the regression routine. The objective function is function that calculates the least squares sum of the differences between the experimental data and the data calculated by the flash routine with the parameter estimations from the Levenberg-Marquardt routine. The objective functions F_{OBJ} used in the regression are relative and absolute objective functions [41]. The absolute objective functions are given by:

$$F_{OBJ} = \sum_i^{ndp} \sum_j^{nc} \left[\frac{(x_{ij}^{I,calc} - x_{ij}^{I,exp})^2}{(S_j^I)^2} + \frac{(x_{ij}^{II,calc} - x_{ij}^{II,exp})^2}{(S_j^{II})^2} \right] \quad (6.18)$$

where ndp = Number of experimental datapoints
 nc = Number of components
 S = Standard deviation

In equation (6.18) x_{ij} may stand for either mole fractions or mass fractions of component j , resulting in two objective functions which perform quite different as will be seen in the next chapter. The standard deviation can also be used as a weighting factor for the component. The relative objective functions are given by:

$$F_{OBJ} = \sum_i^{ndp} \sum_j^{nc} \left[\left(\frac{x_{ij}^{I,calc} - x_{ij}^{I,exp}}{S_j^I \cdot x_{ij}^{I,exp}} \right)^2 + \left(\frac{x_{ij}^{II,calc} - x_{ij}^{II,exp}}{S_j^{II} \cdot x_{ij}^{II,exp}} \right)^2 \right] \quad (6.19)$$

Several ways are possible for obtaining parameters to start the regression. Among them is one method that consists of a regression itself, where the following activity objective function is used:

$$F_{OBJ} = \sum_i^{ndp} \sum_j^{nc} \left[(x_{ij}^{exp} \gamma_{ij}^I)^I - (x_{ij}^{exp} \gamma_{ij}^{II})^{II} \right]^2 \quad (6.20)$$

When the regression is finished, the results are evaluated visually and by calculating the average deviation of the calculated values from the experimental values. The average deviation Δx is defined as [25]:

$$\Delta x = \sqrt{\frac{\sum_i^{ndp} \sum_j^{nc} [(x_{ij}^{I,calc} - x_{ij}^{I,exp})^2 + (x_{ij}^{II,calc} - x_{ij}^{II,exp})^2]}{2 \cdot nc \cdot ndp}} \quad (6.21)$$

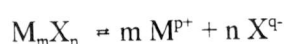
The x 's may again be either mole fractions or mass fractions.

6.5 Levenberg-Marquardt routine

The Levenberg-Marquardt routine was obtained from DSM Research. A detailed description of the numerical method will not be given here. The Levenberg-Marquardt method is a modification of the well-known Gauss-Newton method. The Gauss-Newton method is a least squares estimation method that linearizes the nonlinear regression problem. (In the program only numerical derivatives are used for this linearization.) The Gauss-Newton solves the linearized problem and uses the resulting regression parameters to get a new estimation. Subsequently the system is linearized around the new estimations. The process is repeated until the sum of squared errors does not decrease anymore and the regression parameters do not change either. The Levenberg-Marquardt method is a method to prevent the problem from becoming singular and thus hardly solvable.

6.6 Chemical equilibrium

An optional chemical equilibrium was programmed in order to look at the possibility of improving the fitting results by assuming partial dissociation of the salt in the organic phase. The ionic equilibrium obeys the following dissociation reaction for the systems involved:



The extent of dissociation is given by the dissociation fraction α . The equilibrium compositions are calculated from the dissociation constant K :

$$K = K_Y \cdot K_x = \frac{\gamma_M^m \gamma_X^n \cdot x_M^m x_X^n}{\gamma_{M_m X_n} x_{M_m X_n}} \quad (6.22)$$

The mole fractions of the salt and the ions are given by:

$$x_{M_m X_n} = \frac{x_S(1-\alpha)}{1+(m+n-1)x_S\alpha} \quad (6.23)$$

$$x_M = \frac{m x_S \alpha}{1+(m+n-1)x_S\alpha} \quad (6.24)$$

$$x_X = \frac{n x_S \alpha}{1+(m+n-1)x_S\alpha} \quad (6.25)$$

Insertion of these mole fractions in the equation for the dissociation constant and rewriting, leads to:

$$\alpha = \left(1 - \frac{K_Y(T,x)}{K} \frac{m^m n^n x_S^{m+n} \alpha^{m+n}}{[1+(m+n-1)x_S\alpha]^{m+n-1}} \right) \quad (6.26)$$

where x_S = Salt weight fraction

The procedure programmed to solve the dissociation fraction is given in figure 6.6.

MSA: Contributions to $\ln(\gamma)$

NaCl in water at 25°C

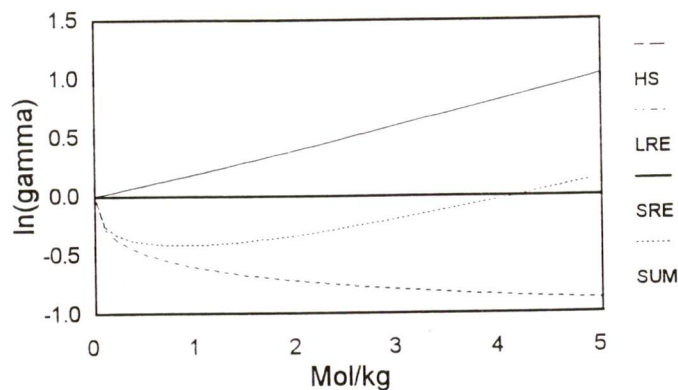


Figure 7.1: The figure shows the influence of the concentration (in mol/kg) on the MSA mean ionic activity coefficient and its contributions (HS = hard sphere term, LRE = long range electrostatic term, SRE = short range electrostatic term, SUM = all contributions)

MSA: Contributions to $\ln(\gamma)$

1 mol/kg NaCl in water at 25°C

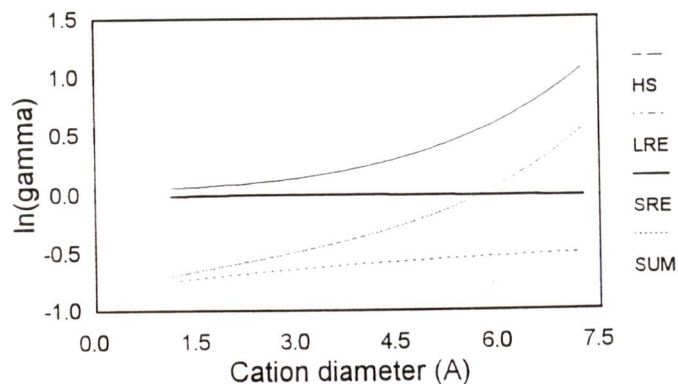


Figure 7.2: The figure shows the influence of the cationic diameter on the MSA mean ionic activity coefficient and its contributions (HS = hard sphere term, LRE = long range electrostatic term, SRE = short range electrostatic term, SUM = all contributions)

7. Calculations

7.1 Examination of the MSA activity coefficient

The MSA mean ionic coefficient is built up from three terms: a long range electrostatic contribution (LRE), a short range electrostatic contribution (SRE) and a hard sphere contribution (HS). The extent to which these contributions contribute to the activity coefficient is dependent on concentration and the ionic diameters. To learn more about this, calculations were carried out for the system water-NaCl and the individual contributions were studied. First, the concentration was maintained constant at 1 mol/kg and the diameter of the sodium ion was varied. The anion diameter was kept constant at the Pauling diameter of 0.36 nm. The results are made visible in figure 7.1. Secondly, the diameters of both the anion and the cation were fixed at respectively the Pauling diameter and a fitted diameter from literature [14] and the concentration of sodium chloride, expressed in moles salt per kg solvent, was varied from 0 to 5 mol/kg. This produced the results presented in figure 7.2.

From figure 7.1 and 7.2 it can be concluded that the long range electrostatic contribution is dominant at lower concentrations. The hard sphere contribution is getting more important at increasing concentration and increasing cation diameter. The short range electrostatic contribution is only small and has a parabolic form with a minimum when the ionic diameters are equal. The electrostatic contributions to $\ln(\gamma_{\pm})$ are negative and thus lower the activity coefficient. The hard sphere contribution is positive (repulsive) and enlarges the ionic activity coefficient.

7.2 Prediction of ionic activity coefficients

The modelling was started with testing the performance of the Mean Spherical Approximation in predicting mean ionic activity coefficients, compared with the Debye-Hückel model. This was done by comparing mean ionic activity coefficients in the MSA model, the Extended Debye-Hückel, the classical Debye-Hückel and the Pitzer-Debye-Hückel. The ionic activity coefficients were calculated for systems of NaCl, LiCl, CaCl₂, ZnSO₄ and (NH₄)₂SO₄ + water. The objective of this choice of the electrolytes was to see if the MSA can cope with different classes of electrolytes (1:1, 1:2, 2:1, 2:2). The experimental ionic activity coefficients were obtained from Robinson and Stokes [36]. Since these are molal activity coefficients, they were converted to molar activity coefficients by:

$$\gamma_{\text{exp}}^{MM} = \gamma_{\text{exp}} \left(1 + \frac{mM}{d_0}\right) \quad (7.1)$$

where: m = Salt molality
 M = Molecular weight of the salt
 d_0 = Density of the pure solvent

An important question arising from the MSA model is what kind of ionic diameter to use. In chapter 4 it was stated that this should be the hard core diameter of the hydrated ion: the diameter of the sphere that cannot be penetrated by another ion. This diameter is not given in literature and hard to determine. The effective diameter of an ion is dependent on the type of solvents present and the ion concentration. Generally, the effective anion and cation diameters decrease as the concentration increases. This is due to decreased availability of the solvent molecules for the secondary hydration shell ($r > \sigma_{\text{water}}$) and

Ionic diameters in MSA NaCl + water

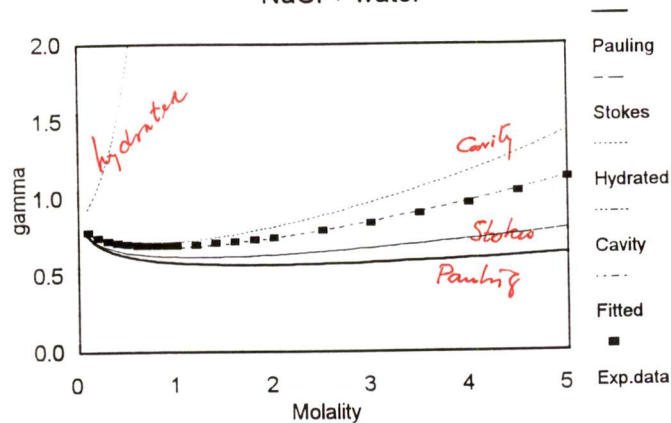


Figure 7.3: Mean ionic activity coefficient of NaCl in the system NaCl-water at 25°C, calculated with different kinds of ionic diameters

NaCl in water Cation diameter = 0.32 nm

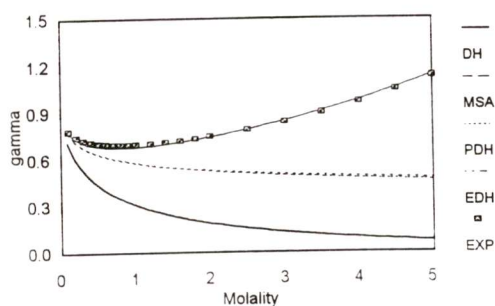


Figure 7.4: Mean ionic activity coefficients for the system water+NaCl at 25°C, calculated from the Debye-Hückel model (DH), the extended Debye-Hückel (EDH), the Pitzer-Debye-Hückel (PDH) and the MSA model. EXP = Experimental data.

Ammonium sulfate in water Cation diameter = 0.08 nm

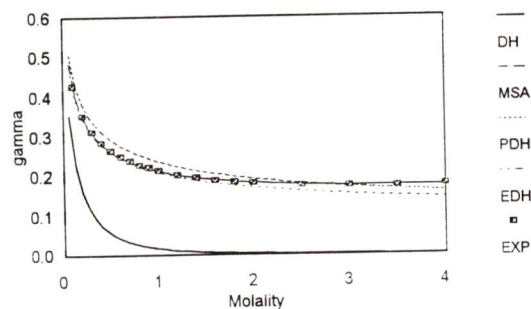


Figure 7.5: Mean ionic activity coefficients for the system water+ammonium sulfate at 25°C, calculated from the Debye-Hückel model (DH), the extended Debye-Hückel (EDH), the Pitzer-Debye-Hückel (PDH) and the MSA model. EXP = Experimental data.

compression of the entire solvation shell. Articles on the MSA report the use of the Pauling diameter or a fitted diameter. (However, these articles are mainly concerned with the calculation for osmotic coefficients.) In some publications, like Simonin et al. [38], a concentration dependent diameter is used, where the ionic diameter may vary with both salt concentrations and solvent ratios. [15]

Nightingale [30] has published three different ionic diameters for a large number of ions. They are:

- Pauling diameter: This diameter has been calculated from the interatomic distances from crystallographic data
- Stokes diameter: This diameter has been calculated from conductance experiments by the relations of Stokes and Einstein.
- Hydrated diameter: This is an effective hydrated diameter, calculated from a solvation model by Nightingale [30]

Rashin and Honig [34] have given radii of the dielectric cavities formed by the ions. These radii were used by them to reproduce experimental hydration enthalpies, using the Born model of ion hydration, with fairly good results.

Table 7.1: Comparison of ionic diameters (in Å) [30,34]

Ion	Pauling	Stokes	Hydrated	Cavity
Na ⁺	1.90	3.68	7.16	3.36
Cl ⁻	3.62	2.42	6.64	3.87
Li ⁺	1.20	4.76	7.64	2.63
Ca ²⁺	1.98	6.20	8.24	3.72
NH ₄ ⁺	2.96	2.50	6.62	4.26
SO ₄ ²⁻	4.80	4.60	7.58	
Zn ²⁺	1.48	6.98	8.60	2.67

Figure 7.3 shows the results of calculations of the mean ionic activity coefficient using Pauling diameters, Stokes diameters, hydrated diameters, dielectric cavity diameters and the results of calculations with a Pauling diameter for the anion and a fitted diameter for the cation. The latter option may be declared from the fact that the anion is hydrated to a smaller extent than the cation generally. This is because the association between anion and hydrogen is generally much weaker than the association between cation and oxygen. Therefore, the anion can be assumed to remain unhydrated.

From figure 7.3 it becomes clear that the Pauling diameter is too small for the NaCl-water system. In fact it is too small for all systems studied, except water + AS which shows a behaviour different from the other electrolytes. The use of Stokes diameters or the ionic cavity diameters can be assumed to account more for the influence of the solvent on the diameter and does produce better results. In figures 7.4 to 7.6 the ionic diameter of the MSA activity coefficient is fitted to the experimental data by least squares estimation. Figures 7.4 and 7.5 show the results for the different electrolyte models for the system NaCl+water and ammonium sulfate + water, respectively. Figure 7.4 can be thought to represent the other systems. Figure 7.5 is shown because of the quite different behaviour and since this system is

MSA ionic activity coefficients

Salt-water systems at 25°C

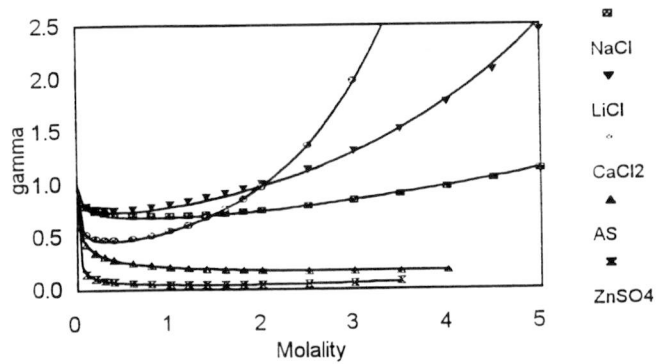


Figure 7.6: MSA mean ionic activity coefficients for salt-water systems at 25°C. Markers represent experimental mean ionic activity coefficients, lines are calculated values. Pauling diameters are used as anionic diameters. Cationic diameters were obtained by regression (Na^+ : 0.325 nm, Li^+ : 0.418 nm, Ca^{2+} : 0.564 nm, Zn^{2+} : 0.265 nm, NH_4^+ : 0.081 nm)

LiCl in water and methanol

Molality LiCl = 1 mol/kg

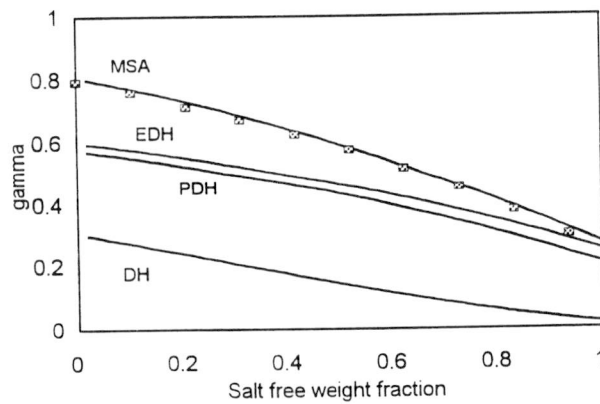


Figure 7.7: Mean ionic activity coefficients for the system water + methanol + 1 mol/kg LiCl at salt free methanol fractions of 0 to 1 kg/kg. Markers are experimental values, lines represent calculated values. (MSA = Mean Spherical Approximation, EDH = Extended Debye-Hückel, PDH = Pitzer-Debye-Hückel, DH = Debye-Hückel)

of interest for the modelling of the experimental data in chapter 5. Figure 7.6 shows the results for some systems studied. Figure 7.4 up to 7.6 show that the MSA theory can describe mean ionic activity coefficients of some common electrolytes up to high concentrations very well. This is especially true for 1:1 electrolytes, but the theory can also satisfactorily describe unsymmetric electrolytes.

To get an indication of the applicability of the MSA-model to mixed solvent systems, the testing was extended to a mixed solvent system with salt. There are not much data with experimental mean ionic activity coefficients of these systems, but a publication was found with experimental ionic activity coefficients of the system water + methanol + lithium chloride. The cation diameter was fixed here at the value found for the system water + LiCl, although it was realized that the diameter is solvent dependent. The results are shown in figure 7.7. It may be concluded that the MSA can handle mixed solvent systems satisfactorily without adaptations. (For comparison of the calculated with the experimental mean ionic activity coefficients the addition of a Born expression like in the electrolyte NRTL is not required. This is only required for the liquid-liquid equilibrium calculations, when the ionic activity coefficients must have the same reference state.)

7.3 Modelling liquid-liquid equilibria of electrolyte solutions

7.3.1 Model 1: MSA + molecular NRTL

The first attempt in modelling liquid-liquid equilibria of electrolyte systems with an NRTL-MSA model was to follow the approach by Lloyd Lee [22]. He used a molecular UNIFAC model for the calculation of the activity coefficients for the molecular species and the MSA for the calculation of the ionic activity coefficients. From Gibbs-Duhem integration he derived an expression for the electrostatic contribution to the molecular species. This contribution has already been discussed in sections 3.2.3 and 4.7. A Born expression was added to the ionic activity coefficient. In this work it was tried to model liquid-liquid equilibria of water + 2-propanol + NaCl measured by De Santis [37] with a corresponding combination of the NRTL and the MSA model. The molecular NRTL of Renon and Prausnitz [35] is used for the activity coefficients of the neutral species. The MSA activity coefficient including the hard sphere term is used for the description of the ionic activity coefficients. The system water + 2-propanol + NaCl was chosen since this system had been modelled before by Liu [25] and Cheluget et al. [11].

First, to get an impression if the molecular NRTL could handle the system without electrostatic terms it was tried to model the system with the molecular NRTL where NaCl was accounted for as an uncharged molecular component. At first the nonrandomness factors were used as proposed by Chen [13]: 0.20 for the salt-molecule parameters and 0.30 for the molecule-molecule parameters. It was found that fitting at least one α greatly improved the goodness of fit. The result of this modelling is shown in figures 7.8 and 7.9. It was found that using only nonelectrostatic contributions, the NRTL can correlate the experimental data with an average deviation of 0.005 mole/mole and of 0.007 w/w when $\alpha_{\text{water,propanol}}$ is not fixed. The correlation of the experimental data is good for this system. However, getting a representation of the experimental data for the system caprolactam + water + ammonium sulfate that is as good, was not possible (see figure 7.9). The parameters obtained from the regression are presented in table 7.2 and are used as estimations for the parameters for the combination of the molecular NRTL and the MSA.

For the combination of a molecular NRTL with MSA, initially fixed ionic diameters were used, that were obtained by the least squares regression with experimental ionic activity coefficients (former section). Since this did not seem to work, the diameters were also fitted, it was tried to use solvent dependent diameters that were mixed on mass fraction basis and it was tried to use concentration dependent diameters (which required programming of additional terms in the MSA and Born activity coefficients, containing the derivatives of the diameter to the concentration). Neither of these approaches led to satisfactory results. Figure 7.10 shows one of the results of this approach, which is characteristic for all the results following the same approach. It can be seen that the calculated two phase line has a slope that deviates largely from the slope experimentally found.

Table 7.2: Parameters and results of using the molecular NRTL on electrolyte solutions of I: water (1) + 2-propanol (2) + NaCl (3) at 25°C and II: water (1) + caprolactam (2) + ammonium sulfate (3) at 20°C. (* = Fixed during regression)

Parameter	System I		System II
τ_{12}	2.562	3.421*	5.084
τ_{21}	0.139	0.941*	-2.873
τ_{13}	24.23	17.56	19.21
τ_{31}	-3.741	-5.268	-7.279
τ_{23}	2.333	2.342	1.717
τ_{32}	25.00	11.236	18.12
α_{12}	0.30*	0.445	0.284
α_{13}	0.20*	0.20*	0.20*
α_{23}	0.20*	0.20*	0.20*
Δx (mole/mole)	0.011	0.005	0.004
Δx (w/w)	0.018	0.007	0.013

It was tried to improve the goodness of fit by accounting for the salt effect on the solution density. This did not improve the results, and is not used further. To improve the performance, it was also investigated how the model performs if partial dissociation is assumed. This assumption is in particular valid for the organic phase, where, due to the low dielectric constant, a large fraction of the salt may be present as molecular salt. Therefore, the influence of this dissociation on the performance of the model was investigated at some values of the dissociation constant. The parameters found with using the molecular NRTL (table 7.2) were chosen for the molecular salt-solvent parameters. The introduction of partial dissociation slowed down the regression a lot, but did result in a only slightly better correlation with the experimental data. Comparison of figure 7.10 and 7.11 illustrates this. The results of figures 7.10 and 7.11 were obtained from regression with the same set of initial parameters and are tabulated in table 7.3.

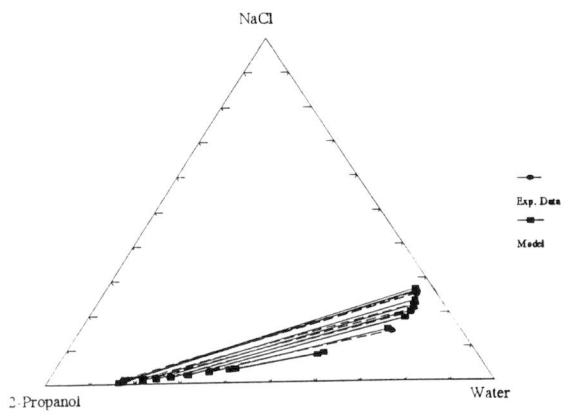


Figure 7.8: Liquid-liquid equilibrium for the system water + 2-propanol + NaCl at 25°C. Representation by the molecular NRTL. All data are in mass fractions.

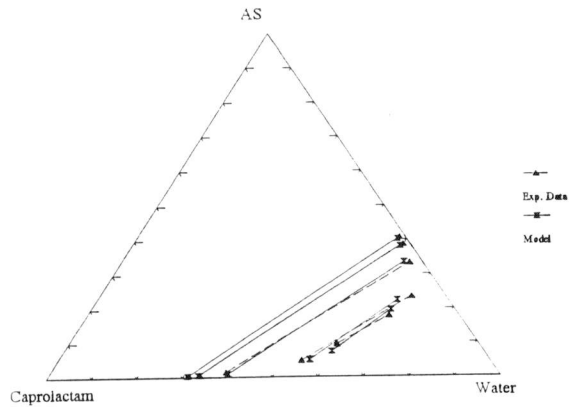


Figure 7.9: Liquid-liquid equilibrium for the system water + caprolactam + ammonium sulfate at 20°C. Representation by the molecular NRTL. All data are in mass fractions

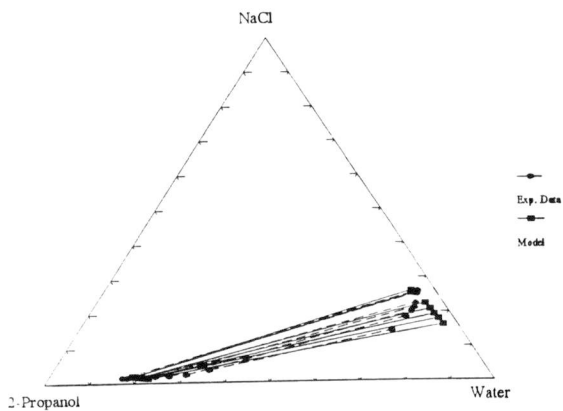


Figure 7.10: Liquid-liquid equilibrium for the system water + 2-propanol + NaCl at 25°C. Representation by molecular NRTL combined with MSA. All data are in mass fractions.

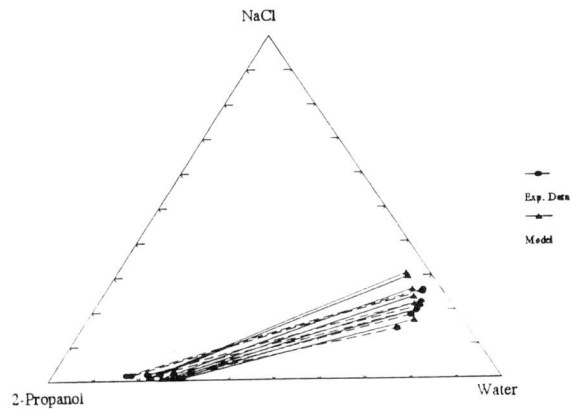


Figure 7.11: Liquid-liquid equilibrium for the system water + 2-propanol + NaCl at 25°C. Representation by the molecular NRTL combined with MSA. Dissociation constant $K = \exp(1)$. All data are in mass fractions

Table 7.3: Parameters and results for the combination of a molecular NRTL with the MSA at different values of the dissociation constant K for the system water (1) + 2-propanol (2) + sodium chloride (3) at 25°C. For the salt-molecule parameters, the values of table 7.2 were used.

Parameter	full dissociation	$\ln(K) = 1$	$\ln(K) = 10$
τ_{12}	7.708	5.087	7.066
τ_{21}	-1.920	-1.746	-1.906
α_{12}	0.201	0.156	0.203
σ_{cation} (nm)	0.08	0.08	0.08
σ_{anion} (nm)	0.36	0.36	0.36
Δx (mole/mole)	0.041	0.029	0.041
Δx (w/w)	0.047	0.030	0.047

From the results and the figures 7.10 and 7.11, it might be concluded that this approach does not represent the experimental liquid-liquid equilibria very well. (Lloyd Lee used this approach for vapour-liquid equilibria with many components = many parameters.)

7.3.2 Model 2: MSA + electrolyte NRTL

Since the combination of molecular NRTL and MSA did not seem to perform well, modelling was continued with a combination of the electrolyte NRTL and MSA. In the electrolyte NRTL [4] the electrostatic Pitzer-Debye-Hückel contribution was replaced by the MSA ionic activity coefficient. It was considered to drop the NRTL contribution in the ionic activity coefficient since the MSA itself can accurately describe the ionic activity coefficient. However, this would be inconsistent since a derivation from the excess Gibbs energy in the electrolyte NRTL would always yield a contribution for the ionic activity coefficients. The electrostatic contribution to the neutral species is still the same. The Born expression is used again to get the same reference state for both liquid phases.

For the ionic diameters the Pauling diameters were taken in this model. Larger ionic diameters were supposed to produce ionic activity coefficients that are too large. Two representative figures are shown in figure 7.12 and 7.13. It can be observed that the model does predict only very small amounts of salt in the organic phase. This may probably be caused by too large ionic activity coefficients in the organic phase. From the equilibrium condition, equation (2.3), it can be seen that large ionic activity coefficients in the organic phase lead to small ionic mole fractions in this phase.

The combination of the electrolyte NRTL and MSA still does not produce the results with the desired accuracy, but performs better than the model in the former subsection. However, Cheluget et al. [11] found a good representation of the system water + 2-propanol + NaCl by a model that also consisted of a local composition model (the Flory-Huggins theory), an electrolyte model (Bromley equation) and a Born contribution, confirming the supposition that a combination of NRTL and MSA must give a good representation.

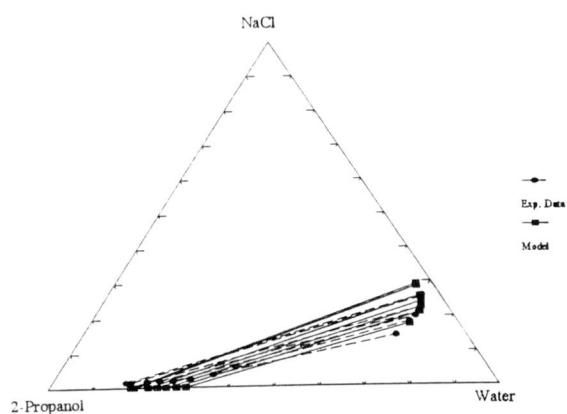


Figure 7.12: Liquid-liquid equilibrium for the system water + 2-propanol + NaCl at 25°C. Representation by electrolyte NRTL + MSA. All data are in mass fractions

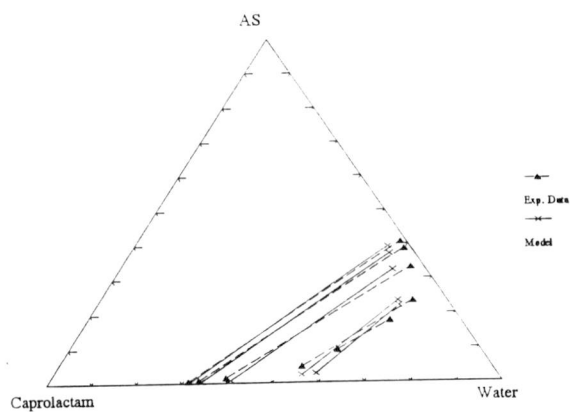


Figure 7.13: Liquid-liquid equilibrium for the system water + caprolactam + ammonium sulfate at 20°C. Representation by electrolyte NRTL + MSA. All data are in mass fractions.

Table 7.4: Parameters and results of using the electrolyte NRTL with the MSA to correlate the experimental data of the system I: water (1) + 2-propanol (2) + NaCl (3) at 25°C and II: water + caprolactam + ammonium sulfate at 20°C. (* = fixed during regressions)

Parameter	I	II
τ_{12}	3.266	3.881
τ_{21}	0.888	-2.485
$\tau_{1,ca}$	23.15	7.066
$\tau_{ca,1}$	2.805	-2.890
$\tau_{2,ca}$	3.314	2.760
$\tau_{ca,2}$	2.051	8.123
α_{12}	0.455	0.122
$\alpha_{1,ca}$	0.20	0.30
$\alpha_{2,ca}$	0.20	0.30
Δx (mole/mole)	0.018	0.008
Δx (w/w)	0.026	0.029

During the attempts to regress the parameters of the model with the objection function of equation (6.18), it was observed that the model predicted hardly any salt in the organic phase (see figure 7.12). Besides by introducing partial dissociation, it was tried to force the model to predict more salt in the organic phase by the application of a weighting factor for the salt in the organic phase, resulting in a modest improvement. The choice of the right objective function proved to have a much greater influence. Initially, the absolute objective function of equation (6.18) was used with mole fractions. In order to let the model predict more salt in the organic phase, the relative objective function of equation (6.19) was applied. An important advantage of this objective function is that large and small mole fractions have an equal influence on the direction of the regression. The salt mass fractions converted to mole fractions are rather small, since the salt usually has a much higher molar mass than the solvent molecules. (In the figures mass fractions are chosen to enlarge the area under the binodal curve in the Gibbs triangle.) An important disadvantage of the relative objective function is that it sometimes sends the regression to a wrong direction due to the large weight given to small mole fractions. Best results for electrolyte systems were obtained in this work by using the absolute objective function of equation (6.18), but now with mass fractions. This way the smallest average deviations in both mass and mole fractions were obtained from the same starting values. A 'penalty function' which enlarges the value of the objective function when the flash routine has not reached convergence, was used when the regression tended to go to a set of parameters, where not all the flash calculations of the datapoints converged.

7.3.3 Model 3: No hard sphere contribution

It was noticed before that the MSA activity coefficient with the hard sphere does not need the short range contribution of the electrolyte NRTL. It can itself give a good description of the ionic activity coefficients in aqueous and mixed-solvent solutions. It was also observed that the hard sphere

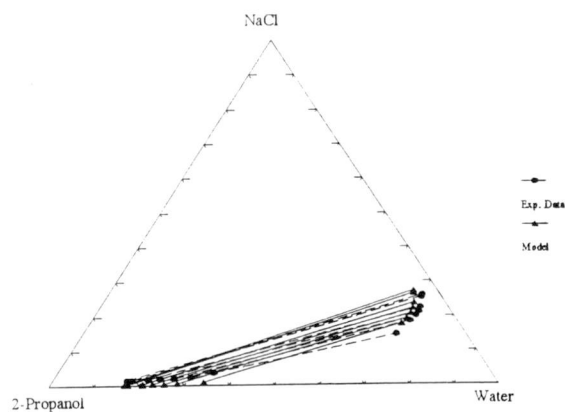


Figure 7.14: Liquid-liquid equilibrium of the system water + 2-propanol + NaCl at 25°C. Representation by the electrolyte NRTL + MSA (without hard sphere contribution). All data are in mass fractions.

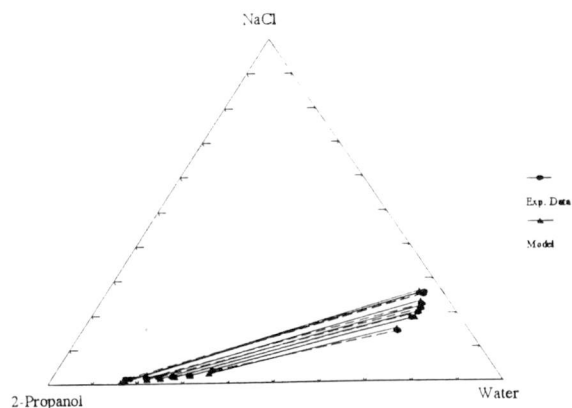


Figure 7.15: Liquid-liquid equilibrium of the system water + 2-propanol + NaCl at 25°C. Representation by the electrolyte NRTL + MSA (without hard sphere contribution, α_{12} obtained by regression). All data are in mass fractions.

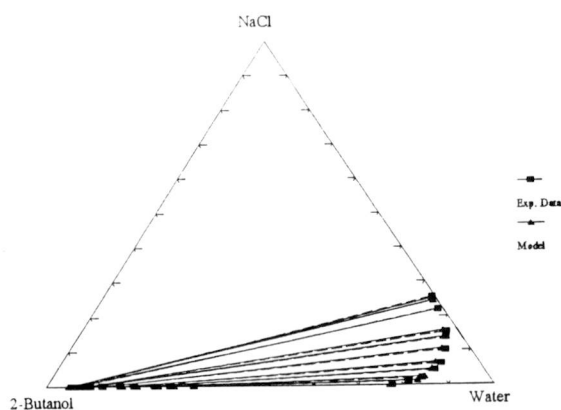


Figure 7.16: Experimental data and correlation by the NRTL-MSA model without hard sphere contribution for the system water + 2-butanol + NaCl at 25°C.

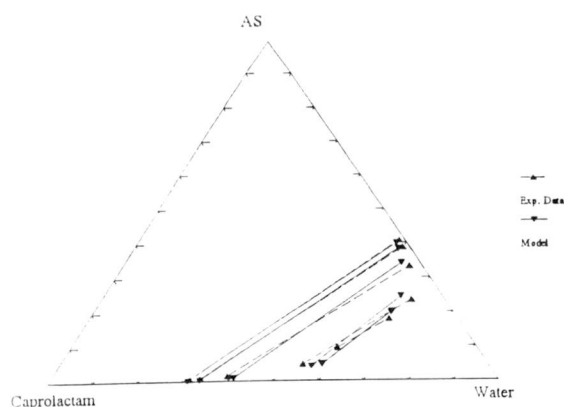


Figure 7.17: Liquid-liquid equilibrium of the system water + caprolactam + ammonium sulfate (AS) at 20°C: experimental data and correlation by the NRTL-MSA model without hard sphere contribution. All experimental tie-lines are used in the regression.

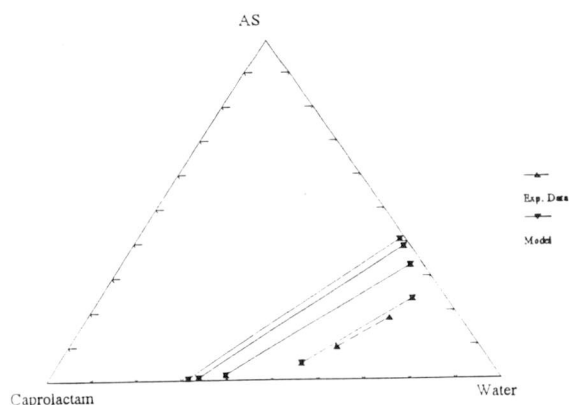


Figure 7.18: Liquid-liquid equilibrium of the system water + caprolactam + ammonium sulfate (AS) at 20°C: experimental data and correlation by the NRTL-MSA model without hard sphere contribution. The last tie-line in the critical region was not used in the regression.

contribution was not present in the original MSA model, but was introduced later to obtain better fits of mean ionic activity coefficients and osmotic coefficients in concentrated aqueous solutions. Thirdly, it was assumed that the short range interactions of the NRTL implicitly include the hard sphere repulsion of the ions. Combining these three led to a model in which the electrolyte NRTL and the MSA are combined but in which the hard sphere contribution in the MSA ionic activity coefficient is omitted. This model has been used to correlate the experimental liquid-liquid equilibria of the systems water + 2-propanol + NaCl, water + 2-butanol + NaCl and water + caprolactam + ammonium sulfate. Stokes diameters were used for the MSA ionic diameters. At first none of the nonrandomness factors was fitted and they were all fixed at 0.3 or 0.2. When it was examined how the agreement with experimental data would be influenced if the nonrandomness factors are adjusted by regression, it was observed that adjustments to even only one of the nonrandomness factors resulted in a large improvement. By a sensitivity analysis, it was determined that adjusting α_{12} by regression had the largest effect on the performance of the model. This way, an average deviation of 0.007 w/w was reached for the system water + 2-propanol + NaCl. Therefore, these results are also given here. The new value of α_{12} may be considered as high, but it was noticed in chapter 3, that although unusual for liquid-liquid equilibria, these values are not uncommon for vapour-liquid equilibria and it was concluded that the nonrandomness factor must be seen as an empirical constant.

The parameters and results obtained are tabulated in table 7.5. A graphical representation of the results is shown in the figures 7.14 up to 7.18. It may be concluded that the combination of electrolyte NRTL + MSA without hard sphere contribution gives the best results of the models studied. However, the behaviour in the vicinity of the critical point has not yet been examined.

Table 7.5: Parameters and results of using the electrolyte NRTL with the MSA (but without hard sphere contribution) to correlate the experimental data of the system I: water (1) + 2-propanol (2) + NaCl (3) at 25°C, II: water (1) + 2-butanol (2) + NaCl (3) at 25°C and III: water + caprolactam + ammonium sulfate at 20°C. (* = not fitted during regression). Concerning system III: the first column are results of fitting all tielines, the last column are results obtained when the last tie-line is not used in the regression.

Parameter	System I		System II	System III	
τ_{12}	2.474	3.421*	4.465	3.455	4.428
τ_{21}	0.227	0.941*	-1.221	-2.107	-1.441
$\tau_{1,ca}$	27.57	26.87	7.126	6.582	6.582
$\tau_{ca,1}$	-2.185	-3.921	-4.327	-2.687	-2.687
$\tau_{2,ca}$	1.940	1.513	2.304	2.362	0.899
$\tau_{ca,2}$	1.192	2.110	14.00	20.44	23.99
α_{12}	0.30*	0.595	0.20*	0.131	0.328
$\alpha_{1,ca}$	0.20*	0.20*	0.40*	0.343	0.30*
$\alpha_{2,ca}$	0.20*	0.20*	0.10*	0.10*	0.10*
Δx (mole/mole)	0.012	0.006	0.008	0.006	0.002
Δx (w/w)	0.018	0.007	0.006	0.018	0.006

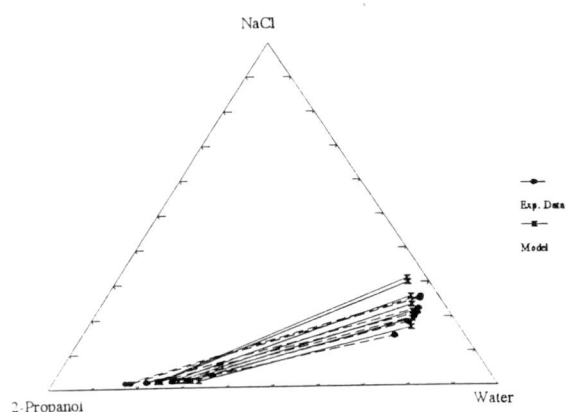


Figure 7.19: Liquid-liquid equilibrium of the system water + 2-propanol + NaCl at 25°C. Representation by the electrolyte NRTL of Chen [12]. Results obtained by Mark Wijtkamp. All data are in mass fractions.

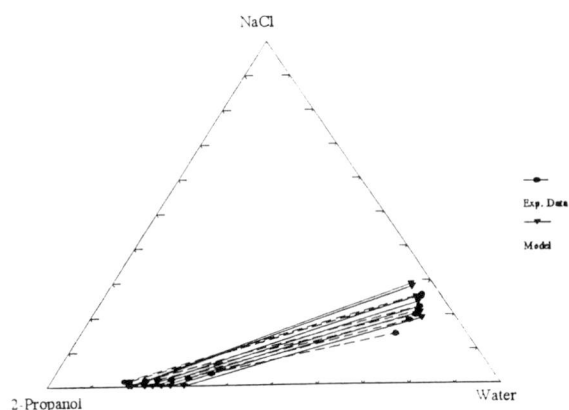


Figure 7.20: Liquid-liquid equilibrium of the system water + 2-propanol + NaCl at 25°C. Representation by the modification of the electrolyte NRTL by Liu [25]. Results obtained by Mark Wijtkamp. All data are in mass fractions.

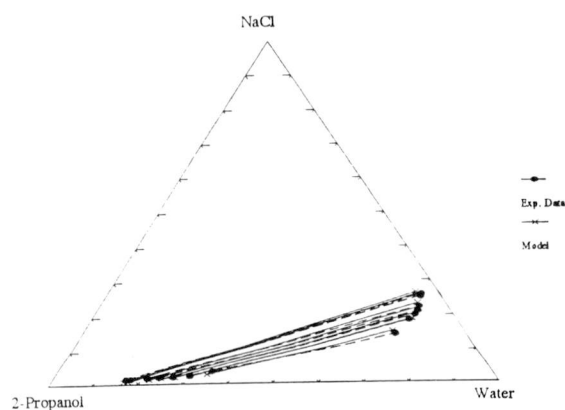


Figure 7.21: Liquid-liquid equilibrium of the system water + 2-propanol + NaCl at 25°C. Representation by the electrolyte NRTL of Chen [12], α_{12} obtained by regression. All data are in mass fractions.

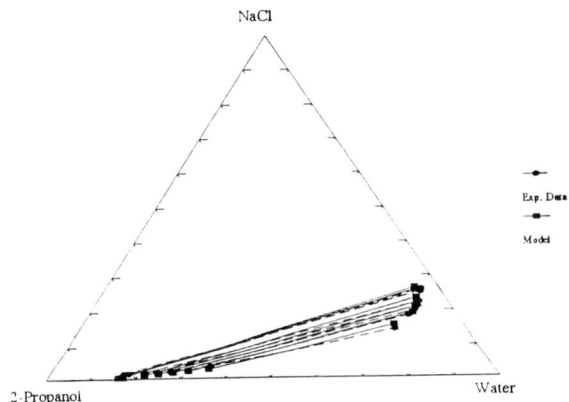


Figure 7.22: Liquid-liquid equilibrium of the system water + 2-propanol + NaCl at 25°C. Representation by the modification of the electrolyte NRTL by Liu [25], α_{12} obtained by regression. All data are in mass fractions.

From comparison of the two sets of parameters given for the system water + caprolactam + ammonium sulfate, it can be seen that the most critical tie-line is determining the direction and quality of the regression.

7.3.4 Model 4: Electrolyte NRTL of Liu

Mark Wijtkamp has performed modelling work with the electrolyte NRTL of Chen [12] and the electrolyte NRTL modification of Liu [25]. His results gave the impression that the modification of the electrolyte NRTL by Liu [25] performs hardly better than the electrolyte NRTL of Chen [25]. Representative results he obtained are given in figure 7.19 and 7.20. The results and parameters are given in table 7.6. Mark Wijtkamp chose not to fit the nonrandomness factors and to use values of 0.2 and 0.3.

Now, it may be interesting to see how the electrolyte NRTL of Chen and its modification by Liu behave when the parameters found in section 7.3.3 for the NRTL-MSA for the system water + 2-propanol + NaCl, with α_{12} fitted, are used as first estimations for the electrolyte NRTL of Chen and Liu. Therefore, these regressions were carried out and it turned out that the results found with the electrolyte NRTL can also be improved greatly. The results of this attempt are also given in table 7.6 and figure 7.21 and 7.22. Although it is not common to do so for liquid-liquid equilibria (see section 3.4.1), it appears that fitting one of the nonrandomness factors outside the range 0.2-0.4 can have a large effect on the performance of the model.

Table 7.6: Parameters and results for the electrolyte NRTL of Chen [12] and its modification by Liu [25] for the system water (1) + 2-propanol (2) + NaCl (3) at 25°C. (* = fixed during regressions)

Parameter	Chen		Liu	
τ_{12}	4.879	3.421*	1.827	3.421*
τ_{21}	-1.145	0.941*	0.131	0.941*
τ_{13}	8.803*	26.88	8.803*	26.30
τ_{31}	-4.514*	-3.795	-4.514*	-4.230
τ_{23}	2.160	1.546	11.31	1.623
τ_{32}	29.76	2.091	7.152	2.399
α_{12}	0.30*	0.598	0.30*	0.619
$\alpha_{1,ca}$	0.20*	0.20*	0.20*	0.20*
$\alpha_{2,ca}$	0.20*	0.20*	0.20*	0.20*
β_{ca}	-	-	-1.956	-1.956*
Δx (mole/mole)	0.040	0.005	0.020	0.007
Δx (w/w)	0.035	0.007	0.029	0.009

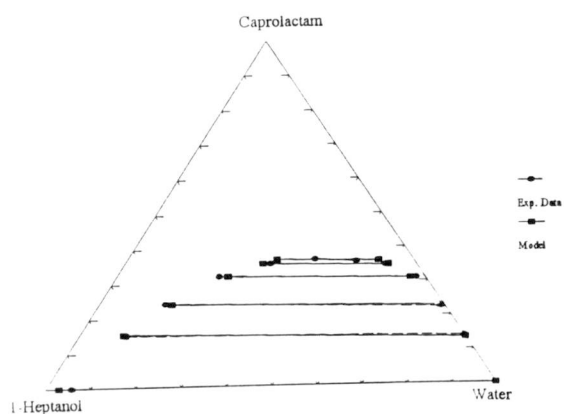


Figure 7.23: Experimental data and correlation by the NRTL model for the system water + 1-heptanol + caprolactam at 20°C

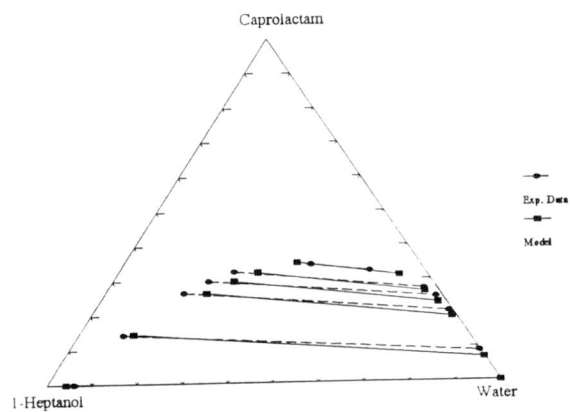


Figure 7.24: Experimental data and correlation by the NRTL model for the system water + 1-heptanol + caprolactam at 40°C

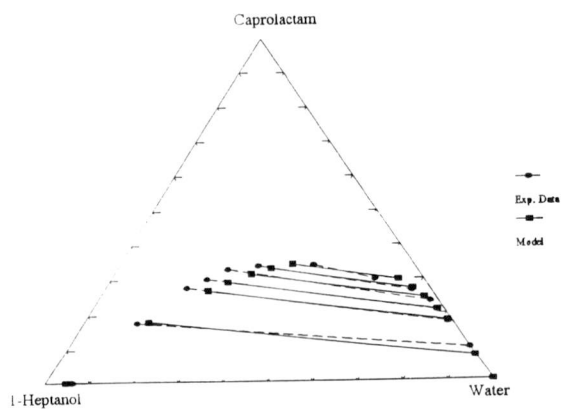


Figure 7.25: Experimental data and correlation by the NRTL model for the system water + 1-heptanol + caprolactam at 60°C

7.4 Modelling of experimental results

Because of the very laborious search for satisfactory results with ternary systems of electrolyte solutions (section 7.3), there was not enough time left to obtain a good fit for the quaternary systems of caprolactam + water + solvent + ammonium sulfate. For a system with four components, the model contains six binary systems, meaning six nonrandomness factors and twelve binary interaction parameters to be fitted. Although several of these parameters can be adopted from ternary systems, the modelling of the quaternary system introduces new difficulties. However, the ternary systems without ammonium sulfate that were determined can be modelled with the NRTL model. This has been done by Mark Wijtkamp. The results he obtained were copied and slightly improved by additional regressions with the relative objective function, equation (6.19). The parameters are given in table 7.7. The triangular diagrams are shown in figure 7.23 up to 7.25.

Table 7.7: Parameters and results of the molecular NRTL for the ternary systems water (1) + 1-heptanol (2) + caprolactam (3) at 20°, 40° and 60°C (* = fixed during regressions)

Parameter	20°C	40°C	60°C
τ_{12}	10.812	9.431	9.613
τ_{21}	0.936	0.329	0.246
τ_{13}	-2.200	-7.991	-2.434
τ_{31}	-1.529	-1.415	-1.480
τ_{23}	-1.907	-6.047	-1.656
τ_{32}	-2.207	-2.715	-2.899
α	0.20*	0.20*	0.20*
α	0.30*	0.30*	0.30*
α	0.30*	0.30*	0.30*
Δx (w/w)	0.032	0.033	0.028
Δx (mol/mol)	0.025	0.029	0.027

The nonrandomness factors were fixed during the regression. From the figures, it can be seen that the NRTL model has difficulties to describe the critical region, where the binodal curve flattens out. This affects the representation of the datapoints outside the critical region. The slope of the tie-lines is well predicted by NRTL.



8. Conclusions & recommendations

The objectives of this work were twofold. The first objective was the collection of liquid-liquid equilibrium data for the system water + 1-heptanol + caprolactam + ammonium sulfate at 20°, 40° and 60°C. Secondly, a dedicated thermodynamic model for the description of liquid-liquid equilibria of mixed solvent electrolyte systems had to be developed to enable modelling of the extraction process of caprolactam.

Liquid-liquid equilibria were measured for the systems water + caprolactam + cyclohexane at 20°C, water + caprolactam + 1-heptanol at 20°, 40° and 60°C, and the system water + caprolactam + 1-heptanol + ammonium sulfate at 40° and 60°C at salt concentrations of approximately 5, 15 and 30 wt %. It was found that cyclohexane is not a good solvent for the extraction of caprolactam: hardly any caprolactam dissolves in the organic phase. A much better solvent seems to be 1-heptanol. Above 20°C, the solubility of caprolactam in 1-heptanol is even larger than in water and the demixing area is large enough to enable the use of 1-heptanol in the extraction process. At increasing temperature, the solubility of caprolactam in 1-heptanol increases to a greater extent than the solubility in water. This means that the forward extraction is favoured by a lower process temperature, whilst the backward extraction is favoured by a higher temperature during extraction. The presence of ammonium sulfate facilitates the extraction. The experiments show that the caprolactam is salted out to the organic phase almost completely. The salt out effect of ammonium sulfate increases with temperature. It may be concluded that the ammonium sulfate introduces a large nonideality to the system. The ammonium sulfate reduces the availability of the solvent (water) molecules to the caprolactam and salt it out to the organic phase. Hardly any ammonium sulfate dissolves in the organic phase, especially at lower temperatures.

In the second part of this graduation work an attempt has been made to model liquid-liquid equilibria of mixed solvent electrolyte solutions. Therefore, the Mean Spherical Approximation [6] activity coefficient expression was programmed in FORTRAN and the performance of the MSA in predicting mean ionic activity coefficients was studied. It appeared that the MSA theory can predict the mean ionic activity coefficients well when a fitted diameter for the cation and the Pauling diameter is used for the anion, respectively. Then the program was extended to carry out liquid-liquid flash calculations for mixed solvent electrolyte solution, using a specified activity coefficient model, with experimental data to regress the parameters. For this purpose the MSA was combined with the Non Random Two Liquid (NRTL) theory of Renon and Prausnitz [35].

At first the approach of Lee [22] was followed, which consists of combining the molecular NRTL for the solvent species with the MSA for the ionic species. Since this did not result in a successful representation, a second approach was followed. Here the MSA model, still explicitly containing the hard sphere contribution, was combined with the local composition contribution of the electrolyte NRTL of Chen [12]. This proved to be an improvement towards the former approach, but the model still did not produce results with the desired accuracy. Since the hard sphere contribution was not present in the first publications of the unrestricted MSA and the NRTL implicitly accounts for this short range contribution, the hard sphere contribution to the ionic activity coefficient was dropped. This worked out well and did produce better results than the former models. Although this new NRTL-MSA model has not been tested enough yet, the first results do look promising. Compared with the modification of the electrolyte NRTL of Liu [25], it may, with some reserves, be concluded that the NRTL-MSA, developed

in this work, performs better than the electrolyte NRTL. Besides this, it must be emphasized that the MSA model has a better physical background than the Debye-Hückel model and takes into account ion size effects. However, a more founded conclusion that can prove the expected superiority of the MSA theory, must be based on more modelling work.

Recommendations

The results of the discussed NRTL-MSA look promising, but the model requires more work. Therefore, the following recommendation are made:

- More modelling work should be done, including examinations on the behaviour of the NRTL-MSA model in the vicinity of the critical region.
- The calculation of the physical properties of the solutions, from those of the individual solvents, should be studied thoroughly, including the taking into account of the mixing rules applied in a correct deviation of the activity coefficient. The use of solvent mole fractions to calculate solution properties, used in the expression for the MSA excess free Helmholtz energy, should result in an additional MSA contribution to the solvent activity coefficient.
- A combination of UNIQUAC and MSA should be considered for the calculation of liquid-liquid equilibria of mixed solvent electrolyte systems. The UNIQUAC model is claimed to be physically more correct and to produce (slightly) better results than the NRTL model [41].
- Since it is physically more correct than the primitive MSA used here and first results are encouraging, the nonprimitive Mean Spherical Approximation should be worked out for mixed solvent systems and be tested on the same systems the NRTL-MSA is applied to.
- It is recommended that more experimental liquid-liquid equilibria are measured to facilitate a solvent choice for the extraction process of caprolactam, to gain more binary interaction parameters of solvents with caprolactam and to extend the selection of systems that can be used to test the NRTL-MSA model.
- A method should be programmed to get better initial parameters for the regression. An option would be to use the Levenberg-Marquardt routine only for the refinement of the parameter regressions and to use a more global method, like a sophisticated grid search for the restriction of the parameter region.

systematic

pattern

eq by γ_{\pm}^{∞}

$\ln \gamma_{\pm}^{\infty}$

References

1. Aspen Technology. Inc., 'Physical property methods & models', ASPEN PLUS manual release 9, volume 2. (1988)
2. Riedel-de Haën, 'Hydranal manual', Seelze (1994)
3. Akerlof, G., 'Activity coefficients of sodium, potassium and lithium chlorides and hydrochloric acid at infinite dilution in water-methyl alcohol mixtures', *Journal of the American Chemical Society*, **1930**, 52, p2353-2369.
4. Austgen, D.M. et al., 'Model of vapor-liquid equilibria for aqueous acid gas-alkanolamine systems using the electrolyte-NRTL equation', *Industrial Engineering and Chemistry Research*, **1989**, 28, p1060-1073.
5. Ball, F.X., H. Planche, W.Furst, H. Renon, 'Representation of deviation from ideality in concentrated aqueous solutions of electrolytes using a mean spherical approximation molecular model' *AIChE Journal*, **1985**, 31, 8, p1233-1240
6. Blum, L., 'Mean spherical model for asymmetric electrolytes. I. Method of solution' *Molecular Physics*, **1975**, 30, 5, p1529-1535.
7. Blum, L. and J.S. Hoye, 'Mean spherical model for asymmetric electrolytes. 2. Thermodynamic properties and the pair correlation function', *Journal of Physical Chemistry*, **1977**, 81, 13, p1311-1316.
8. Blum, L., D.Q. Wei, 'Analytical solution of the mean spherical approximation for an arbitrary mixture of ions in a dipolar solvent', *Journal of Chemical Physics*, **1987**, 87, 1, p555-565.
9. Cardoso, M.J.E. de M., J.P. O'Connell, 'Activity coefficients in mixed solvent electrolyte solutions', *Fluid Phase Equilibria*, **1987**, 33, p315-326.
10. Chandler, D., H.C. Andersen, 'Mode expansion in equilibrium statistical mechanics. II. A rapidly convergent theory of ionic solutions', *Journal of Chemical Physics*, **1971**, 54, 1, p26-35.
11. Cheluguet, E.L. et al, 'Equilibrium in biphasic aqueous systems: A model for the excess Gibbs energy' *Journal of Solution Chemistry*, **1994**, 23, 2, p275-305.
12. Chen, C.C. et al, 'Local composition model for excess Gibbs energy of electrolyte systems' *AIChE Journal*, **1982**, 28, 4, p588-596
13. Chen, C.C., L.B. Evans, 'A local composition model for the excess Gibbs energy of aqueous electrolyte systems' *AIChE Journal*, **1986**, 32, 3, p444-454.
14. Corti, H.R., 'Prediction of activity coefficients in aqueous electrolyte mixtures using the mean spherical approximation' *Journal of Physical Chemistry*, **1987**, 91, p686-689
15. Gering, K.L., Lloyd L. Lee and L.H. Landis, 'A molecular approach to electrolyte solutions: Phase behaviour and activity coefficients for mixed-salt and multisolvent systems.' *Fluid Phase Equilibria*, **1989**, 48, p111-139.
16. Haase, K., unpublished results
17. Humffray, A.A., 'Comment on: "Theoretical single ion activity of calcium and magnesium ions in aqueous electrolyte mixture"', *Journal of Physical Chemistry*, **1983**, 87, p5521-5522
18. Koak, N., Some computational and experimental aspects of polymer solution phase behaviour, Ph.D. thesis University of Calgary (1997)
19. Kroschwitz. J.I., M. Howe Grant (Eds.), Kirk-Othmer Encyclopedia of Chemical Technology, 4th ed. (1991-1998)

20. Lebowitz, J.L. and J.K. Percus, 'Mean spherical model for lattice gases with extended hard cores and continuum fluids' *Physical Review*, **1966**, 144, 1, p251-258.
21. Lee, Lloyd L., *Molecular Thermodynamics of Nonideal Fluids*, Boston (1988)
22. Lee, Lloyd L., 'Accurate prediction of physical properties for acid gas treating', *Proceedings of the seventy-fifth GPA annual convention*, **1996**, p92-101
23. Li, C., Y. Lu, L. Yang, 'Study of ionic activity coefficients in aqueous electrolytes by the non-primitive mean spherical approximation equation', *Fluid Phase Equilibria*, **1996**, 124, p99-110.
24. Lide, R. (Ed.), *CRC Handbook of Chemistry and Physics*. 76th ed., Boca Raton (1995)
25. Liu, Y, S.Watanasari, 'Representation of liquid-liquid equilibrium of mixed solvent electrolyte systems using the extended electrolyte NRTL model' *Fluid Phase Equilibria*, **1996**, 116, p193-200.
26. Luckas, M., D.M.Eden, 'Improved representation of the vapor-liquid equilibrium of HCl-H₂O', *AIChE Journal*, **1995**, 41, 4, p1041-1043.
27. Mansoori, G.A., N.F. Carnahan, K.E. Starling, T.W.Leland, 'Equilibrium thermodynamic properties of the mixture of hard spheres' *Journal of Chemical Physics*, **1971**, 54, 4, p1523-1525
28. Mazo, R.M. and C.Y.Mou, In: *Activity Coefficients in Electrolyte Solutions*, K.S. Pitzer (Ed), 2nd Ed., Boca Raton (1991)
29. McMillan, W.G. and J.E. Mayer, 'The statistical thermodynamics of multicomponent systems' *Journal of Chemical Physics*, **1945**, 13, 7, p276-305.
30. Nightingale, E.R., 'Phenomenological theory of ion solvation. Effective radii of hydrated ions.', *Journal of Physical Chemistry*, **1959**, 63, p1381-1387
31. Passarello, J.P., W. Fürst, 'Representation of the equilibrium properties of the H₂O-HNO₃-N₂O₅ system using the MSA electrolyte model.' *Fluid Phase Equilibria*, **1996**, 116, p177-184.
32. Perry, R. (Ed.), *Perry's Chemical Engineer's Handbook*, 7th ed. (1997)
33. Planche, H., H. Renon, 'Mean spherical approximation applied to a simple but nonprimitive model of interaction for electrolyte solutions and polar substances' *Journal of Physical Chemistry*, **1981**, 85, p3924-3929.
34. Rashin, A.A., B.Honig, 'Reevaluation of the Born model of ion hydration', *Journal of Physical Chemistry*, **1985**, 89, 26, p5588-5593.
35. Renon, H., J.M.Prausnitz, 'Local compositions in thermodynamic excess functions for liquid mixtures' *AIChE Journal*, **1968**, 14, 1, p135-144
36. Robinson, R.A., R.H.Stokes, *Electrolyte solutions*, London (1959)
37. Santis, R. de, 'Liquid-liquid equilibria in water-aliphatic alcohol systems in the presence of sodium chloride' *The Chemical Engineering Journal*, **1976**, 11, p207-214.
38. Simonin, J.P, L.Blum, P.Turq, 'Real ionic solutions in the Mean Spherical Approximation. 1. Simple salts in the primitive model' *Journal of Physical Chemistry*, **1996**, 100, p7704-7709
39. Simonin, J.P., 'Real ionic solutions in the Mean Spherical Approximation. 2. Pure strong electrolytes up to very high concentrations, and mixtures, in the primitive model' *Journal of Physical Chemistry*, **1997**, 101, p4313-4320
40. Simons, A.J.F., N.F.Haasen, In: *Handbook of Solvent Extraction*, T.C. Lo et al. (Eds.) (1991)
41. Sørensen, J.M. et al., 'Liquid-liquid equilibrium data: their retrieval, correlation and prediction, part II: Correlation', *Fluid Phase Equilibria*, **1979**, 3, p47-82.
42. Sun, T., J.L.Lenard, A.S. Teja, 'A simplified mean spherical approximation for the prediction of the osmotic coefficients of aqueous electrolyte solutions' *Journal of Physical Chemistry*, **1994**, 98, p6870-6875

43. Triolo, R., J.R.Griger and L.Blum, 'Simple electrolytes in the Mean Spherical Approximation' *Journal of Physical Chemistry*, **1976**, 80, 17, p1858-1861.
44. Triolo, R., L. Blum and M.A. Floriano, 'Simple electrolytes in the mean spherical approximation. III. A workable model for aqueous solutions' *Journal of Chemical Physics*, **1978**, 67, 12, p5956-5959.
45. Waisman, E. and J.L. Lebowitz, 'Exact solution of an integral equation for the structure of a primitive model of electrolytes' *Journal of Chemical Physics*, **1970**, 52, p4307-4309.
46. Waisman, E. and J.L. Lebowitz, 'Mean spherical model integral equation for charged hard spheres, I. Method of solution' *Journal of Chemical Physics*, **1972**, 56, 6, p3086-3093.
47. Waisman, E. and J.L. Lebowitz, 'Mean spherical model integral equation for charged hard spheres. II. Results', *Journal of Chemical Physics*, **1972**, 56, 6, p3093-3099.
48. Walas, S.M., Phase equilibria in chemical engineering, London (1985)
49. Wu, R.S, L.L.Lee, 'Vapor-liquid equilibria of mixed solvent electrolyte solutions: ion-size effects based on the MSA theory', *Fluid Phase Equilibria*, **1992**, 78, p1-24
50. Zerres, H., J.M.Prausnitz, 'Thermodynamics of phase equilibria in aqueous-organic systems with salt', *AIChE Journal*, **1994**, 40, 4, p676-691

List of symbols

a	Closest approach parameter extended Debye-Hückel
A	Helmholtz free energy
A, B	Debye-Hückel parameter
c	Concentration
C	Debye-Hückel parameter
C	Electrolyte NRTL parameter
C_{ij}	Direct correlation function
d	Solution density
e	Charge of an electron
F_n	Variable in hard sphere equation
F_{OBJ}	Objective function
G_i	Gibbs energy component i
ΔG_m	Gibbs energy of mixing
g_{ij}	Radial distribution function
g_{ji}	Energy of interaction between molecules of type i and j
h_{ij}	Total correlation function
I	Ionic strength
I_x	Mole fraction based ionic strength
k	Boltzmann constant
K_i	Distribution coefficient
K	Dissociation constant
m	Damping or acceleration factor
m	Salt molality
M_B	Solvent molar mass
M	Molar weight
n_i	Number of moles i
n_s	Number of solvents
ndp	Number of experimental datapoints
nc	Number of components
N	Number of particles N
N_A	Avogadro's number
P	Pressure
P_n	MSA Coupling parameter (electrostatic effects to geometric effects)
q_i	Charge on i -th type ion
Q	Partition function
r_{ij}	Distance between centres molecule i and j
r_i^{Born}	Ionic cavity radius or Born radius
R	Universal gas constant
S	Standard deviation
S	Entropy
$t_{\alpha/2}$	Value Student's distribution
T	Temperature
u_{ij}	Interaction energy
U	Internal energy

U_j	Energy of the j -th quantum state
$\langle v_i \rangle$	Partial molar volume
V	Volume
w	Mass fraction
W_{ij}	Parameter nonprimitive MSA
x_i	Mole fraction component i
X_{ij}	Local mole fraction of i in the direct neighbourhood of j
X_n	Variable in hard sphere equation
y	Variable in hard sphere equation
z	Valence
z_i	Overall mole composition
Z_i	Absolute charge number
Z	Compressibility factor
α_{ij}	NRTL nonrandomness factor
α	Parameter
α	Dissociation fraction
α	Probability
β	Boltzmann thermal factor $= (kT)^{-1}$
β	Brønsted-Guggenheim parameter
β	Fraction of phase I
γ_i	Activity coefficient component i
γ_{\pm}	Mean ionic activity coefficient
Γ	MSA shielding parameter
δ	Dirac function
Δ	Volume fraction of the solvent
Δx	Average deviation
ε	Dielectric constant
ζ	Chain sum
κ	Debye-Hückel shielding parameter
μ_i	Chemical potential component i in phase I or II
μ	Dipole moment
ν_i	Stoichiometric coefficient
ξ	Variable in hard sphere equation
Ξ	Partition function of the grand canonical ensemble
Π	Osmotic pressure
ρ	Numerical density, molecules per volume
ρ	Closest approach parameter Pitzer Debye-Hückel
σ	Mean ionic diameter
σ_i	MSA Hard core diameter of molecule i
σ_{ij}	MSA Closest distance of approach
$\sigma^{(i)}$	Parameter
τ_{ji}	NRTL binary interaction parameter
ϕ	Osmotic coefficient
Φ^{mnl}	Angular function
Ω	MSA parameter
ψ	Electrostatic potential

Gas chromatography: calibration

Caprolactam

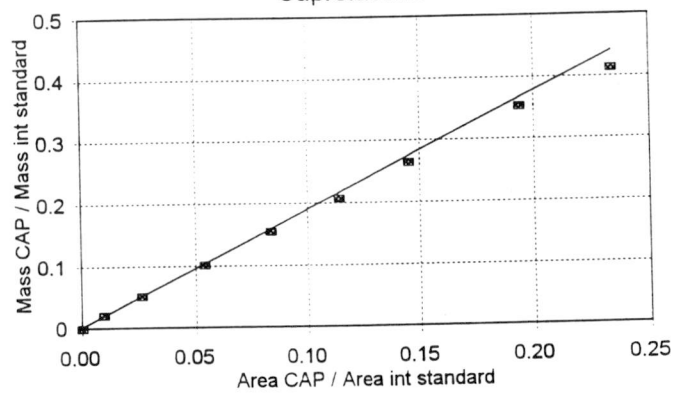


Figure I.1: Example of an regression line, used to calculate the caprolactam mass fraction of a sample with an expected mass fraction of 0.05

Appendices

Appendix I : Analyses

This appendix gives a short description of the analytical methods and procedures used in the liquid-liquid equilibrium measurements. Gas chromatography was used to determine caprolactam, cyclohexane and 1-heptanol concentrations, Karl-Fischer titration was used to determine the water concentrations, while titration with barium perchlorate was used for the determination of ammonium sulfate concentrations.

1. Gas chromatography

1.1 Principles

Gas chromatography is a well-known method for qualitative and quantitative determination of organic substances by means of a stationary and a mobile phase. Separation of the components in a mixture is based on differences of interaction of the component molecules in the mobile gas phase with the material of the stationary phase (a liquid film on a capillary column). The sample is injected as a liquid and directly vaporized. The carrier gas (helium) carries the sample through the column. The components distribute in both phases. The extent of interaction with the stationary phase determines the retention time, the time passed before the components leave the column. The components are usually detected using a Flame Ionisation Detector. The resulting signal can be used for the determination of the components. The retention time is used for the qualitative determination. The magnitude of the signal indicates the amount of a certain component present in the sample. The retention times may be reduced by a temperature program, which increases the temperature during the process. The exact composition of a sample can be determined using the internal standard method: a known amount of a compound (not present in the sample) is injected with the sample to correct for fluctuations which affect the magnitude of the signal. Standards of each component in the sample are used to relate the signal to a concentration.

1.2 Procedure

Either 0.15 grams (top phase) or 0.30 grams (bottom phase) of the sample is diluted with 20 ml methanol. About 0.15 grams of the internal standard toluene are added to the dilution. The use of methanol as the solvent causes the dissolved salt in the sample to precipitate, which would disturb the performance of the capillary column or would lead to blockage of the injector. After the salt is precipitated, the dilution is pipetted in a vial which is put in the automatic sampler of the gas chromatograph. The integrator connected to the GC records and interprets the signals from the detector and prints the retention time and the magnitude of the signal in a number of units. The retention time is used to identify the components, the solvent and the internal standard. The number of units of a component relative to the number of units of the internal standard is used for the determination of the mass fraction, using a calibration line of at least five standards. It was tried to have at least one standard or calibration within 10% of each sample concentration. Since the regression line is not a straight line (see figure I.1) only the nearest three to five points were used in the regression.

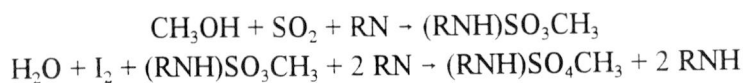
1.3 Equipment

The analyses were performed using an HP 5890 Series II gas chromatograph with an HP 7673 automatic sampler (injected volume: 0.5 μ l) and an HP 3396 Series II integrator. The sampling was performed using split injection with a split ratio of 1:57 and an injection temperature of 225°C. Detection was performed by a Flame Ionization Detector operating at a temperature of 260°C. The column was a 30 m \times 0.53 mm DB5 (J&W Scientific) .

2. Karl-Fischer titration

2.1 Principles

In 1935 Karl-Fischer published his new method for the determination of water. Nowadays his method is has been developed into a worldwide use analytical method. The Karl-Fischer titration is based on a water consuming reaction in which sulfur dioxide reacts with an alcohol to form alkyl sulfurous acid. This alkyl sulfite anion is oxidated by iodine to the alkyl sulfate. The equations for this reaction are:



where RN is a base to neutralize the ester formed by the reaction of the alcohol and sulfur dioxide. The base currently used is imidazole, which has proven to ensure a rapid and accurate Karl-Fischer titration. Methanol is the used alcohol and serves as the solvent. The endpoint is reached when the potential of the solution remains constant for a specified length of time.

2.2 Procedure

The titrator consists of a continuously stirred glass vessel tightly closed with a plastic seal. In this vessel about 40 ml solvent is brought by a pump. A known amount of sample is introduced using a syringe. Consequently, the solution is automatically titrated using a dispensing burette. The titre is, dependent on the expected water content (0- 40% or 40-100% water), a solution of sulfur dioxide and imidazole in methanol which reacts with about 2 or 5 mg water per ml titre. The end point is automatically determined by the titrator. The water determination of each sample is repeated 5 times. The titre is regularly calibrated using sodium tartrate dihydrate, which has a water content of 15.66%. Although the reservoirs of the titre and the solvent are protected from atmospheric water penetrating the glass vessel by drying tubes, the results are corrected for water penetrating the vessel. This is done by measuring the water consumption without sample introduced (the so-called drift) for about 5 minutes. [2]

2.3 Equipment

The analyses were performed using a Mettler DL 35 Karl-Fischer titrator. Two titrants were used: for high water concentrations Hydranal titrant 5 was used, for low concentrations Hydranal titrant 2. The solvent was Hydranal solvent. (Titrant and solvent were obtained from Riedel-de Haen.). The used electrode was a Mettler DM 142 electrode.

AS titration curve

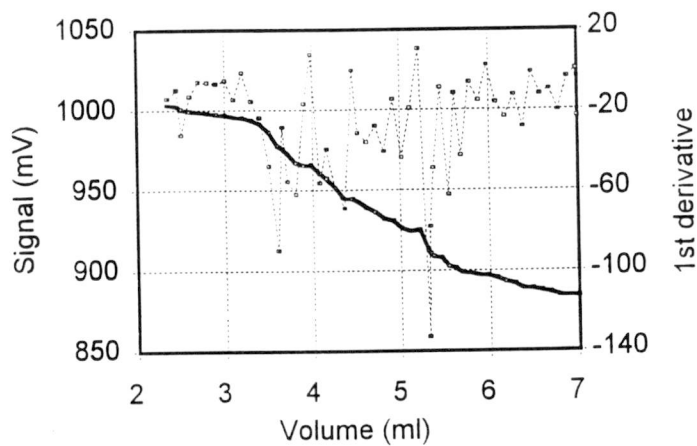
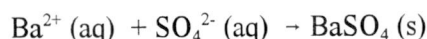


Figure V.2: Example of a result of an ammonium sulfate mass fraction determination. illustrating the difficulties of the endpoint determination.

3. Determination of ammonium sulfate

3.1 Principles

Ammonium sulfate contents are determined using titration with barium perchlorate (= Ba(ClO₃)₂). The titration is based on the precipitation of barium sulfate:



The endpoint can be determined photometrically using thorin as adsorption indicator. The reaction of barium with sulfate can be interfered by other metal ions that can block the indicator. Interference by other anions is also possible. Since water has a disturbing effect on the phototrode, a mixture of an alcohol and water has to be used as solvent.

3.2 Procedure

Before titration, samples have to be diluted to a mass fraction of ammonium sulfate of about 0.005. Then 0.5 grams of the dilution are weighted and mixed with 60 ml of a solvent, which consists of 20% water, 80% propanol and 0.005 mol/l Ba(ClO₄)₂. Some drops of thorin are added to the solution and the pH is adjusted to about 3-4 with 0.1 mol/l HClO₄. The titration is carried out using an apparatus comparable to that of the Karl-Fischer titration. A phototrode is used to detect the colour change from orange to pink. A signal is sent to a computer that interprets the data. The endpoint is (afterwards) determined from the first derivative of the signal from the phototrode. The endpoint is assumed to be at the maximum of this first derivative. Since the phototrode is very sensitive and there is only a slight colour change, a lot of scattering is found in the data, which leads to uncertainties in the endpoint determination (see for example figure ?). (Fitting the data to a function such as arctan(x) does not result in a significant improvement.) The concentration of the titre was checked by atomic spectrometry. Results that deviated more than 5% were ignored.

3.3 Equipment

The ammonium sulfate titrations were performed using a Mettler DL21 Titrator. The endpoint was detected by a Mettler DP 550 Phototrode.

Appendix II : Error analysis experiments

To obtain an indication of the errors in the mass fraction determinations, a series of five “samples” was prepared with known compositions over the whole range of the compositions in the experiments. The compositions were chosen in such a way that no demixing occurred. The samples were analysed several times on the way described in appendix I. Table II.1 and II.2 give the real mass fractions and the mass fractions resulting from the analyses:

Table II.1: Real mass fractions of the samples used to estimate the experimental errors

	Caprolactam	Water	1-Heptanol	AS
1	0.2998	0.1001	0.6001	-
2	0.1005	0.8495	-	0.0500
3	0.1501	0.0501	0.7998	-
4	-	0.7000	-	0.3000
5	0.4001	0.2001	0.3998	-

Table II.2: Measured mass fractions of the samples in table II.1

	Caprolactam	Water	1-Heptanol	AS	SUM
1	0.3021	0.1015	0.5949	-	99.9 %
2	0.0972	0.8403	-	0.0512	98.9 %
3	0.1466	0.0527	0.7938	-	99.3 %
4	-	0.6960	-	0.3102	100.6 %
5	0.4037	0.1983	0.3976	-	100.0 %

From repeated analyses of the samples, both the test samples from table II.1 and the real samples, an indication can be obtained of the statistical errors in the analyses. The calculation of statistical errors is performed in the usual way and is summarized in the equations below:

$$S_{abs} = \sqrt{\frac{\sum (x_i - \bar{x})^2}{n-1}} \quad (\text{II.1})$$

$$S_{rel} = \frac{S_{abs}}{\bar{x}} \cdot 100\% \quad (\text{II.2})$$

$$\Delta x = \frac{t_{\alpha/2} S_{abs}}{\sqrt{n}} \quad (\text{II.3})$$

where: S_{abs} = Absolute sample standard deviation
 S_{rel} = Relative sample standard deviation
 Δx = Statistical error
 $t_{\alpha/2}$ = Value Student's distribution at a probability α and $n-1$ degrees of freedom

- n = Number of datapoints
 x_i = Sample value

A short discussion will now follow for each of the used analytical methods. For α a value of 5% was taken in the calculations. (This means there is a probability of 95% that a sample falls within the average value plus or minus the statistical error. Systematic errors are not accounted for.)

Gas chromatography

All test samples were analysed four times on caprolactam and 1-heptanol. Four test samples contained caprolactam, three of the test samples contained 1-heptanol. From these samples mean statistical errors and standard deviations can be calculated. They are tabulated in table II.3:

Table II.3: Average standard deviations and errors of the GC analysis of heptanol and caprolactam mass fractions

	Caprolactam	1-Heptanol
Relative standard deviation	0.013	0.005
Absolute statistical error	0.004	0.004
Relative statistical error	0.020	0.007
Deviation from real value	0.003	0.004

It was observed that the absolute error remained more or less the same over the concentration range and thus may be considered as not dependent on the concentration. It can be seen from the table that the results for caprolactam and 1-heptanol are almost equal. The mean relative standard deviation and mean relative error in the caprolactam mass fraction is higher due to the higher 1-heptanol concentrations used. The errors in the mass fraction determination may be due to several reasons: errors are introduced with the making of the dilution, with the injection in the gas chromatograph, with the detection and with the interpretation of the results.

It may be noticed that the real mass fractions (table II.1) do not always lie in the confidence interval of the measured fractions, but one should keep in mind that there are other errors which cannot be determined in this way. For instance those related to the regression line, since the same regression line was used for all the test samples. The regression line may be changed by evaporation of solvent from the standards and is also subjected to weighting errors, which have an increasing influence on lower concentrations. The weighting errors are for caprolactam enlarged by the high hygroscopy of this compound.

Karl-Fischer titration

Since all the water determinations had to be repeated at least five times for all the samples, an error estimation can be based on a large amount of measurements, besides the test samples. The water determinations can be divided into two water concentration ranges: from 0 to 40 and from 40 up to 100 mass percent. The water fractions in these ranges were respectively determined with a 2g/ml titrant and a 5 ml burette and a 5 g/ml titrant and a 25 ml burette. This division can also be found in table II.4, where the standard deviations and estimated statistical errors are tabulated.

Table II.4: Average standard deviations and statistical errors of the water analysis using Karl-Fischer titration

	0-40% water	40-100% water
Relative standard deviation	0.0207	0.0107
Absolute statistical error	0.0037	0.0088
Relative statistical error	0.0232	0.0115

The determination of water may introduce an absolute deviation of almost 1% follows from the table. This is rather large, but the determination of a water content is known to be difficult. The proper use of Karl-Fischer titration is for the determination of low water concentrations. The method can be used for larger concentration when large amounts of chemicals are used or only very small amounts of a sample are used. The small amounts of sample (about 10-50 μ l) is the main reason for the errors being rather large. Also, excluding water from outside totally is impossible and the amount of this drift is not constant and can only be estimated. However, the determination of water by analysis is always better than calculation from a mass balance. At lower concentrations a relatively larger error is made. This may be because the uncertainties in the drift velocity have a higher impact on small concentrations than on larger concentrations.

Ammonium sulfate titration

The determination of ammonium sulfate was carried out using photometric titration. This method is rather time consuming and interpretation of the results is tricky and sensitive to errors as mentioned in appendix II. However, better methods were not available or feasible in the laboratory. The used method led to the results as tabulated in table II.5:

Table II.5: Average standard deviations and estimated statistical errors of the ammonium sulfate analysis using titration with barium perchlorate

Relative standard deviation	0.0351
Absolute statistical error	0.0075
Relative statistical error	0.0455

The relative errors remain rather constant over the concentration range. The absolute error changes from 0.002 at 5% ammonium sulfate to 0.014 at the highest concentrations. This is rather high and must be due to two reasons: the sample is diluted about 60 times, so titration errors are multiplied by a factor 60 and this large dilution itself also introduces larger errors, since weighting errors have an increasing influence at higher dilutions. (The relative error in the ammonium sulfate determination at DSM's Chemlab is 4.5% using ionic chromatography)

Appendix III : Experimental results

- x_1 = water mass fraction
 x_2 = 1-heptanol mass fraction
 x_3 = caprolactam mass fraction
 x_4 = ammonium sulfate

Table III.1: Results and overall compositions of the experiments on the ternary system water + 1-heptanol + caprolactam

Temperature (°C)	Overall compositions			Organic phase				Aqueous phase			
	x_1	x_2	x_3	x_1	x_2	x_3	$\sum x_i$	x_1	x_2	x_3	$\sum x_i$
20.0	0.5000	0.5000	0.0000	0.0587	0.9500	0.0000	100.87%	0.9955	0.0000	0.0000	99.55%
	0.4500	0.4004	0.1496	0.1057	0.7429	0.1516	100.03%	0.8446	0.0000	0.1373	98.19%
	0.4935	0.2758	0.2307	0.1471	0.6112	0.2424	100.07%	0.7600	0.0069	0.2226	98.95%
	0.4795	0.2113	0.3092	0.2285	0.4525	0.3207	100.18%	0.6708	0.0210	0.3099	100.16%
	0.4704	0.1803	0.3493	0.3282	0.3255	0.3604	101.41%	0.5855	0.0710	0.3501	100.67%
	-	-	-	0.4147	0.2155	0.3644	99.46%	0.5093	0.1272	0.3574	99.39%
40.0	0.5000	0.5000	0.0000	0.0612	0.9483	0.0000	100.95%	0.9892	0.0000	0.0000	98.92%
	0.4803	0.3994	0.1203	0.0998	0.7578	0.1429	100.06%	0.9023	0.0000	0.0890	99.13%
	0.4935	0.2758	0.2307	0.1723	0.5528	0.2612	98.63%	0.7787	0.0080	0.2034	99.02%
	0.5028	0.2288	0.2684	0.2125	0.4883	0.2994	100.03%	0.7393	0.0149	0.2498	100.40%
	0.5029	0.2004	0.2967	0.2580	0.4204	0.3278	100.62%	0.6962	0.0274	0.2719	99.55%
	0.5007	0.1664	0.3329	0.4180	0.2393	0.3441	100.14%	0.5574	0.1219	0.3268	100.61%
60.0	0.5000	0.5000	0.0000	0.0611	0.9476	0.0000	100.87%	0.9942	0.0000	0.0000	99.42%
	0.4892	0.3667	0.1441	0.1206	0.7019	0.1776	100.01%	0.8982	0.0000	0.0995	99.77%
	0.4955	0.2770	0.2274	0.1871	0.5482	0.2842	101.95%	0.8036	0.0097	0.1731	98.64%
	0.4987	0.2421	0.2591	0.2171	0.4800	0.3022	99.93%	0.7682	0.0168	0.2080	99.30%
	0.4999	0.2206	0.2795	0.2488	0.4175	0.3289	99.52%	0.7357	0.0181	0.2317	98.55%
	0.5002	0.1998	0.3000	0.3133	0.3470	0.3413	100.16%	0.6869	0.0426	0.2665	99.60%
	0.4987	0.1831	0.3182	0.4294	0.2173	0.3355	98.22%	0.5836	0.1042	0.2970	98.49%

Table III.2: Quaternary system water + 1-heptanol + caprolactam + ammonium sulfate at 40 and 60°C

T	Overall compositions				Organic phase					Aqueous phase				
	x_1	x_2	x_3	x_4	x_1	x_2	x_3	x_4	$\sum x_i$	x_1	x_2	x_3	x_4	$\sum x_i$
40°C	0.5153	0.4616	0.0000	0.0231	0.0558	0.9460	0.0000	0.0000	100.18%	0.9442	0.0000	0.0000	0.0497	99.38%
	0.4936	0.3866	0.0958	0.0240	0.0884	0.7735	0.1395	0.0000	100.15%	0.8857	0.0000	0.0569	0.0468	98.93%
	0.5059	0.2812	0.1891	0.0239	0.1352	0.6080	0.2552	0.0000	99.84%	0.8166	0.0033	0.1339	0.0489	100.27%
	0.4872	0.1966	0.2903	0.0259	0.2315	0.4002	0.3700	0.0018	100.35%	0.7086	0.0085	0.2155	0.0487	98.13%
	0.4897	0.4373	0.0000	0.0731	0.0528	0.9562	0.0000	0.0000	100.90%	0.8503	0.0000	0.0000	0.1421	99.25%
	0.4192	0.4159	0.0940	0.0708	0.0837	0.7700	0.1500	0.0000	100.36%	0.8075	0.0000	0.0255	0.1599	99.28%
	0.4873	0.2650	0.1779	0.0699	0.1346	0.5739	0.2957	0.0000	100.42%	0.7837	0.0000	0.0765	0.1386	99.88%
	0.4863	0.1777	0.2676	0.0683	0.2335	0.3523	0.4142	0.0026	100.25%	0.7364	0.0000	0.1163	0.1421	99.49%
	0.3779	0.4752	0.0000	0.0731	0.0436	0.9543	0.0000	0.0000	99.79%	0.6882	0.0000	0.0000	0.3111	99.93%
	0.3821	0.3779	0.0951	0.1469	0.0735	0.7527	0.1822	0.0000	100.84%	0.6976	0.0000	0.0092	0.3085	101.53%
	0.4064	0.2774	0.1783	0.1380	0.1169	0.5604	0.3413	0.0000	101.85%	0.6998	0.0000	0.0200	0.2755	99.53%
	0.4556	0.1673	0.2497	0.1273	0.2006	0.3327	0.4612	0.0022	99.67%	0.7034	0.0000	0.0375	0.2531	99.40%
60°C	0.5344	0.4384	0.0000	0.0272	0.0573	0.9492	0.0000	0.0000	100.65%	0.9475	0.0000	0.0000	0.0454	99.29%
	0.5397	0.3358	0.0976	0.0269	0.0988	0.7576	0.1500	0.0000	100.65%	0.8926	0.0020	0.0532	0.0451	99.30%
	0.5417	0.2246	0.2050	0.0288	0.1642	0.5359	0.3035	0.0000	100.36%	0.8112	0.0037	0.1342	0.0554	100.46%
	0.5443	0.1158	0.3109	0.0289	0.3567	0.2487	0.3952	0.0077	100.83%	0.6610	0.0336	0.2531	0.0481	99.58%
	0.5092	0.4069	0.0000	0.0839	0.0560	0.9522	0.0000	0.0000	100.82%	0.8441	0.0000	0.0000	0.1447	98.88%
	0.5088	0.3075	0.0978	0.0860	0.0954	0.7210	0.1852	0.0000	100.16%	0.8142	0.0000	0.0311	0.1471	99.24%
	0.5053	0.2134	0.1962	0.0851	0.1620	0.4873	0.3562	0.0007	100.63%	0.7764	0.0000	0.0664	0.1632	100.59%
	0.5624	0.0763	0.2815	0.0799	0.3711	0.1633	0.4471	0.0125	99.41%	0.7243	0.0000	0.1388	0.1521	101.53%
	0.4304	0.4087	0.0000	0.1609	0.0481	0.9682	0.0000	0.0000	101.63%	0.7134	0.0000	0.0000	0.2925	100.59%
	0.4379	0.3047	0.0954	0.1620	0.0845	0.7109	0.2067	0.0000	100.21%	0.7004	0.0000	0.0098	0.2980	100.82%
	0.4596	0.1860	0.1874	0.1670	0.1498	0.4565	0.4217	0.0006	102.86%	0.6862	0.0000	0.0188	0.3060	101.09%
	0.5443	0.1158	0.2566	0.1457	0.2393	0.2446	0.5108	0.0036	99.83%	0.6902	0.0000	0.0320	0.2869	100.91%

Table III.3: Quaternary system water + 1-heptanol + caprolactam + ammonium sulfate at 20°C. Experiments and analysis (except water analysis) performed by K.Haase, AS fraction bottom phase calculated by mass balances

Organic phase					Aqueous phase			
x_1	x_2	x_3	x_4	$\sum x_i$	x_1	x_2	x_3	x_4
0.0764	0.8185	0.1061	0.0000	100.10%	0.8643	0.0000	0.0473	0.0884
0.1058	0.7075	0.1826	0.0000	99.60%	0.8267	0.0000	0.1217	0.0516
0.1691	0.5383	0.2958	0.0000	100.32%	0.7285	0.0059	0.2177	0.0479
0.0710	0.8592	0.0822	0.0000	101.16%	0.7730	0.0000	0.0102	0.2168
0.0773	0.7975	0.1271	0.0000	100.19%	0.8235	0.0000	0.0323	0.1442
0.1259	0.6147	0.2587	0.0000	99.93%	0.7714	0.0000	0.0850	0.1436
0.0710	0.8040	0.1341	0.0000	100.90%	0.7216	0.0000	0.0097	0.2687
0.1075	0.6334	0.2762	0.0000	101.72%	0.7019	0.0000	0.0175	0.2807
0.1237	0.5634	0.3107	0.0000	99.78%	0.7055	0.0000	0.0260	0.2685

For the system water-cyclohexane-caprolactam only GC analyses were carried out. The following symbols are used in table III.4:

- x_1 = water mass fraction
 x_2 = cyclohexane mass fraction
 x_3 = caprolactam mass fraction

Table III.4: Ternary system water + caprolactam + cyclohexane at 20°C. The water content was not measured

Overall compositions			Organic phase		Aqueous phase	
x_1	x_2	x_3	x_2	x_3	x_2	x_3
0.5000	0.5000	0.0000	1.0000	0.0000	0.0000	0.000
0.4533	0.4329	0.1138	1.0000	0.0000	0.0000	0.1923
0.2526	0.4474	0.3000	0.9962	0.0000	0.0000	0.5320
0.1382	0.4482	0.4136	0.9848	0.0081	0.0121	0.7267
0.1014	0.5991	0.2994	0.9918	0.0078	0.0147	0.7401
0.0805	0.4699	0.4497	0.9873	0.0079	0.0330	0.8109

Appendix IV : Electrolyte NRTL model

$$\ln \gamma_i = \ln \gamma_i^{PDH} + \ln \gamma_i^{Born} + \ln \gamma_i^{NRTL}$$

$$\ln \gamma_i^{PDH} = - \left(\frac{2\pi N_A d}{M_B} \right)^{\frac{1}{2}} \left(\frac{e^2}{\epsilon_w kT} \right)^{\frac{3}{2}} \left(\frac{2z_i^2}{\rho} \ln(1 + \rho \sqrt{I_x}) + \frac{z_i^2 \sqrt{I_x} - 2I_x \sqrt{I_x}}{1 + \rho \sqrt{I_x}} \right)$$

$$I_x = \frac{1}{2} \sum x_i z_i^2$$

$$\ln \gamma_i^{Born} = \frac{e^2}{2kT} \left(\frac{1}{\epsilon} - \frac{1}{\epsilon_w} \right) \frac{z_i^2}{r_i}$$

$$\ln \gamma_M^{lc} = \frac{\sum_j X_j G_{jM} \tau_{jM}}{\sum_k X_k G_{kM}} + \sum_m \frac{X_m G_{Mm}}{\sum_k X_k G_{km}} \left(\tau_{Mm} - \frac{\sum_k X_k G_{km} \tau_{km}}{\sum_k X_k G_{km}} \right) + \frac{X_c G_{Sc}}{\sum_k X_k G_{kc}} \left(\tau_{Mc} - \frac{\sum_k X_k G_{kc} \tau_{kc}}{\sum_k X_k G_{kc}} \right) + \frac{X_a G_{Ma}}{\sum_k X_k G_{ka}} \left(\tau_{Ma} - \frac{\sum_k X_k G_{ka} \tau_{ka}}{\sum_k X_k G_{ka}} \right)$$

$$\frac{1}{Z_c} \ln \gamma_c^{lc} = \frac{\sum_k X_k G_{kc} \tau_{kc}}{\sum_k X_k G_{kc}} + \sum_m \frac{X_m G_{cm}}{\sum_k X_k G_{km}} \left(\tau_{cm} - \frac{\sum_k X_k G_{km} \tau_{km}}{\sum_k X_k G_{km}} \right) + \frac{X_a G_{ca}}{\sum_k X_k G_{ka}} \left(\tau_{ca} - \frac{\sum_k X_k G_{ka} \tau_{ka}}{\sum_k X_k G_{ka}} \right) - \tau_{wc} - G_{cw} \tau_{cw}$$

$$\frac{1}{Z_a} \ln \gamma_a^{lc} = \frac{\sum_k X_k G_{ka} \tau_{ka}}{\sum_k X_k G_{ka}} + \sum_m \frac{X_m G_{am}}{\sum_k X_k G_{km}} \left(\tau_{am} - \frac{\sum_k X_k G_{km} \tau_{km}}{\sum_k X_k G_{km}} \right) + \frac{X_c G_{ac}}{\sum_k X_k G_{kc}} \left(\tau_{ac} - \frac{\sum_k X_k G_{kc} \tau_{kc}}{\sum_k X_k G_{kc}} \right) - \tau_{wa} - G_{aw} \tau_{aw}$$

where j,k = Any component
 m = Molecular components
 c = Cation
 a = Anion
 w = Water

[1,13]

Appendix V : Electrostatic contribution neutral species

For the derivation of the electrostatic contribution to the activity coefficient of the neutral species, Lee [22] and Cardoso and O'Connell [9] found the same expression, although derived in a quite different way. This appendix gives a short description of both.

1. Derivation from Gibbs-Duhem integration

This derivation is not given in the article [22] where it was applied, but was obtained by Mark Wijtkamp from Lloyd Lee and is copied here without modifications. It was derived for the model which consisted of a combination of the molecular UNIFAC for the neutral species and the MSA for the ionic species.

The Gibbs-Duhem equation can be written in excess chemical potential or activity coefficient as:

$$S^E dT - V^E dP + \sum_i n_i d\mu_i^E = 0 \quad (\text{V.1})$$

$$S^E dT - V^E dP + RT \sum_i n_i d\ln\gamma_i = 0 \quad (\text{V.2})$$

At constant temperature and pressure, Eq. V.1 and V.2 can be written as:

$$RT \sum_j n_j d\ln\gamma_j + \sum_k n_k d\mu_k^E = 0 \quad (\text{V.3})$$

where j refers to all neutral species and k refers to all ions. Because

$$\sum_k n_k d\mu_k^E = V d\Pi, \quad (\text{V.4})$$

Eq. V.3 becomes:

$$\sum_j n_j d\ln\gamma_j = -\frac{V}{RT} d\Pi \quad (\text{V.5})$$

Integrate from a hypothetical solution containing only all neutral species to the real situation at constant neutral species concentrations and same conditions. We can obtain the electrostatic contribution on neutral species

$$\sum_j n_j \int_{\ln\gamma_j^0}^{\ln\gamma_j} d\ln\gamma_j = -\int_0^{\Pi} \frac{V}{RT} d\Pi \quad (\text{V.6})$$

where $\ln \gamma_j^0$ is calculated from UNIFAC, we can also express it as $\ln \gamma_i^{\text{UNIFAC}}$

$$\sum_j (\ln \gamma_j - \ln \gamma_j^{\text{UNIFAC}}) = -\frac{\langle V \rangle}{RT} \Pi \quad (\text{V.7})$$

The osmotic pressure Π can be obtained from MSA theory

$$\frac{\Pi}{RT} = -\frac{\Gamma^3}{3\pi} - \frac{\alpha^2}{8} \left(\frac{P_n}{\Delta} \right)^2 + Z^{\text{HS}} \sum_k \rho_k \quad (\text{V.8})$$

It was assumed that the excess pressure contribution is distributed to individual neutral species according to their concentration ratio. Eq. (V.7) then, can be written for each neutral species as

$$\ln \gamma_j - \ln \gamma_j^{\text{UNIFAC}} = \frac{1}{\sum_j \rho_j} \left[\frac{\Gamma^3}{3\pi} + \frac{\alpha^2}{8} \left(\frac{P_n}{\Delta} \right)^2 - Z^{\text{HS}} \sum_k \rho_k \right] \quad (\text{V.9})$$

2. Osmosis

The McMillan-Mayer thermodynamic system can be seen schematically as a container, consisting the solvent components and the salt. The container is divided in two compartments. The first compartment (A) only contains the solvents. The second compartment (B) contains the salt and also the solvents (with a different composition). The compartments are separated by a membrane permeable only to the solvents. The pressure in compartment B is equal to the pressure in compartment A plus the osmotic pressure. The equality of fugacities can be written for the solvent components:

$$x_i^A \gamma_i^A(T, P_0, x^A) f_i^0(T, P_0) = x_i^B \gamma_i^B(T, P_0 + \Pi, x^B) f_i^0(T, P_0 + \Pi) \quad (\text{V.10})$$

$$= x_i^B \gamma_i^B(T, P_0, x^B) f_i^0(T, P_0) \exp \left(\int_{P_0}^{P_0 + \Pi} \frac{\bar{v}_i(T, P_0 + \Pi, x^B)}{RT} dP \right) \quad (\text{V.11})$$

$$\equiv x_i^B \gamma_i^B(T, P_0, x^B) f_i^0(T, P_0) \exp \left[\frac{\langle \bar{v}_i \rangle \Pi}{RT} \right] \quad (\text{V.12})$$

Lewis-Randall models can provide expressions for the activity coefficients of the solute free system A, McMillan-Mayer models can provide an expression for the osmotic pressure Π . Since the solvent mole fractions in compartment A do usually not equal those in compartment B, the activity coefficients still can not be found. However, in practice the Lewis-Randall model is designed to include short range contributions to the solvents as well as to the solutes and thus also accounts for the short range contribution to the osmotic pressure (Π^{SR}). The ideal contribution to is given by equation (V.13). (This relation is valid for an ideal solvent solution with point solutes.) This yields the equation for the solvent activity coefficients:

$$\frac{\Pi^*}{RT} = -\frac{1}{\langle v_i \rangle} \ln(x_i^B/x_i^A) \quad (\text{V.13})$$

$$\gamma_i^B(T, P_0, x^B) = \frac{x_i^A}{x_i^B} \gamma_i^A(T, P_0, x^A) \exp \left[-\frac{\langle \bar{v}_i \rangle}{RT} (\Pi^* + \Pi^{SR} + \Pi^{ELEC}) \right] \quad (\text{V.14})$$

$$= \gamma_i^{LR}(T, P_0, x^A) \exp \left[-\frac{\langle \bar{v}_i \rangle \Pi^{ELEC}}{RT} \right] \quad (\text{V.15})$$

where ELEC = Electrostatic contribution
 SR = Short range contribution
 LR = Lewis-Randall model

Equation gives the activity coefficient of a solvent species in an electrolyte solution, built up from an excess Gibbs energy model (that also accounts for the short range contribution of the ions) and an electrostatic contribution from a Debye-Hückel or MSA model. [9]

Appendix VI : Example of an input file

In this appendix an example of an input file for the regression program for liquid-liquid equilibria of electrolytes is shown. The notes refer to the explanation that follows after the example. The input files can be used both for the programs of Mark Wijtkamp and for the NRTL-MSA program.

1. Example

```

'Water' (1)
'2-Propanol'
'NaCl'
'Na+'
'Cl-'
'*' (2)
0.0 18.01520 3.0D-10 (3)
0.0 60.09592 3.0D-10
0.0 58.44280 3.0D-10
1.0 22.98980 3.0D-10
-1.0 35.45300 3.0D-10

249.21 -0.79069 7.2997D-4 0.0000D0 (4)
104.16 -0.41011 4.2049D-4 0.0000D0
0.0000D0 0.0000D0 0.0000D0 0.0000D0
0.0000D0 0.0000D0 0.0000D0 0.0000D0
0.0000D0 0.0000D0 0.0000D0 0.0000D0

0.0000D0 0.0000D0 0.0000D0 0.0000D0 (5)
508.3 47.62 0.2504D0 0.0000D0
0.0000D0 0.0000D0 0.0000D0 0.0000D0
0.0000D0 0.0000D0 0.0000D0 0.0000D0
0.0000D0 0.0000D0 0.0000D0 0.0000D0

0.0000D0 0.0000D0 (6)
7.68988D-2 298.15D0
0.0000D0 0.0000D0
0.0000D0 0.0000D0
0.0000D0 0.0000D0

50 4 4 5 0.00D0 (7)

'tau12' 3.26669 -100.0 100.0 10.0 1.0 0 (8)
'tau21' .888221 -100.0 100.0 10.0 1.0 0
'tau14' 26.0643 -100.0 100.0 10.0 1.0 0
'tau41' -4.0670 -100.0 100.0 10.0 1.0 0
'tau24' 1.90137 -100.0 100.0 10.0 1.0 0
'tau42' 1.67909 -100.0 100.0 10.0 1.0 0
'alfa12' .612009 -1.0 1.0 1.0 1.0 0

```

'alfa14'	0.2	0.0	1.0	1.0	1.0	0	
'alfa24'	0.2	0.0	1.0	1.0	1.0	0	
'sigma41'	3.68E-10	1.E-11	8.E-10	5.E-11	1.0E-10	0	
'sigma51'	2.42E-10	1.E-11	8.E-10	5.E-11	1.0E-10	0	
'*'							(9)
'C'	'WF'						(10)
'D'	25.0	0.1657	0.819	0.701	0.040		(11)
'D'	25.0	0.1762	0.808	0.703	0.044		
'D'	25.0	0.2115	0.771	0.714	0.062		
'D'	25.0	0.2373	0.744	0.717	0.072		
'D'	25.0	0.2676	0.712	0.717	0.084		
'D'	25.0	0.3038	0.673	0.711	0.104		
'I'	25.0	0.348	0.615	0.699	0.155		
'*'							(12)
1.000	1.000	1.000	1.000	1.000	1.000		(13)
0	0.1	1.0D-10	5000				(14)
5.45900	.305420	647.130	.810000E-01				(15)
1.24000	.273420	508.300	.235300				
.000000	.000000	.000000	.000000				
0.76239	.000000	.000000	.000000				
.000000	.000000	.000000	.000000				

2. Explanation

- (1) Names of the components. For salts both the molecular salt and the ions must be given. The components must be given in this order: Water> solvents>molecular salt >cation>anion
- (2) Asterisk indicates end of component list. Used to determine number of components.
- (3) Valence of the components (must be given as a real value, for programming reasons), molar weight of the components (g/mol), Born radius (m) used in programs Mark Wijtkamp
- (4) Parameters A, B, C and D for the calculation of the dielectric constant. Parameters can be found in Perry's Chemical Engineer's Handbook [32]
- (5) Parameters for density calculations with the Racket equation (used in programs Mark Wijtkamp): critical temperature (K), critical pressure (bar), Racket compressibility factor.
- (6) Parameters for density calculations with the Racket equation: experimental density (m³/kmole), reference temperature (K)
- (7) Maximum number of iterations Levenberg-Marquardt routine
 Printing value: lower printing values produce more outout to screen (5 = only iteration results, 4 = print whether not the flash calculation of a datapoint has converged, 3 = Gibbs excess energies, 2 = print details flash calculation, 1 = print activity coefficients each calculation, 0 = print all)
 Number of optimalization function (0 = absolute mole fractions, 1 = relative objective function, 2 = objective function with activity coefficients, 3 = 1+2, 4 = absolute mass fractions)

- Model number:
1. Molecular NRTL
 2. Electrolyte NRTL of Chen
 3. Electrolyte NRTL, modification of Liu
 4. Electrolyte NRTL with MSA (+ hard sphere)
 5. Electrolyte NRTL with MSA (- hard sphere)
 6. Molecular NRTL (excl. molecular salt) + MSA
 7. Molecular NRTL (incl. molecular salt) + MSA
 8. MSA

Natural logarithm of dissociation constant, if zero, chemical equilibrium subroutine is skipped

- (8) Regression parameters for the activity coefficient subroutine. From left to right: initial values for the parameters, minimum value, maximum value, maximum stepsize, scaling parameter for LM routine, hold value (0= fixed parameter, 1=fit parameter)
- (9) Asterisk indicates end of parameter list, used to determine number of parameters
- (10) Temperature experimental data is given in °C (C) or K (K). Experimental data are given as mole fractions (MF), mole percents (MP), weight fractions (WF), weight percents (WP).
- (11) Experimental datapoints: (I)/(?) means ignore/use datapoint, temperature, experimental data (n-1) molecular components in phase I and phase II.
- (12) Asterisk indicates and of list. Used to determine number of datapoints.
- (13) Standard deviations or inverse weighting factors per component per liquid phase
- (14) Iteration parameters flash routine: acceleration (0=no), damping factor, tolerance, maximum number of iterations.
- (15) Parameters for density calculations (can be found in the Handbook of Chemistry and Physics, [24])

Appendix VII : Source code CHEMEQ

```

SUBROUTINE EQUILIBRIUM(EPSILON,X, TEMP)

C   Subroutine to calculate dissociation within the flash routine, the
C   dissociation fraction epsilon (or alpha) is solved with the secant method.
C   Subroutine uses the activity coefficient subroutine ACTCOEFF.

IMPLICIT REAL*8 (A-H,O-Z), INTEGER (I-N)

PARAMETER      (NMAX=10)
REAL*8         KEQ
DIMENSION      X(NMAX)

COMMON /NCOMP/  NC, NM, NAION, NCIION
COMMON /CHEM/   XX, YY, KEQ
COMMON /PRINT/  IPRINT

C   Convert true into apparent mole fractions
IF (XX.EQ.1.0D0) THEN
    XTOT = 1.0D0-X(NM+2)
ELSE IF (YY.EQ.1.0D0) THEN
    XTOT = 1.0D0-X(NM+1)
ENDIF

DO J=1, (NM-1)
    X(J)=X(J)/XTOT
ENDDO

X(NM) = (X(NM)+X(NM+1)/XX)/XTOT

X(NM+1)=0.0D0
X(NM+2)=0.0D0

C   Calculate initial values for secant method iteration
DEPS1 = EPSCALC(EPSILON*0.9D0, X, TEMP) - EPSILON*0.9D0
DEPS2 = EPSCALC(EPSILON, X, TEMP) - EPSILON
IF(DABS(DEPS1).LT.DABS(DEPS2))THEN
    EPS2 = EPSILON*0.9D0
    EPS1 = EPSILON
    SWAP = DEPS1
    DEPS1 = DEPS2
    DEPS2 = SWAP
ELSE
    EPS1 = EPSILON*0.9D0
    EPS2 = EPSILON
ENDIF

C   Use secant method to solve for EPSILON
ERR=1.0D0
DO WHILE (ERR.GT.(1.0D-6))
    SLOPE = (DEPS2 - DEPS1)/(EPS2 - EPS1)
    EPS1 = EPS2
    DEPS1 = DEPS2
    EPS2 = EPS2 - DEPS2/SLOPE
    IF (EPS2.LT.0.0D0) EPS2 = EPS1
    IF (EPS2.GT.1.0D0) EPS2 = (1.0D0-1.0D-10)
    DEPS2 = EPSCALC(EPS2, X, TEMP) - EPS2
    ERR = 2.0D0*DABS(EPS1-EPS2)/(EPS1+EPS2)
END DO

C   Use last EPSILON
EPSILON = EPS2
IF (IPRINT.LE.1) WRITE(6,*)'Dissociation fraction = ',EPS2

```


Appendix VIII : Source code ACTCOEFF

```

SUBROUTINE ACTCOEFF(TEMP, Z, GAMMA)

C      LAST MODIFIED 29-07-1998,
C      GERARD VAN BOCHOVE, MARK WIJTKAMP
C      TU-DELFT
C
C      THIS SUBROUTINE CALCULATES THE ACTIVITY COEFFICIENTS OF THE COMPONENTS IN AN
C      ELECTROLYTE SOLUTION, CONTAINING ONE SALT AND ONE OR MORE SOLVENTS.
C
C      MODELS:
C      ' 1. m-NRTL (Renon)
C      ' 2. e-NRTL + PDH + BORN (Chen)
C      ' 3. e-NRTL + PDH + BG + BORN (Liu)
C      ' 4. e-NRTL + MSA + HS + BORN
C      ' 5. e-NRTL + MSA + BORN (no HS-contribution)
C      ' 6. m-NRTL + MSA + BORN
C      ' 7. m-NRTL + MSA + BORN (molecular salt in NRTL)
C      ' 8. MSA
C      '10. 4 + solvent dependent diameter
C      '11. 5 + solvent dependent diameter
C      '12. 6 + solvent dependent diameter
C      '13. 7 + solvent dependent diameter
C
C      IMPLICIT DOUBLE PRECISION (A-H,O-Z), INTEGER (I-N)
C
C      PARAMETER      ( MAXNOION=2,
C      +              NMAX=10,
C      +              BOLTZMAN = 1.38066E-23,
C      +              PI= 3.141592653589793D0,
C      +              AV = 6.02214D23,
C      +              Q = 1.6021773D-19,
C      +              EO = 8.85419D-12*4.0D0*PI)
C      DOUBLE PRECISION MM(NMAX), DIAMETER(NMAX,NMAX), KEQ
C      DIMENSION X(NMAX), SIGMA(MAXNOION), Z(NMAX),
C      +          DCA(NMAX), DCB(NMAX), DCC(NMAX), GAMMA(NMAX),
C      +          DENS(NMAX), DC(NMAX), GNRTL(NMAX), DCD(NMAX),
C      +          DP(NMAX, 4), GMSA(NMAX), CHARGE(NMAX),
C      +          GBORN(NMAX), dSdrHO(MAXNOION, MAXNOION),
C      +          dEPSdrHO(MAXNOION), RADIUS(NMAX),
C      +          TCR(NMAX), PC(NMAX), ZRA(NMAX), OMEGA(NMAX),
C      +          VEXP(NMAX), TDENS(NMAX), GBG(NMAX)
C      +          NC, NM, NAION, NCIION
C      COMMON /NCOMP/
C      COMMON /CHARGE/ CHARGE
C      COMMON /DIELEC/ DCA, DCB, DCC, DCD
C      COMMON /MOLWEIGHT/ MM
C      COMMON /DENS/ DP
C      COMMON /SOLUTION/ DIELMX, DENSITY, SIGMA
C      COMMON /SIGMA/ DIAMETER
C      COMMON /PRINT/ IPRINT
C      COMMON /MODEL/ IMODEL
C      COMMON /RACKETT/ TCR, PC, ZRA, OMEGA, VEXP, TDENS
C      COMMON /CHEM/ XX, YY, KEQ
C      COMMON /DERIV/ dSdrHO, dEPSdrHO
C      COMMON /RADIUS/ RADIUS
C
C      CCCCCCCCCCCCCCCCCCCCCCCCCCCCCCCCCCCCCCCCCCCCCCCCCCCCCCCCCCCCCCCCCCCCCCCCCCCCC
C
C      If ions present, calculate solution properties:
C      IF (NC.GT.NM.AND.IMODEL.NE.1) THEN
C
C      Calculation of mass fractions
C      SUMMZ = 0.0D0
C      DO I=1, NC
C      SUMMZ = SUMMZ + Z(I)*MM(I)
C      END DO
C      DO I=1, NC
C      X(I) = Z(I)*MM(I)/SUMMZ
C      END DO
C
C      Molecular salt is not treated as a solvent and is assumed not to
C      have any influence on dielectric constant or density
C      NOSOLVENT = NM - 1
C
C      Dielectric constants (DC) of the solvents
C      DO I=1, NOSOLVENT
C      DC(I) = DCA(I) + DCB(I)*TEMP + DCC(I)*TEMP**2.0D0+
C      + DCD(I)*TEMP**3.0D0
C      END DO
C
C      Densities of pure components
C      DO I=1, NOSOLVENT
C      IF (DP(I,1).NE.0.0D0) THEN
C      DENS(I) = MM(I)*DP(I,1)/DP(I,2)**(1.0D0+(1.0D0-

```



```

DO I=1, NC
  WRITE(6,FMT='(15,6F12.5)')I, Z(I), DEXP(GMSA(I)),
  & DEXP(GNRTL(I)),DEXP(GBORN(I)+GBG(I)),GAMMA(I)
END DO

WRITE(6,*)

END IF

END

END

CCCCCCCCCCCCCCCCCCCCCCCCCCCCCCCCCCCCCCCCCCCCCCCCCCCCCCCCCCCC
SUBROUTINE PMSA(TEMP, Z, GMSA)

C
C This subroutine calculates the ionic activity coefficient using the
C primitive MSA model. The Carnahan-Starling equation for mixtures
C (Mansoori et al) is used to calculate the hard sphere contribution.
C
C EXPLANATION OF THE MOST IMPORTANT VARIABLES:
C
C AV      : Avagadro's number
C BOLTZMAN : Boltzman constant
C CHARGE  : Valence of an ion
C DATA   : Name of file containing physical properties
C DELTA   : Parameter MSA
C DENSITY : Density of the solution
C DIELMX  : Dielectric constant/permittivity solvent mixture
C GAMMA   : Inverse shielding length in MSA theory
C KAPPA   : Inverse Debye-Huckel length
C NMAX    : Maximum number Of components, including ions,
C           excluding molecular salts
C MAXNOION : MAXimum Number Of IONS
C MM      : Molar weight of a component
C NM      : Number of Molecular components
C NOION   : Number Of IONS
C NC      : Number Of Components
C NOSOLVENT : Number Of SOLVENTS
C OMEGA   : Parameter MSA
C PN      : Parameter MSA
C Q       : Charge of an electron
C SIGMA   : Ion diameter
C TEMP    : Temperature
C Z       : Mole fractions (salts as ions)

IMPLICIT DOUBLE PRECISION (A-H,O-Z), INTEGER (I-N)

PARAMETER      ( MAXNOION=2,
+              NMAX=10,
+              BOLTZMAN = 1.380658D-23,
+              PI= 3.141592653589793D0,
+              AV = 6.02214D23,
+              E0 = 8.85419D-12*4.0D0*PI,
+              Q = 1.6021773D-19)
DOUBLE PRECISION IONSTR, MM(NMAX)
DIMENSION        SIGMA(MAXNOION), RHO(NMAX), CHARGE(NMAX),
+              GMSA(NMAX), Z(NMAX), dSdrHO(MAXNOION,MAXNOION),
+              dEPSdrHO(MAXNOION)
COMMON /SOLUTION/ DIELMX, DENSITY, SIGMA
COMMON /MSAPARS/  GAMMA, DELTA, OMEGA, PN
COMMON /NCOMP/    NC, NM, NAION, NCION
COMMON /CHARGE/   CHARGE
COMMON /PRINT/    IPRINT
COMMON /MOLWEIGHT/ MM
COMMON /MODEL/    IMODEL
COMMON /DERIV/    dSdrHO, dEPSdrHO

NOION = NAION + NCION

C
C Calculation of numerical density RHO = #/m3 (used in MSA)
SUMMZ = 0.0D0
DO I=1, NC
  SUMMZ = SUMMZ + Z(I)*MM(I)
END DO
DO I=1, NC
  RHO(I) = Z(I)/SUMMZ*1.0D3*AV*DENSITY
END DO

C
C The first part of this subroutine calculates the MSA inverse shielding length,
C the main parameter in the unrestricted primitive MSA (Blum).
IONSTR = 0.0D0
DO I=NM+1, NC
  IONSTR = IONSTR+0.5D0*(CHARGE(I)**2.0D0)*RHO(I)*Q*Q
END DO

C
C Calculation of kappa/2 as first estimation of GAMMA
ESTGAMMA = 0.5D0*DSQRT(8.0D0*PI*IONSTR/
+ (BOLTZMAN*TEMP*DIELMX))

C
C Calculation of GAMMA as described by Simonin et al (1996)
ESTGAMMA = DSQRT(1.0D0+2.0D0*ESTGAMMA*(SIGMA(1)+SIGMA(2))) -
+ 1.0D0/(SIGMA(1)+SIGMA(2))

```

```

C Since it is difficult to calculate derivative of gamma and ..
C "NEWTON-RAPHSON with numerical derivatives is in one
C dimension always dominated by the secant method"
C (Numerical Recipes p365)
C --> SECANT METHOD IS USED

DGAMMA1 = CALCGAMMA(TEMP, RHO, ESTGAMMA*0.9D0) - ESTGAMMA*0.9D0
DGAMMA2 = CALCGAMMA(TEMP, RHO, ESTGAMMA) - ESTGAMMA
IF (DABS(DGAMMA1).LT.DABS(DGAMMA2)) THEN
  GAMMA2 = ESTGAMMA*0.9D0
  GAMMA1 = ESTGAMMA
  SWAP = DGAMMA1
  DGAMMA1 = DGAMMA2
  DGAMMA2 = SWAP
ELSE
  GAMMA1 = ESTGAMMA/0.9D0
  GAMMA2 = ESTGAMMA
ENDIF

ERRGAMMA=1.0D0
DO WHILE (ERRGAMMA.GT.(1.0D-6))
  SLOPE = (DGAMMA2 - DGAMMA1)/(GAMMA2 - GAMMA1)
  GAMMA1 = GAMMA2
  DGAMMA1 = DGAMMA2
  GAMMA2 = GAMMA2 - DGAMMA2/SLOPE
  DGAMMA2 = CALCGAMMA(TEMP, RHO, GAMMA2) - GAMMA2
  ERRGAMMA = 2.0D0*DABS(GAMMA1-GAMMA2)/(GAMMA1+GAMMA2)
END DO

C The error made by skipping the iteration is rather small, so
C it is possible to do it. If so, use this equation:
C GAMMA = CALCGAMMA(TEMP, RHO, ESTGAMMA)

C End of iteration

CCCCCCCCCCCCCCCCCCCCCCCCCCCCCCCCCCCCCCCCCCCCCCCCCCCCCCCCCCCCCCCC
C The following part calculates the activity coefficients of the ions
C from a hard sphere contribution and an electrostatic contribution.
C
C Calculation of hard sphere contribution (without dependencies) from the
C Mansoori-Leland-Carnahan-Starling approximation
C The expression for the activity coefficient as derived by Simonin et al
C is used. (See: J.Phys.Chem (1996),100, p7704-7709)

X0=0.0D0
X1=0.0D0
X2=0.0D0
X3=0.0D0
DO I=1, NOION
  X0 = X0 + PI/6.0D0*RHO(NM+I)
  X1 = X1 + PI/6.0D0*RHO(NM+I)*SIGMA(I)
  X2 = X2 + PI/6.0D0*RHO(NM+I)*SIGMA(I)**2.0D0
  X3 = X3 + PI/6.0D0*RHO(NM+I)*SIGMA(I)**3.0D0
END DO
F2 = 3*X1/(1.0D0-X3) + 3.0D0*X2*X2/(X3*(1.0D0-X3)**2.0D0) +
+ 3.0D0*X2*X2/(X3*X3)*DLOG(1.0D0-X3)
F3 = (X0-(X2**3.0D0)/(X3*X3))/(1.0D0-X3)+(3.0D0*X1*X2-(X2**3.0D0)
+ /(X3*X3))/(1.0D0-X3)**2.0D0 + 2.0D0*(X2**3.0D0)/(X3*
+ (1.0D0-X3)**3.0D0)-2.0D0*(X2**3.0D0)/(X3**3.0D0)*DLOG(1.0D0-X3)

DO J=1, NOION
  HS = - DLOG(1.0D0-X3)+ SIGMA(J)*3.0D0*X2/(1.0D0-X3)+
+ (SIGMA(J)**2.0D0)*F2 + (SIGMA(J)**3.0D0)*F3
C Calculation of MSA parameter ALPHA
  ALPHA = Q*DSQRT(4.0D0*PI/(DIELMX*BOLTZMAN*TEMP))
C Calculation of short range electrostatic contribution
  SRE = -(ALPHA*PN)**2.0D0/(8.0D0*DELTA)*
+ (2.0D0*SIGMA(J)*CHARGE(NM+J)/(PN*(1.0D0+GAMMA*SIGMA(J)))-
+ SIGMA(J)**3.0D0*PI/(2.0D0*DELTA*(1.0D0+GAMMA*SIGMA(J)))+
+ PI*(SIGMA(J)**3.0D0)/(6.0D0*DELTA) )
C Calculation of (Coulombic) long range electrostatic contribution
  CLRE = - 0.25D0*ALPHA*ALPHA*GAMMA/PI*
+ CHARGE(NM+J)**2.0D0/(1.0D0+GAMMA*SIGMA(J))
C Contributions due to concentration dependency ionic diameters
  IF (dSdRHO(J,J).NE.0.0D0) THEN
    SUMHS = 0.0D0
    DO I=1, (NC-NM)
      SUMHS = SUMHS + (3.0D0*X2/(1.0D0-X3)+2.0D0*SIGMA(I)*F2+
+ 3.0D0*SIGMA(I)*SIGMA(I)*F3)*RHO(NM+I)*dSdRHO(I,J)
    ENDDO
    HS = HS + SUMHS
    SUMELEC = 0.0D0
    DO I=1, (NC-NM)
      SUMELEC = SUMELEC + RHO(NM+I)*ALPHA*ALPHA/(4.0D0*PI)*
+ ((GAMMA*CHARGE(NM+I)/(1.0D0+GAMMA*SIGMA(I)))**2.0D0
+ PN*PI*0.5D0/DELTA*(PN*PI*0.5D0/DELTA*SIGMA(I))*

```

```

+          SIGMA(I)*(2.0D0-(GAMMA*SIGMA(I))**2.0D0)-2.0D0*
+          CHARGE(NM+I))/(1.0D0+GAMMA*SIGMA(I))**2.0D0)*
+          dSdrHO(I,J)

      ENDDO
      CLRE = CLRE + SUMELEC

ENDIF

C Contribution due to concentration dependency dielectric constant
ESUM = 0.0D0
DO I=1, NOION
  ESUM = ESUM + RHO(I+NM)*(CHARGE(I+NM)**2.0D0)/
  (1.0D0+GAMMA*SIGMA(I))
ENDDO

EMSA = -Q*Q/DIELMX*(GAMMA*ESUM+PI/(2.0D0*DELTA)* OMEGA*PN*PN)
      / (BOLTZMAN*TEMP)

IF (dEPSdrHO(J).NE.0.0D0) CLRE = CLRE + EMSA/DIELMX*dEPSdrHO(J)

C Calculation of ionic activity coefficients
GMSA(NM+J) = HS + CLRE + SRE

IF (IMODEL.EQ.5.OR.IMODEL.EQ.11) GMSA(NM+J) = CLRE + SRE

C Write MSA contributions (for use with SIGMAFIT.FOR or ACTMSA.FOR)
IF (IPRINT.EQ.41.OR.IPRINT.EQ.42) THEN
  IF (J.EQ.1) THEN
    HSC = HS
    CLREC = CLRE
    SREC = SRE
  ELSE IF (J.EQ.2) THEN
    HS = (RHO(NM+1)*HSC+RHO(NC)*HS)/(RHO(NM+1)+RHO(NC))
    CLRE = (RHO(NM+1)*CLREC+RHO(NC)*CLRE)/(RHO(NM+1)+RHO(NC))
    SRE = (RHO(NM+1)*SREC+RHO(NC)*SRE)/(RHO(NM+1)+RHO(NC))
    WRITE(6,'(3F15.8)')HS, CLRE, SRE
  END IF
END IF

END DO

CCCCCCCCCCCCCCCCCCCCCCCCCCCCCCCCCCCCCCCCCCCCCCCCCCCCCCCCCCCCCCCCCCCC
C The contribution of the MSA to the activity coefficients of the
C neutral species is calculated in the same way Lloyd Lee does in
C Proc. Ann. Conv. GPA, 1996, p92-101

C Calculation of ion density
RHOION = 0.0D0
RHOMOLEC = 0.0D0
DO I=1, NC
  IF (I.GT.NM) RHOION = RHOION + RHO(I)
  IF (I.LE.NM) RHOMOLEC = RHOMOLEC + RHO(I)
END DO

C Electrostatic contribution:
ELEC = -GAMMA**3.0D0/(3.0D0*PI*RHOMOLEC)-ALPHA**2.0D0/
      (8.0D0*RHOMOLEC)*(PN/DELTA)**2.0D0

C Hard sphere contribution:
HS = X3/(1.0D0-X3)+3.0D0*X1*X2/(X0*(1-X3)**2.0D0)+
      X2**3.0D0*(3.0D0-X3)/(X0*(1-X3)**3.0D0)*RHOION/RHOMOLEC

C Total contribution to activity coefficient of neutral species
DO I=1, NM
  GMSA(I) = - (ELEC + HS)
  IF (IMODEL.EQ.5.OR.IMODEL.EQ.11) GMSA(I)=-ELEC
END DO

END
CCCCCCCCCCCCCCCCCCCCCCCCCCCCCCCCCCCCCCCCCCCCCCCCCCCCCCCCCCCCCCCCCCCC
FUNCTION CALCGAMMA(TEMP, RHO, ESTGAMMA)

C This function calculates the MSA shielding parameter (one iteration)

IMPLICIT DOUBLE PRECISION (A-H,O-Z), INTEGER (I-N)

PARAMETER ( NMAX=10,
+           MAXNOION=2,
+           BOLTZMAN = 1.38066E-23,
+           PI = 3.141592653589793D0,
+           Q = 1.6021773D-19 )
DIMENSION SIGMA(NMAX), RHO(NMAX), CHARGE(NMAX)
COMMON /SOLUTION/ DIELMX, DENSITY, SIGMA
COMMON /CHARGE/ CHARGE
COMMON /MSAPARS/ GAMMA, DELTA, OMEGA, PN
COMMON /NCOMP/ NC, NM, NAION, NCIION

NOION = NAION + NCIION

C Calculation of MSA parameters
DELTA = 1.0D0

```



```

C Initialization
DO I=1,NMAX
  DO J=1,NMAX
    USRGN(I,J) = 0.0D0
    USRGT(I,J) = 0.0D0
    ALPHA(I,J) = 0.0D0
    TAU(I,J) = 0.0D0
    G(I,J) = 1.0D0
  ENDDO
  GNRTL(I)=0.0D0
  C(I)=0.0D0
ENDDO

C Calculation of all parameters in NRTL equations.
C ASPEN Reference Manual Vol. 2 Rel. 3; Appendix B :eq. 37 --> 48.

DO I=1, NC
  DO J=1, NC
    USRGN(I,J) = GMUN(I,J)
    USRGT(I,J) = GMUT(I,J)
  ENDDO
ENDDO

C IF (NC.GT.NM.AND.KEQ.GT.0.0D0) THEN
C DO I=1, NC
C   USRGT(NM, I) = USRGT(NM+1,I)
C   USRGT(I, NM) = USRGT(I,NM+1)
C   USRGN(NM,I) = USRGN(NM+1,I)
C   USRGN(I,NM) = USRGN(I,NM+1)
C ENDDO
C ENDIF

C Convert ALPHA_ij into ALPHA_ji
DO I=1,(NC-1)
  DO J=I+1, NC
    USRGN(J,I)=USRGN(I,J)
  ENDDO
ENDDO

C Initialize parameter Ci
DO I=1, NC
  IF ((CHARGE(I)).NE.0.0D0) THEN
    C(I) = DABS(CHARGE(I))
  ELSE
    C(I) = 1.0D0
  ENDF
ENDDO

C STEP 1 : G(1->NM,1->NM), TAU(1->NM,1->NM), ALPHA(1->NM)

DO I=1,NM
  DO J=1,NM
    ALPHA(I,J)=USRGN(I,J)
    TAU(I,J)=USRGT(I,J)
    G(I,J)=DEXP(-ALPHA(I,J)*TAU(I,J))
  ENDDO
ENDDO

IF (NCION.NE.0.AND.NAION.NE.0) THEN

C STEP 2a : G(NM+1->NM+NCION,1->NM)
C b : G(NM+NCION+1->NC,1->NM)

IJ = NM+1
I2 = NM+NCION+1

DO J=1,NM
  G(IJ,J) = DEXP(-USRGN(IJ,J)*USRGT(IJ,J)) ! 2a
  G(I2,J) = DEXP(-USRGN(IJ,J)*USRGT(IJ,J)) ! 2b
ENDDO

C STEP 3a : ALPHA(1->NC,NM+1->NM+NCION)
C b : ALPHA(1->NC,NM+NCION+1->NC)

IJ = NM+1
I2 = NM+NCION+1

DO J=1,NM
  ALPHA(IJ,J) = USRGN(IJ,J) ! 3a
  ALPHA(J,IJ) = USRGN(J,IJ)
  ALPHA(I2,J) = USRGN(IJ,J) ! 3b
  ALPHA(J,I2) = USRGN(J,IJ)
ENDDO

C STEP 4a : TAU(NM+1->NM+NCION,1->NM)
C b : TAU(NM+NCION+1->NC,1->NM)

TINY=1.0D-64
IJ = NM+1
I2 = NM+NCION+1
DO J=1,NM

```

```

      TAU(IJ,J) = -DLOG(G(IJ,J))/(ALPHA(IJ,J)+TINY)      . 4a
      TAU(I2,J) = -DLOG(G(I2,J))/(ALPHA(I2,J)+TINY)      . 4b
      ENDDO

C   STEP 5a      :      TAU(1->NC,NM+1->NM+NCION)
C   b           :      TAU(1->NC,NM+NCION+1->NC)

      DO IJ = 1,NM
        J = NM+1
        J2 = NM+NCION+1
        TAU(IJ,J) = USRGT(IJ,J)                          ! 5a
        TAU(IJ,J2) = USRGT(IJ,J)                        ! 5b
C       TAU(IJ,J) = TAU(J,IJ) - USRGT(J,IJ) + USRGT(IJ,J) ! 5a
C       TAU(IJ,J2) = TAU(J2,IJ) - USRGT(J2,IJ) + USRGT(IJ,J2) ! 5b
      ENDDO

C   STEP 6a      :      G(1->NC,NM+1->NM+NCION)      OK
C   b           :      G(1->NC,NM+NCION+1->NC)

      IJ = NM+1
      I2 = NM+NCION+1
      DO J=1,NM
        G(J,IJ) = DEXP(-ALPHA(J,IJ)*TAU(J,IJ))          ! 6a
        G(J,I2) = DEXP(-ALPHA(J,I2)*TAU(J,I2))          ! 6b
      ENDDO

C   STEP 7      :      t(NM+1,NM+1)=t(NM+2,NM+2)=-oo
C               :      G(NM+1,NM+1)=G(NM+2,NM+2)=0

      TAU(NM+NCION,NM+NCION)=1.0D16
      TAU(NC,NC)=1.0D16

      G(NM+NCION,NM+NCION)=0.0D0
      G(NC,NC)=0.0D0

      ENDIF

***** The NRTL expression for the activity coefficient, GNRTL *****

C The equations are divided into several contributions,
C namely NRTL1 --> NRTL10
C These contributions are described on page B-9,
C ASPEN Reference Manual Vol. 2 Rel. 9; Appendix B ;eq. 37 -> 48.
C Gamma,molecular = NRTL1 + NRTL2 + NRTL3 + NRTL4
C Gamma,cation    = NRTL5 + NRTL6 + NRTL7
C Gamma,anion     = NRTL8 + NRTL9 + NRTL10

***** NRTL 1 *****

      NRTL1 = 0.0D0
      NRTL3 = 0.0D0
      NRTL2 = 0.0D0
      NRTL4 = 0.0D0
      NRTL5 = 0.0D0
      NRTL6 = 0.0D0
      NRTL7 = 0.0D0
      NRTL8 = 0.0D0
      NRTL9 = 0.0D0
      NRTL10 = 0.0D0
      TINY = 1.0D-64

      DO I=1,NM
        NRTL11 = 0.0D0
        NRTL12 = 0.0D0
        DO J=1,NC
          NRTL11 = NRTL11 + C(J)*Z(J)*G(J,I)*TAU(J,I)
          NRTL12 = NRTL12 + C(J)*Z(J)*G(J,I)
        ENDDO
        NRTL1 = NRTL11/(NRTL12+TINY)
      ENDDO

C ***** NRTL 2 *****

      NRTL2 = 0.0D0
      DO J=1,NM
        NRTL21 = 0.0D0
        NRTL22 = 0.0D0
        DO K=1,NC
          NRTL21 = NRTL21 + C(K)*Z(K)*G(K,J)*TAU(K,J)
          NRTL22 = NRTL22 + C(K)*Z(K)*G(K,J)
        ENDDO
        NRTL2 = NRTL2 + ((C(J)*Z(J)*G(I,J))/
          (NRTL22+TINY))*(TAU(I,J)-(NRTL21/(
          NRTL22+TINY)))
      ENDDO

      IF (NCION.NE.0.AND.NAION.NE.0) THEN

C ***** NRTL 3 *****

      J = NM+1

```

```

      NRTL31 = 0.0D0
      NRTL32 = 0.0D0+TINY
      DO L=1,NC
        NRTL31 = NRTL31 + C(L)*Z(L)*G(L,J)*TAU(L,J)
        NRTL32 = NRTL32 + C(L)*Z(L)*G(L,J)
      ENDDO
      NRTL3 = ((C(J)*Z(J)*G(I,J)/NRTL32)*
        (TAU(I,J)-(NRTL31/NRTL32)))
      J=NM+1
C ***** NRTL 4 *****
      J=NM+NCION+1
      NRTL41 = 0.0D0
      NRTL42 = 0.0D0+TINY
      DO L=1,NC
        NRTL41 = NRTL41 + C(L)*Z(L)*G(L,J)*TAU(L,J)
        NRTL42 = NRTL42 + C(L)*Z(L)*G(L,J)
      ENDDO
      NRTL4 = ((C(J)*Z(J)*G(I,J)/NRTL42)*
        (TAU(I,J)-(NRTL41/NRTL42)))
      ENDIF
C Calculate NRTL term for molecular species
      GNRTL(I) = NRTL1 + NRTL2 + NRTL3 + NRTL4
      ENDDO
.....
      IF (NCION.NE.0.AND.NAION.NE.0) THEN
        I = NM+1
C ***** NRTL 5 *****
      NRTL51=0.0D0
      NRTL52=0.0D0
      DO K=1,NC
        NRTL51 = NRTL51 + C(K)*Z(K)*G(K,I)*tau(K,I)
        NRTL52 = NRTL52 + C(K)*Z(K)*G(K,I)
      ENDDO
      NRTL5 = NRTL51/(NRTL52+tiny)
C ***** NRTL 6 *****
      NRTL6=0.0D0
      DO J=1,NM
        NRTL61=0.0D0
        NRTL62=0.0D0
        DO K=1,NC
          NRTL61 = NRTL61 + C(K)*Z(K)*G(K,J)*tau(K,J)
          NRTL62 = NRTL62 + C(K)*Z(K)*G(K,J)
        ENDDO
        NRTL6 = NRTL6 + ((C(J)*Z(J)*G(I,J)/(NRTL62+
          & tiny))*tau(I,J)-(NRTL61/(NRTL62+
          & tiny)))
        ENDDO
C ***** NRTL 7 *****
      J=NM+NCION+1
      NRTL71=0.0D0
      NRTL72=0.0D0
      DO L=1,NC
        NRTL71 = NRTL71 + C(L)*Z(L)*G(L,J)*tau(L,J)
        NRTL72 = NRTL72 + C(L)*Z(L)*G(L,J)
      ENDDO
      NRTL7 = ((C(J)*Z(J)*G(I,J)/(NRTL72+tiny))
        *tau(I,J)-(NRTL71/(NRTL72+tiny)))
C ***** Ln Gamma, cation (infinite diluted), GCINF *****
      GCINF = TAU(1,NM+1) + TAU(NM+1,1)*G(NM+1,1)
C Calculate NRTL term for cations
      GNRTL(I) = (NRTL5 + NRTL6 + NRTL7 - GCINF)*DABS(CHARGE(I))
      I = NM+NCION+1
C ***** NRTL 8 *****
      NRTL81=0.0D0
      NRTL82=0.0D0
      DO K=1,NC
        NRTL81 = NRTL81 + C(K)*Z(K)*G(K,I)*tau(K,I)
        NRTL82 = NRTL82 + C(K)*Z(K)*G(K,I)
      ENDDO
      NRTL8 = NRTL81/(NRTL82+tiny)
C ***** NRTL 9 *****

```

```

NRTL9=0.0D0
DO J=1,NM
  NRTL91=0.0D0
  NRTL92=0.0D0
  DO K=1,NC
    NRTL91 = NRTL91 + C(K)*Z(K)*G(K,J)*tau(K,J)
    NRTL92 = NRTL92 + C(K)*Z(K)*G(K,J)
  ENDDO
  NRTL9 = NRTL9 + ((C(J)*Z(J)*G(I,J))
& / (NRTL92+tiny))*tau(I,J)-
& (NRTL91/ (NRTL92+tiny)))
ENDDO

C ***** NRTL 10 *****

J=NM+1
NRTL101=0.0D0
NRTL102=0.0D0
DO L=1,NC
  NRTL101 = NRTL101 + C(L)*Z(L)*G(L,J)*TAU(L,J)
  NRTL102 = NRTL102 + C(L)*Z(L)*G(L,J)
ENDDO
NRTL10 = ((C(J)*Z(J)*G(I,J))/(NRTL102+TINY))*
& (TAU(I,J)-(NRTL101/(NRTL102+TINY)))

GAINF = TAU(1,NM+NCION+1) + TAU(NM+NCION+1,1)
& *G(NM+NCION+1,1)

C Calculate NRTL term for anions
  GNRTL(I) = (NRTL8 + NRTL9 + NRTL10 - GAINF)*DABS(CHARGE(I))

ENDIF

C NRTL expression for the excess Gibbs energy, GENRTL
C
C This contribution consists of three parts, namely
C GENRTL1, GENRTL2, and GENRTL3
C These contributions are described on page B-9,
C ASPEN Reference Manual Vol. 2 Rel. 9; Appendix B :eq. 37 -> 48.
C Gexcess,molecular = GENRTL1
C Gexcess,cation = GENRTL2
C Gexcess,anion = GENRTL3

GENRTL1 = 0.0D0
GENRTL2 = 0.0D0
GENRTL3 = 0.0D0

DO I=1, NM
  GENSUM11 = 0.0D0
  GENSUM12 = 0.0D0
  DO J=1, NC
    GENSUM11 = GENSUM11 + Z(J)*C(J)*G(J,I)*TAU(J,I)
    GENSUM12 = GENSUM12 + Z(J)*C(J)*G(J,I)
  ENDDO
  GENRTL1 = GENRTL1 + C(I)*Z(I)*(GENSUM11
& / (GENSUM12+TINY))
ENDDO

L = NM+1
GENSUM21 = 0.0D0
GENSUM22 = 0.0D0
DO I=1, NC
  GENSUM21 = GENSUM21 + Z(I)*C(I)*G(I,L)*TAU(I,L)
  GENSUM22 = GENSUM22 + Z(I)*C(I)*G(I,L)
ENDDO
GENRTL2 = C(L)*Z(L)*(GENSUM21/ (GENSUM22+TINY))

M = NM+NCION+1
GENSUM31 = 0.0D0
GENSUM32 = 0.0D0
DO I=1, NC
  GENSUM31 = GENSUM31 + Z(I)*C(I)*G(I,M)*TAU(I,M)
  GENSUM32 = GENSUM32 + Z(I)*C(I)*G(I,M)
ENDDO
GENRTL3 = C(M)*Z(M)*(GENSUM31/ (GENSUM32+TINY))

GENRTLINF = C(L)*Z(L)*GCINF + C(M)*Z(M)*GAINF

GENRTL = GENRTL1 + GENRTL2 + GENRTL3 - GENRTLINF

GENRTL22 = 0.0D0
DO I=1, NM
  GENRTL22 = GENRTL22 + Z(I)*GNRTL(I)
ENDDO
GENRTL22 = GENRTL22 + Z(M)*GNRTL(M)+Z(L)*GNRTL(L)

IF (IPRINT.EQ.3) THEN
  WRITE(6,98)' NRTL excess Gibbs energy = ',GENRTL
  WRITE(6,98)' Sum x(i)*ln[gamma(i)] = ',GENRTL22
  WRITE(6,98)' Difference = ',DABS(GENRTL-GENRTL22)
  WRITE(6,98)' Quotient = ',DABS(GENRTL/GENRTL22)
  WRITE(6,*)

```



```

C     These contributions are described on page B-9,
C     ASPEN Reference Manual Vol. 2 Rel. 9; Appendix B ;eq. 37 -> 48.
C     Gamma,molecular = NRTL1 + NRTL2 + NRTL3 + NRTL4
C     Gamma,cation    = NRTL5 + NRTL6 + NRTL7    ---> HERE NOT USED
C     Gamma,anion     = NRTL8 + NRTL9 + NRTL10   ---> HERE NOT USED

TINY = 1.0D-32

C     IF (NC.EQ.NM.OR.KEQ.NE.0.0D0.OR.IMODEL.EQ.10.OR.IMODEL.EQ.11) THEN
C     IF (NC.EQ.NM.OR.KEQ.NE.0.0D0.OR.IMODEL.EQ.7.OR.IMODEL.EQ.13) THEN
IMAX = NM
ELSE
IMAX = NM-1
END IF

C     ***** NRTL 1 *****

DO I=1,NC
NRTL1 = 0.0D0
NRTL2 = 0.0D0
GNRTL(I) = 0.0D0
IF (I.LE.IMAX) THEN
NRTL11 = 0.0D0
NRTL12 = 0.0D0+TINY
DO J=1,IMAX
NRTL11 = NRTL11 + C(J)*Z(J)*G(J,I)*TAU(J,I)
NRTL12 = NRTL12 + C(J)*Z(J)*G(J,I)
ENDDO
NRTL1 = NRTL11/NRTL12

```

```

C     ***** NRTL 2 *****

DO J=1,IMAX
NRTL21 = 0.0D0
NRTL22 = 0.0D0+TINY
DO K=1,IMAX
NRTL21 = NRTL21 + C(K)*Z(K)*G(K,J)*TAU(K,J)
NRTL22 = NRTL22 + C(K)*Z(K)*G(K,J)
ENDDO
NRTL2 = NRTL2 + (C(J)*Z(J)*G(I,J)/
& NRTL22)*(TAU(I,J)-NRTL21/NRTL22)
ENDDO

```

```

C     Calculate NRTL term for molecular species
GNRTL(I) = NRTL1 + NRTL2

END IF
END DO

C     NRTL expression for the excess Gibbs energy, GENRTL
C
C     This contribution consists of three parts, namely
C     GENRTL1, GENRTL2, and GENRTL3
C     These contributions are described on page B-9,
C     ASPEN Reference Manual Vol. 2 Rel. 9; Appendix B ;eq. 37 -> 48.
C     Gexcess,molecular = GENRTL1
C     Gexcess,cation    = GENRTL2    -> not used
C     Gexcess,anion     = GENRTL3    -> not used

GENRTL = 0.0D0

DO I=1, NM
GENSUM1 = 0.0D0
GENSUM2 = 0.0D0
DO J=1, NC
GENSUM1 = GENSUM1 + Z(J)*C(J)*G(J,I)*TAU(J,I)
GENSUM2 = GENSUM2 + Z(J)*C(J)*G(J,I)
ENDDO
GENRTL = GENRTL + C(I)*Z(I)*(GENSUM1
& / (GENSUM2+TINY))
ENDDO

GENRTL22 = 0.0D0
DO I=1, NM
GENRTL22 = GENRTL22 + Z(I)*GNRTL(I)
ENDDO

IF (IPRINT.EQ.3) THEN
WRITE(6,98)' NRTL excess Gibbs energy = ',GENRTL
WRITE(6,98)' Sum x(i)*ln[gamma(i)] = ',GENRTL22
WRITE(6,98)' Difference = ',DABS(GENRTL-GENRTL22)
WRITE(6,98)' Quotient = ',DABS(GENRTL/GENRTL22)
WRITE(6,*)
ENDIF

98 FORMAT(A,G12.6)

END

```